

Computer visualization of ternary and quaternary fluid-phase equilibria

by

Kong Sen Tian

A thesis submitted to the graduate faculty
in partial fulfillment of the requirements for the degree of
MASTER OF SCIENCE

Major: Chemical Engineering

Major Professor: Kenneth R. Jolls

Iowa State University

Ames, Iowa

1997

Copyright © Kong Sen Tian, 1997. All rights reserved.

Graduate College
Iowa State University

This is to certify that the Master's thesis of
Kong Sen Tian
has met the thesis requirements of Iowa State University

Signatures have been redacted for privacy

TABLE OF CONTENTS

	Page
LIST OF FIGURES	iv
LIST OF TABLES	viii
ACKNOWLEDGMENTS	x
ABSTRACT	xi
CHAPTER 1. INTRODUCTION	1
CHAPTER 2. GEOMETRIC REPRESENTATION OF PHASE DIAGRAMS	8
Unary systems	8
Binary systems	12
Ternary systems	16
Quaternary systems	21
Quinary systems	28
CHAPTER 3. THEORIES AND APPLICATIONS	30
Equations of state	30
Phase equilibrium	33
Vapor-liquid equilibrium	34
Application	47
Liquid-liquid equilibrium	50
CHAPTER 4. MAKING OF THREE-DIMENSIONAL BINARY DIAGRAMS	51
Generating phase-equilibrium data	51
Generating data points in the critical region	56
Generating images using Open Inventor software	58
CHAPTER 5. MAKING OF THREE-DIMENSIONAL TERNARY DIAGRAMS	59
Thermodynamic surface triangulation	86
CHAPTER 6. MAKING OF THREE-DIMENSIONAL QUATERNARY DIAGRAMS	113
Triangulation of the quaternary surface	126
CHAPTER 7. CONCLUSIONS AND RECOMMENDATIONS	137
APPENDIX	139
BIBLIOGRAPHY	140

LIST OF FIGURES

	Page
Figure 1.1 Isothermal P-xy diagram for cyclohexane-cyclohexanone, T = 500 K.	2
Figure 1.2 Isobaric T-xy diagram for cyclohexane-cyclohexanone, P = 10 bar.	3
Figure 1.3 P-xy diagram for cyclohexanone-cyclohexane with three constant-temperature curves.	4
Figure 2.1 Pressure-temperature diagram for a pure substance that contracts on freezing.	9
Figure 2.2 Three-dimensional PVT diagram [2, page 96].	11
Figure 2.3 Isothermal T-xy diagram for the AB binary.	13
Figure 2.4 Pressure-temperature diagram for component A.	13
Figure 2.5 Pressure-temperature diagram for component B.	14
Figure 2.6 P-T-xy diagram for cyclohexane(A)-cyclohexanone(B).	15
Figure 2.7 Triangular plots for representing the compositions of ternary mixtures.	17
Figure 2.8 Two-dimensional diagram representing VLE in a ternary system at a fixed temperature and pressure. Component A is the least volatile.	19
Figure 2.9 Isothermal P-xy diagrams for the A-B, A-C, and B-C binaries.	20
Figure 2.10 Planar diagram for the A-B-C ternary consistent with Figure 2.9.	21
Figure 2.11 Planar representation of a quaternary system for fixed X_D .	23
Figure 2.12 Equilateral tetrahedron for representing phase equilibrium in a quaternary system at constant temperature and pressure.	24
Figure 2.13 Constant-composition plane lying parallel to the triangular base ABC.	25

Figure 2.14	P-xy diagrams for the six binary sub-systems at temperature T_1 .	27
Figure 2.15	Outline structure of the quaternary diagram obtained from the binaries in Figure 2.14.	28
Figure 3.1	Flow sheet diagram for bubble-point pressure calculation [9].	46
Figure 3.2	P-xy phase diagram for cyclohexane and cyclohexanone illustrating a bubble-point pressure calculation at $x = 0.7$.	47
Figure 3.3	Setting up vapor-liquid equilibrium calculations using the FLASH2 routine.	48
Figure 4.1	Coordinate box for a binary diagram.	64
Figure 4.2	PTx diagram for cyclohexanone and cyclohexane.	67
Figure 4.3	PTx diagram for cyclopentane and acetone.	68
Figure 4.4	Magnified PTx diagram for cyclopentane and acetone.	69
Figure 5.1	The order of components A, B and C in the (unturned) prism.	73
Figure 5.2	Surface contour lines projected onto a triangular base (equally spaced).	74
Figure 5.3	Surface contour lines with equal (default) spacing ($a=1$, $b=0$).	76
Figure 5.4	Surface contour-line spacing with $a=1$ and $b=0.2$.	78
Figure 5.5	Surface contour-line spacing with $a=-3$ and $b=0.1$.	78
Figure 5.6	Surface contour-line spacing with $a=-4$ and $b=0.1$.	78
Figure 5.7	Dew-point surface with triangular elements of unequal size.	79
Figure 5.8	Dew-point surface with triangular elements of roughly the same size.	79
Figure 5.9	Schematic representation of the coordinate transformation, Cartesian (left) to equilateral triangular prism.	83
Figure 5.10	Square with two triangular elements drawn with MOVIE.BYU.	84

Figure 5.11	Model ternary phase surface with 5 constant-composition lines and 16 triangular elements.	86
Figure 5.12	FORTRAN code for triangulating upright triangles.	88
Figure 5.13	FORTRAN code for triangulating inverted triangles.	89
Figure 5.14	Ternary p-xy diagram for the system benzene, acetone, n-butane at $T=298.15$ K.	94
Figure 5.15	Isothermal pressure-composition prism for the n-pentane, nitrobenzene, iso-butane ternary at $T=398.15$ K (bubble-point surface is transparent).	95
Figure 5.16	P-xy diagram for nitrobenzene and n-pentane at $T=398.15$ K. The wavy bubble point curve indicates immiscible liquid phases.	96
Figure 5.17	P-xy diagram for nitrobenzene, n-pentane at $T=398.15$ K. Three phase line is at $P = 8.617$ bar.	97
Figure 5.18	LLE and VLE tie lines for the ternary mixture, $T = 398.15$ K.	99
Figure 5.19	Isothermal ternary phase diagram for n-pentane, nitrobenzene, i-butane showing the VLLE coexistence curves and tie lines.	100
Figure 5.20	Complete, isothermal, pressure-composition diagram for the n-pentane, nitrobenzene, i-butane ternary mixture.	101
Figure 5.21	Schematic diagram showing a series of base points and circular search paths to find LLE critical points (exaggerated scale).	106
Figure 5.22	Magnified drawing of a particular base point and its circular search path.	107
Figure 5.23	Two views of the isothermal p-xy diagram for the acetonitrile, benzene, ethanol ternary, $T = 333.15$ K.	108
Figure 5.24	P-xy diagram for the ethylbenzene, acetic acid, pyridine ternary at $T=373.15$ K (two views).	110
Figure 5.25	Flowsheet for locating the composition of a saddle azeotrope.	111

Figure 6.1	Two views of a unit-length tetrahedron for representing quaternary systems.	113
Figure 6.2	Schematic representation of a quaternary coordinate transformation: Cartesian to equilateral tetrahedron.	115
Figure 6.3	Schematic diagram for flash calculation using Design-Spec.	118
Figure 6.4	Outline structure of the bubble- and dew-point surfaces in the phase diagram for a simple quaternary mixture (two orientations).	120
Figure 6.5	Outline structure of the bubble-point surface in Figure 6.4(b) as viewed from the top of the tetrahedron.	120
Figure 6.6	Outline structure of the dew-point surface in Figure 6.4(b).	125
Figure 6.7	Quaternary phase diagram for benzene, acetone, n-pentane, n-butane at $T=298.15$ K and $P=0.5$ bar.	127
Figure 6.8	Outline structure of the quaternary bubble-point and dew-point surfaces using straight-line approximations in the ternary faces.	131
Figure 6.9	Enlargement of bubble-point surface near the benzene vertex in Figure 6.8.	132
Figure 6.10	Phase diagram for the acetonitrile, benzene, ethanol, acetone quaternary, $T=333.15$ K, $P=0.6$ bar.	135
Figure 6.11	Phase diagram for acetone, benzene, ethanol and acetonitrile, $T=333.15$ K, $P=0.6377$ bar.	136

LIST OF TABLES

	Page	
Table 4.1	CR program input file for the ethylene/n-butane binary.	57
Table 4.2	A sample <i>iv</i> file.	60
Table 4.3	Box coordinates.	64
Table 5.1	The format of a script file for the TS program.	72
Table 5.2	Sample geometric-format data file.	85
Table 5.3	Connectivities for triangulating the surface shown in Figure 5.11.	87
Table 5.4	Sample <i>iv</i> file for constructing bubble point surface.	92
Table 5.5	The coordinates of the prism.	93
Table 5.6	Input flash conditions for calculating the three-phase locus for the ternary mixture n-pentane, nitrobenzene, i-butane, T = 398.15 K.	98
Table 5.7	Three-phase compositions for n-pentane, nitrobenzene, i-butane, T = 398.15 K.	98
Table 5.8	CRLI input file format for the n-pentane, nitrobenzene, i-butane ternary.	104
Table 6.1	Coordinates of the vertices of the tetrahedron.	114
Table 6.2	Binary interaction parameters used for the quaternary system.	116
Table 6.3	Coexisting compositions for binary sub-mixtures. T=298.15 K, P=0.5 bar.	119
Table 6.4	Ternary compositions calculated on the lines where $X_D=0$ and $X_A=0$.	123
Table 6.5	Interaction parameters used for the binary pairs.	128

Table 6.6	Coexisting points for binary sub-mixtures at T=333.15 K, P=0.6 bar.	130
Table 6.7	ASPEN PLUS parameter settings for evaluating ternary bubble-point compositions for a specific triangular section.	133
Table 6.8	Ternary bubble-point compositions for the parameters specified in Table 6.7.	133

ACKNOWLEDGMENTS

I would like to express my sincere gratitude to my major Professor, Dr. Kenneth R. Jolls, for patiently guiding and constantly encouraging me through this research. I have always liked to bring hundreds and thousands of lines of words in books to the lively computer visualization world.

I am also grateful to the members of my thesis committee, Professors Hugo Franzen, Glenn Schrader, and Dennis Vigil for their thoughtful attention.

I would further like to thank Professor Dean Ulrichson for his assistance with various ASPEN PLUS problems that I encountered during the work generating phase-equilibrium data points. Finally, Professor Judy Vance and Mr. Perry Miller from the Mechanical Engineering Department of Iowa State provided tremendous help with the use of Open Inventor software.

Financial support from the General Electric Foundation is gratefully acknowledged.

ABSTRACT

This work focused on producing three-dimensional, fluid-phase equilibrium diagrams (vapor-liquid and liquid-liquid) for binary, ternary, and quaternary systems. Although vapor-solid and liquid-solid equilibria occur also, they are not discussed in this project. The ternary and quaternary systems consisted mostly of light hydrocarbon compounds in mixtures at temperatures and pressures below the lowest pure-component critical temperature and pressure in the system. There was no direct chemical reason for choosing the mixtures studied. Rather, their phase diagrams simply fit into distinct and geometrically interesting categories.

The Peng-Robinson equation of state was used through the ASPEN PLUS chemical process simulator to generate meshes of data points. Two kinds of visualization software were used to render those data into graphic displays. The first, MOVIE.BYU, produces static graphics, but it also provides a way for the user to set different viewing positions from the keyboard. Other visualizing attributes, such as wireframe, smooth and flat shading, light-source control, color, and transparency are also available in MOVIE.BYU. More importantly, MOVIE can save these visual settings in a file for later retrieval.

The second, Open Inventor, is a powerful, object-oriented, programming and graphics tool. It has two convenient programs called `ivview` and `SceneViewer` that read `iv`-format data for graphics rendering. Open Inventor provides for interaction between the user and the on-screen graphics. One can rotate, translate,

and enlarge the displays in real time to expose the fine details of the structures being shown.

CHAPTER 1. INTRODUCTION

I will begin by quoting a familiar saying, "Seeing is believing." It is true that visualization can be an important aid in understanding thermodynamics. Instead of reading thousands of lines of words in a textbook and trying to understand what the author is saying, students can find that understanding through graphics and images. It is like embedding an object in the brain – once students understand a concept through the aid of graphics, it usually stays fresh and lasts longer. This is the power of visualization that words often don't have.

Thermodynamicists use phase diagrams to express the effects of temperature, pressure, and composition on the behavior of chemical systems. Almost all substances exist in three states: the solid, liquid, and gaseous states. If two or even three states of a chemical system coexist in a stable manner at a particular temperature and pressure, they are said to be in a state of phase equilibrium, where the chemical potential of each component distributed among those phases is uniform. Said a little differently, there is no net transport of heat, mass, or momentum between the phases.

Because of the ease of construction, two-dimensional phase diagrams are the most widely used graphical tool in textbooks and among scientists. However, 2-D diagrams are limited to showing only the direct relationship between two variables, one dependent and the other independent. Depending upon the number of chemical species in a system and the amount of information needed, the planar

phase diagram may not have the ability to show the effects on phase behavior of the third or an even greater number of variables. For a binary system in vapor-liquid equilibrium, Figure 1.1 shows a planar pressure-composition diagram for the cyclohexanone-cyclohexane binary at a temperature of 500 K. Data for Figure 1.1 were generated using the ASPEN PLUS chemical process simulator. This figure shows the full range of composition (independent variable) and the effective range of pressure (dependent variable). However, it cannot show the continuing effects of temperature on phase equilibrium.

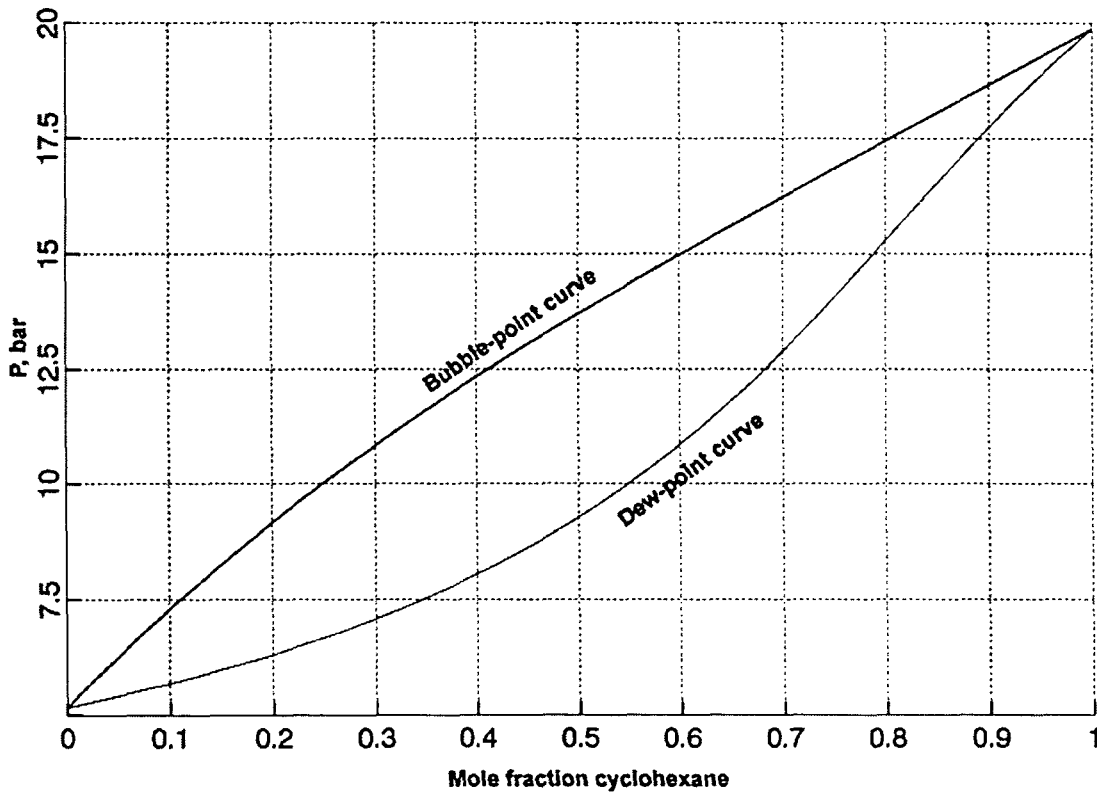


Figure 1.1 Isothermal P-xy diagram for cyclohexane-cyclohexanone, T = 500 K.

In the same manner, a planar T-xy phase diagram, drawn at a constant pressure, shows a full range of composition and an effective range of temperature. It cannot show the continuing effects of pressure on phase equilibrium. Figure 1.2 shows an isobaric T-xy diagram for the same binary mixture at a constant pressure of 10 bar.

In order to show the continuing effects of both temperature and pressure, a sequence of P-xy or T-xy diagrams can be generated, each at a different value of the constant property. Figure 1.3 shows a planar pressure-composition diagram

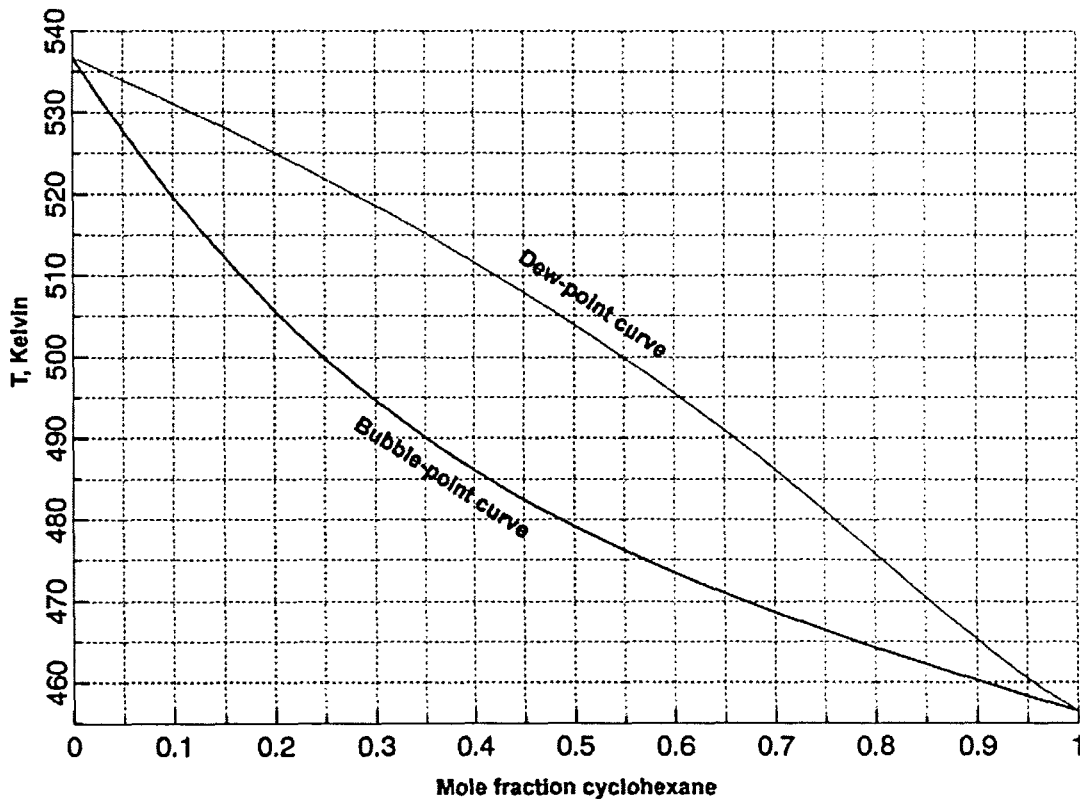


Figure 1.2 Isobaric T-xy diagram for cyclohexane-cyclohexanone, $P = 10$ bar.

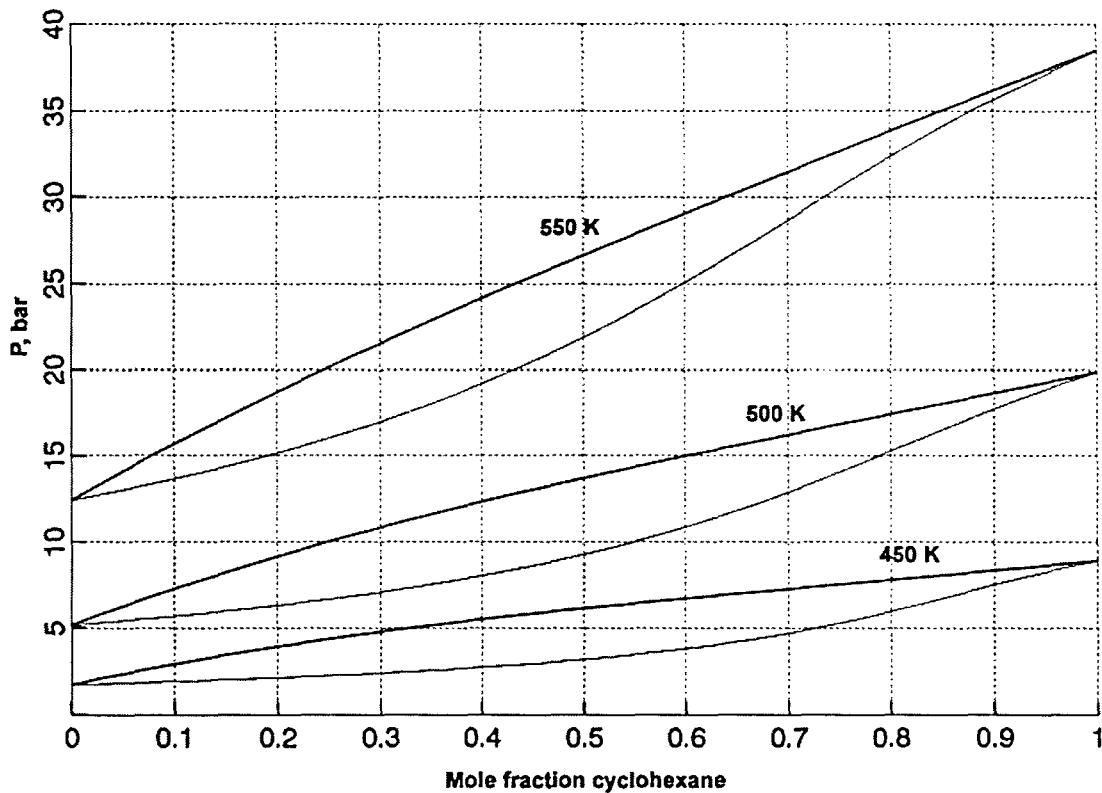


Figure 1.3 P-xy diagram for cyclohexanone-cyclohexane with three constant-temperature curves.

with three constant-temperature curves at 450 K, 500 K, and 550 K for the cyclohexanone-cyclohexane binary.

A series of constant-pressure T-xy curves can be drawn in a similar manner. The problem with drawings such as Figure 1.3 is that the bubble- and dew-point lines will be squeezed together as the range is extended, and the problem of overlapping cannot be avoided when the plots are too close together. An alternate way of making Figure 1.3 would be three separate P-xy diagrams, each at a different temperature. However, that scheme loses the sense of the relative

temperature effect. So no matter what type of planar phase diagram is used, it is always ineffective for presenting the effects of a third or an even greater number of variables on the system.

In 1990, Michael Schmitz [1] developed a method to visualize accurately the effect of a third variable on a binary-mixture phase diagram. He used a high-performance Silicon Graphics workstation to make three-dimensional (spatial) P-T-xy drawings. Physical data points were calculated by using the Peng-Robinson equation of state and were obtained from the ASPEN PLUS chemical process simulator. Composition, pressure, and temperature variables were plotted on the x, y and z axes, respectively, according to the right-hand rule as defined in computer graphics. In his M.S. thesis ([1], Page 61, Fig. 5.7), Schmitz was able to show clearly the continuing effects of temperature on P-xy curves. This approach solved the problems with planar diagrams mentioned earlier. Since constructing three-dimensional phase diagrams involves geometric visualization techniques, sophisticated computer skills as well as thermodynamic knowledge are needed. Few people have these abilities while many others try to avoid such complicated procedures. Other Iowa State graduate students (Gary Willers [2], Jeff Haseman [20], and Dr. Daniel Coy [3]) have also made contributions to this field since 1975.

In the absence of equations of state, the phase behavior of various substances must be studied in the laboratory. Measurements for a single phase diagram can require several days to make. In order to show the effects of added variables (temperature or pressure in the case of binary, fluid-phase systems),

repeated experiments and large amounts of time are required. To make a complete ternary phase diagram, one must deal with an additional chemical substance introduced to the system. As a result, procedures for making phase diagrams experimentally are slow, costly, and tedious.

Following the first equation of state by Van der Waals (1873 [4]), several improved cubic equations were subsequently developed. Among these are the Redlich-Kwong [21], the Soave-Redlich-Kwong [5], and the Peng-Robinson [6] equations. Because of the invention of high-speed digital computing, the prediction of phase behavior using cubic equations of state has become common and standard. Cubic equations provide the ability to calculate smooth and continuous liquid- and vapor-phase properties [19]. With the recent addition of high-performance graphics workstations, generating three-dimensional phase diagrams has now become possible, and this method can play a crucial role in developing an understanding of the phase behavior of mixtures.

James Clerk Maxwell, the famous physicist at Cambridge University in the late 1800s, was the first scientist to construct a three-dimensional thermodynamic property model. After reading Gibbs' papers on predicting thermodynamic behavior from an energy-entropy-volume (USV) surface, Maxwell spent an entire winter in his laboratory making a model of Gibbs' USV surface for water. Recently, with the aid of computer graphics technology and visualization skills, Iowa State University graduate student Daniel Coy was able to produce such a USV surface on a computer screen. At the same time, he was able to apply similar techniques to

more complicated binary and ternary mixtures. For those who have difficulty analyzing and understanding thermodynamic models from the mathematics alone, Dr. Coy has provided an alternate but powerful way to acquire that understanding.

The objective of this project has been to extend the work performed by Michael Schmitz and Daniel Coy and to visualize vapor-liquid and liquid-liquid equilibria for ternary systems and vapor-liquid equilibria for a quaternary system. Fluid-phase thermodynamic properties are calculated by ASPEN PLUS using the Peng-Robinson equation of state. Data points are constructed in formats appropriate for displaying geometrical structures through MOVIE.BYU and Open Inventor graphics software. This has been one of the first attempts to apply interactive graphics to complex multicomponent phase diagrams. With the aid of these powerful features, viewers can rotate and translate the displays and visualize the detailed structure of the drawings. Viewers can also zoom in to specific points on the diagrams. These features provide a more flexible way to visualize thermodynamic properties than through static graphics displays. To achieve the same effect as with interactive graphics, one must construct many static images showing different viewpoints. We are hopeful that the ideas proposed in this thesis will lead to new thinking about thermodynamic property relationships.

CHAPTER 2. GEOMETRIC REPRESENTATION OF PHASE DIAGRAMS

Depending on the number of species present, the conditions of phase equilibrium are defined by the temperature, pressure, and composition of a system. Phase equilibrium occurs when two states of aggregation, e.g., vapor-liquid or liquid-liquid, coexist at the same temperature and pressure, and uniformity of all chemical potentials. In a graphical representation, two coexisting phases can be connected by a tie line to denote the equilibrium states. There are an infinite number of tie lines that can be drawn to connect the coexisting phases of most systems. The continued connection of such phases forms a smooth envelope. Inside the envelope the phases mix together. In equilibrium, they split to form two coexisting phases according to the tie line that represents the bulk properties of the mixture.

The graphical representation of these phases is called a phase-equilibrium diagram. There are several ways to draw such a diagram, depending on the number of components present in the system. The greater the number of components, the more complicated geometrically is the diagram, since more variables affect the phase behavior.

Unary systems

In a unary system there is only a pure substance, and thus volume, temperature, and pressure become the variables that indicate whether the

substance is in the solid, liquid, or vapor state. According to the Gibbs phase rule for a non-reacting, system,

$$F = C - P + 2 \quad (2.1)$$

where,

F: number of degrees of freedom

C: number of components

P: number of phases

For a unary system in vapor-liquid equilibrium, there exists one degree of freedom, which means that there is only one independent intensive variable that can be fixed to find the dependent variables of the system. These then provide sufficient information to define the equilibrium state. In this case, either temperature or pressure can vary independently in the system while the remaining variables are dependent. The phase diagram of a unary system can be plotted as pressure versus temperature in the two-dimensional form shown in Figure 2.1.

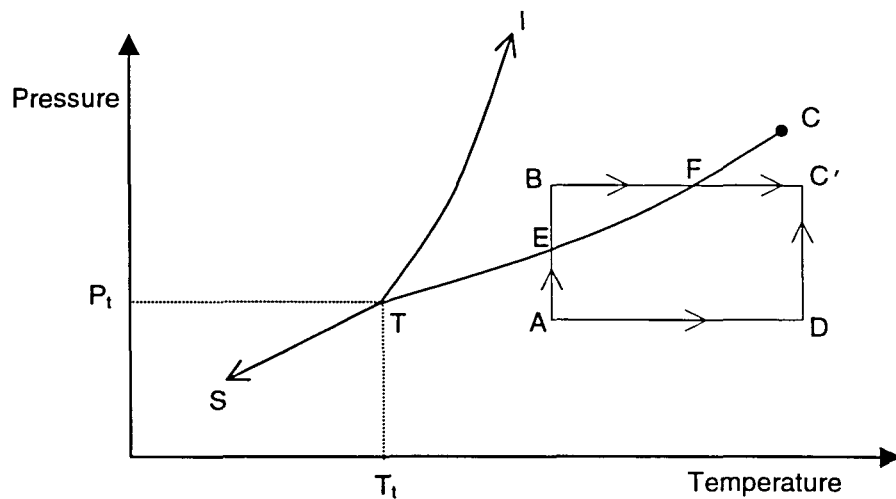


Figure 2.1 Pressure-temperature diagram for a pure substance that contracts on freezing.

The line TS represents the vapor-solid or sublimation curve. To the left and above the vapor-solid curve, the substance exists in the solid state, and to the right and below the substance exists in the vapor state. This process of phase change is called sublimation. Both vapor and solid coexist on the TS curve in the equilibrium state. TI represents the liquid-solid or fusion curve. To the left of the liquid-solid curve, as before, the substance exists in the solid state, and to the right it exists in the liquid state. This process of phase change is called fusion. Both liquid and solid coexist on the TI curve.

TC is the common vapor-liquid or vaporization curve. To the left and above the vapor-liquid curve exists the liquid state, and to the right and below the vapor state. This process of phase change is known as vaporization, and in the equilibrium state both vapor and liquid phases coexist on the TC curve. At the temperature T_t and pressure P_t , all three phases coexist at the condition called the triple point. Point C is the critical state of the substance. If either the temperature or the pressure is above its critical value T_c or P_c , the substance is called a dense fluid of indistinguishable liquid or vapor phase (sometimes called supercritical).

Phase diagrams are important for many chemical processes as they show the route to achieve certain changes of state. As shown in Figure 2.1, there are different routes to get the substance from vapor state A to vapor state C'. Route ABC' passes through phase changes accomplished by condensation and vaporization before it gets to the final state C'. It begins by compressing vapor state A isothermally. The substance undergoes a phase change at point E on the

TC curve, then enters the liquid state, and finally moves to point B. Then it is heated isobarically and undergoes another phase change at point F on the TC curve to return to the vapor phase before arriving at the final state C'. Route ADC', on the other hand, does not go through a phase-change process. Starting at liquid state A, the substance is heated isobarically to point D and then it is compressed isothermally to the final state C'.

The planar plot is restricted to show only the phase-change pressure of a substance at a certain temperature. A question arises when one asks about the volumes of the coexisting liquid and vapor states. Two-dimensional diagrams do not show the effects of the third variable very well – volume in this case. But the three-dimensional PVT diagram provides the extra dimension to show the relationship of volume within the overall phase behavior. Figure 2.2 shows a PVT diagram generated by Gary Willers in his 1978 M.S. Thesis at Iowa State University [2].

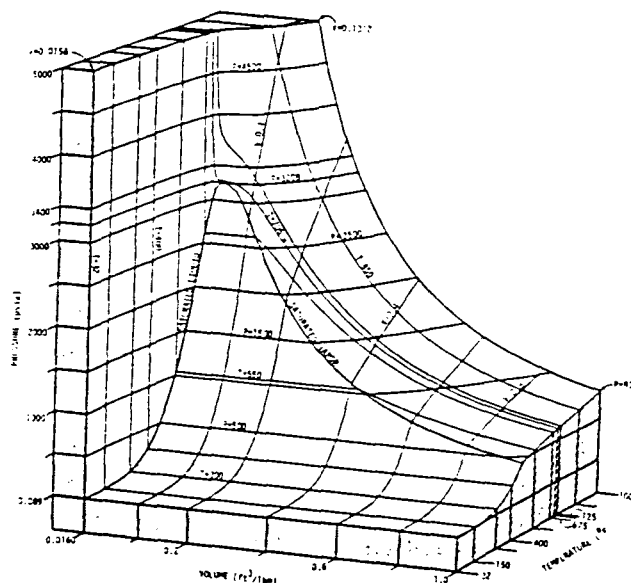


Figure 2.2 Three-dimensional PVT diagram [2, page 96]

Binary systems

Systems of two components have a composition variable that increases the number of degrees of freedom. The composition variable may be expressed as a mole fraction so that the sum of the fractions equals one ($x_A + x_B = 1$). The expression of composition in mole fraction is important since it lowers the overall dimensionality of the system. Hence, a dependent variable in a binary system of two phases is a function of two other independent variables. Either temperature or pressure can be the dependent variable while the independent variables might be pressure or temperature and the mole fraction of one component.

Thus,

$$P = f(T, x_A) = f(T, 1 - x_B) \quad (2.2)$$

or,

$$T = f(P, x_A) = f(P, 1 - x_B) \quad (2.3)$$

If the system is specified extensively and relative molar flow rates (eg., F_A) are used to define composition (in a chemical process situation), the dependent variable (T or P) will be a function of three variables (P or T, F_A , and F_B). This raises the problem to a higher dimension and increases the difficulty in solving the system of equations.

In most cases two-dimensional binary diagrams are plotted as pressure versus mole fraction (P-xy) or temperature versus mole fraction (T-xy). Although pressure versus temperature (P-T) diagrams are also possible, they are not often used. Figure 2.3 shows a simple binary P-xy phase diagram plotted at a fixed temperature.

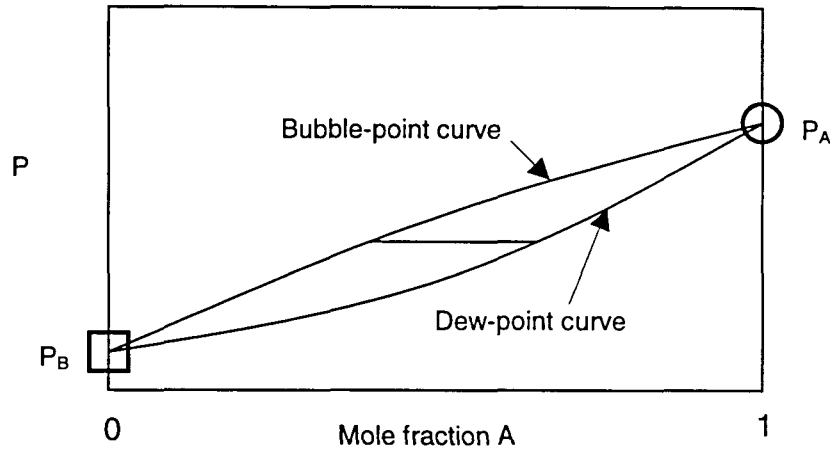


Figure 2.3 Isothermal P-xy diagram for the AB binary.

The region above the bubble-point curve (the saturated liquid curve) is the subcooled-liquid state, and the region below the dew-point curve (saturated vapor) is the superheated-vapor state. In between, vapor and liquid are mixed together. They coexist in equilibrium according to tie lines drawn at a constant pressure. In Figure 2.4 the circled point on the pure-A pressure-temperature curve is the vapor pressure of component A at temperature T_1 . In Figure 2.5, the point surrounded by

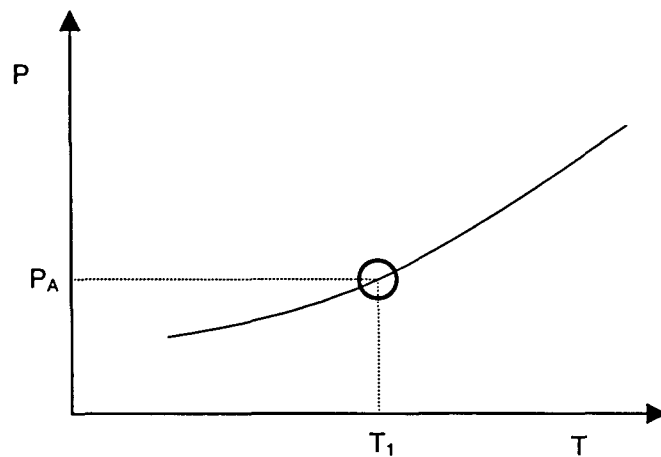


Figure 2.4 Pressure-temperature diagram for component A.

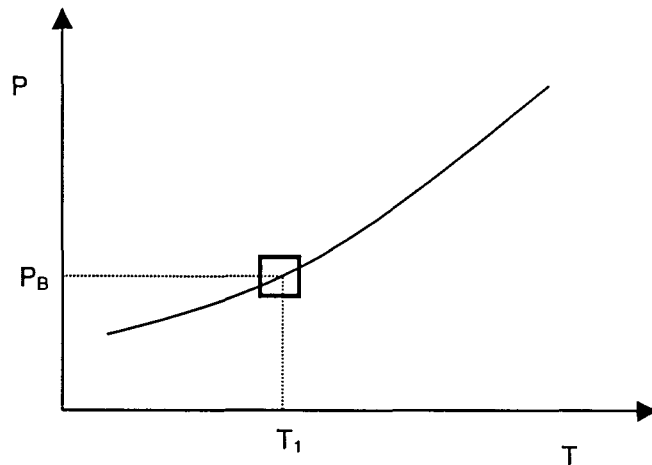


Figure 2.5 Pressure-temperature diagram for component B.

the square on the pure-B pressure-temperature curve is the vapor pressure of component B at temperature T_1 .

These two points (P_A and P_B) are located on the P-xy diagram in Figure 2.3 before the complete bubble-point and dew-point curves are drawn. The shapes of the bubble-point and dew-point curves are not easily predictable and depend wholly on the natural characteristics and non-ideality of the mixture. The curves can be obtained by experiment or by computation via an equation of state using appropriate mixing rules with a binary interaction parameter. An alternate computational method uses activity coefficients.

It is important to show the effect of temperature on the P-xy phase diagram. In other words, how do these bubble-point and dew-point curves change with temperature. One way to do this would be to make several constant-temperature bubble-point and dew-point curves on the same P-xy diagram. Figure 1.3 showed an example of such a plot. However, this could cause confusion when the

temperature difference is small and adjacent bubble-point and dew-point curves overlap one another. One other way is by making separate P-xy phase diagrams for different temperatures. But the best solution for showing the continuing effect of temperature is to make a spatial, three-dimensional P-T-xy diagram as shown in Figure 2.6

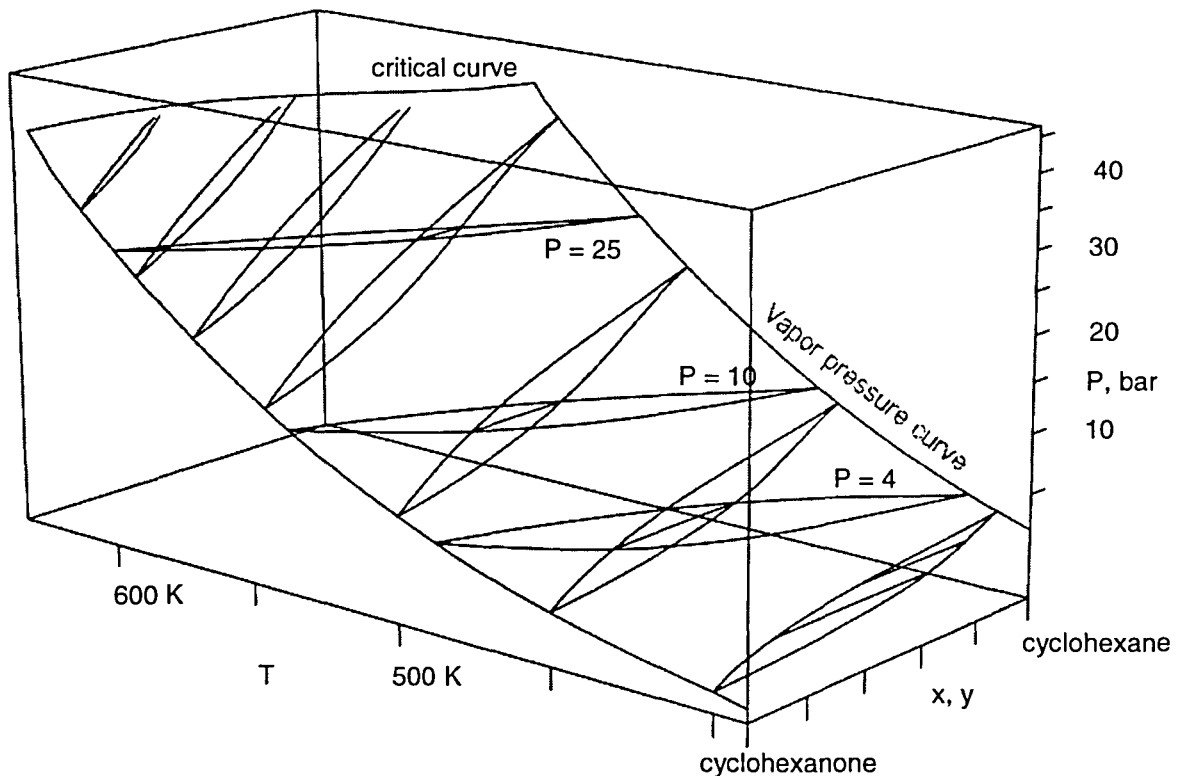


Figure 2.6 P-T-xy diagram for cyclohexane(A)-cyclohexanone(B).

The coordinates are drawn according to the left-hand rule. The composition variable in mole fraction is plotted positively toward the right on the x-axis. The far end of the axis represents pure component A (cyclohexane), and the near end of the axis represents pure component B. At any point in the middle of the axis, the

two mole fractions sum to one. Pressure is plotted positively upward on the y-axis, and temperature is plotted positively into the paper (right to left) on the z-axis.

Ternary systems

Most textbooks are limited to considering binary phase diagrams because of the graphical complexity of ternary and higher-order drawings. Again, according to the Gibbs phase rule there are three degrees of freedom in a ternary system with two phases. This implies a four-dimensional problem with one dependent variable (either temperature or pressure) given as a function of three independent variables, two compositions and pressure or temperature.

$$P = f(T, x_A, x_B) \quad (2.4)$$

or

$$T = f(P, x_A, x_B) \quad (2.5)$$

Dealing with a four dimensional problem is not difficult computationally, but when it comes to representing four-dimensional data graphically (since we live in a three-dimensional world), certain visualization and solving techniques are required to cope with the problem. That is why many people fail to understand ternary or higher-order phase diagrams. A three-dimensional ternary diagram is incapable of showing the continuing effects of all variables on the system. The extra independent variable must be fixed at a certain value in order to create a three-dimensional figure for plotting. Only with this approach can a three-dimensional phase diagram show the continuing effects of two independent variables on ternary

phase behavior. Thus, either temperature or pressure is chosen as the fixed variable.

$$P = f(x_A, x_B)_T \quad (2.6)$$

$$T = f(x_A, x_B)_P \quad (2.7)$$

Before moving to three-dimensional ternary diagrams, consider the simpler case of a two-dimensional plot. As shown in Figure 2.7, the composition of a ternary mixture can be represented on an equilateral triangle having unit sides. The components A, B, and C are located at the vertices of the triangle.

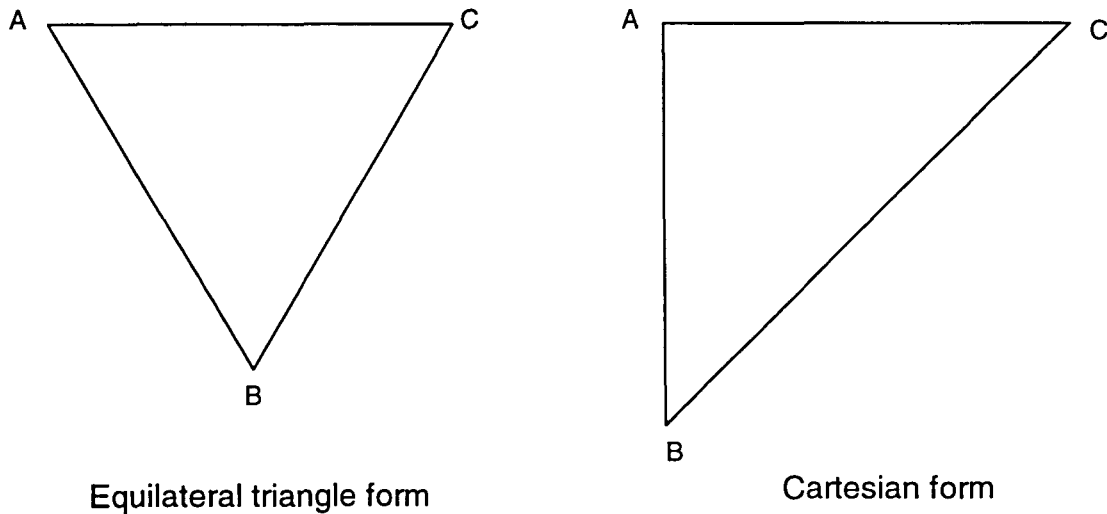


Figure 2.7 Triangular plots for representing the compositions of ternary mixtures.

Point A on each triangle represents pure component A. The contours of constant-A composition are lines parallel to line BC, where the mole fraction of component A equals zero. The composition then increases toward point A where the mole fraction of A equals one. In a similar manner, points B and C represent those pure components. On line AC the mole fraction of component B equals zero, which then increases toward point B where its value becomes one. The equilateral triangle has the property that the summation of the perpendicular distances from each side (AB, BC, AC) to any fixed point in the triangle equals the altitude, which can be thought of as a constant equal to one. Therefore, for any fixed point in the triangle the mole fractions of components A, B, and C always sum to one. On the other hand, to define a point in the triangle, two of the composition variables must be specified. The composition of the third component can then be found by difference, $X_C = 1 - X_A - X_B$.

Recall that a two-phase ternary system requires a four-dimensional display, with three independent variables [pressure (or temperature), and two compositions] and one dependent variable [temperature (or pressure)]. Figure 2.8 shows a planar ternary phase diagram drawn at a fixed temperature *and* pressure. Once these variables are fixed, only one of the remaining composition variables is independent. Now the system becomes a pseudo two-dimensional problem and can be represented by a two-dimensional drawing.

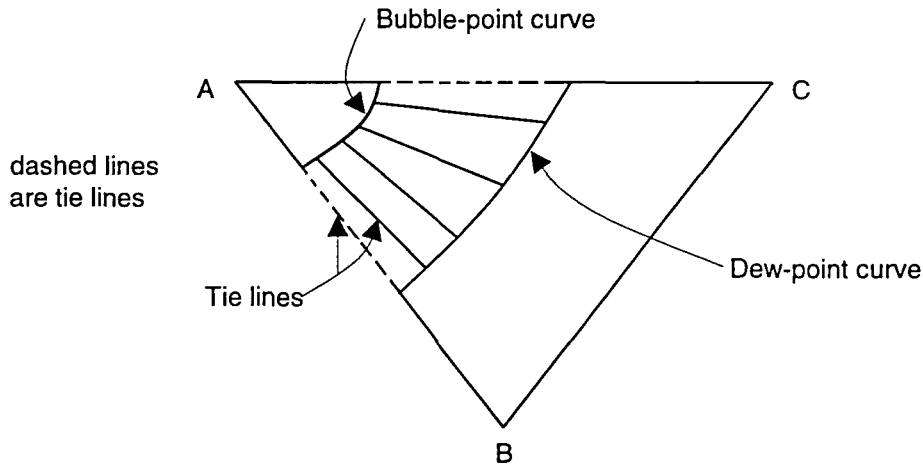


Figure 2.8 Two-dimensional diagram representing VLE in a ternary system at a fixed temperature and pressure. Component A is the least volatile.

For two-phases in equilibrium:

$$X_A = f(X_B)_{T,P} \quad (2.8)$$

$$X_C = 1 - X_A - X_B \quad (2.9)$$

The vapor and liquid states coexist in phase equilibrium at the given temperature and pressure. The composition in the saturated liquid phase is represented by a bubble-point curve. Along the bubble-point curve there are infinitely many compositions that coexist with the saturated vapor-phase compositions on the dew-point curve. Such pairs are connected by tie lines. Any composition that lies inside the two-phase region will split according to a particular tie line to form coexisting liquid and vapor states, located separately on the bubble- and dew-point curves. The shapes of these curves depend on the chosen

temperature and pressure and also on the natural characteristics (non-ideality) of the components and of the mixture. The ternary diagram shown in Figure 2.8 has relatively simple bubble- and dew-point curves because the system consists of three non-azeotropic binaries, A-B, A-C, and B-C, each of whose three-dimensional PT-xy diagram is similar to Figure 2.6. The information on the binary diagrams can be used to predict roughly the shape of the bubble- and dew-point curves on the ternary diagram. Figure 2.9 shows the P-xy diagrams for the A-B, A-C and B-C binaries at a fixed temperature T_1 . If the pressure is chosen to be above the vapor pressure of components A and B but below the vapor pressure of C, the bubble- and dew-point curves in the ternary diagram will connect the A-C and B-C binaries, as shown in Figure 2.10.

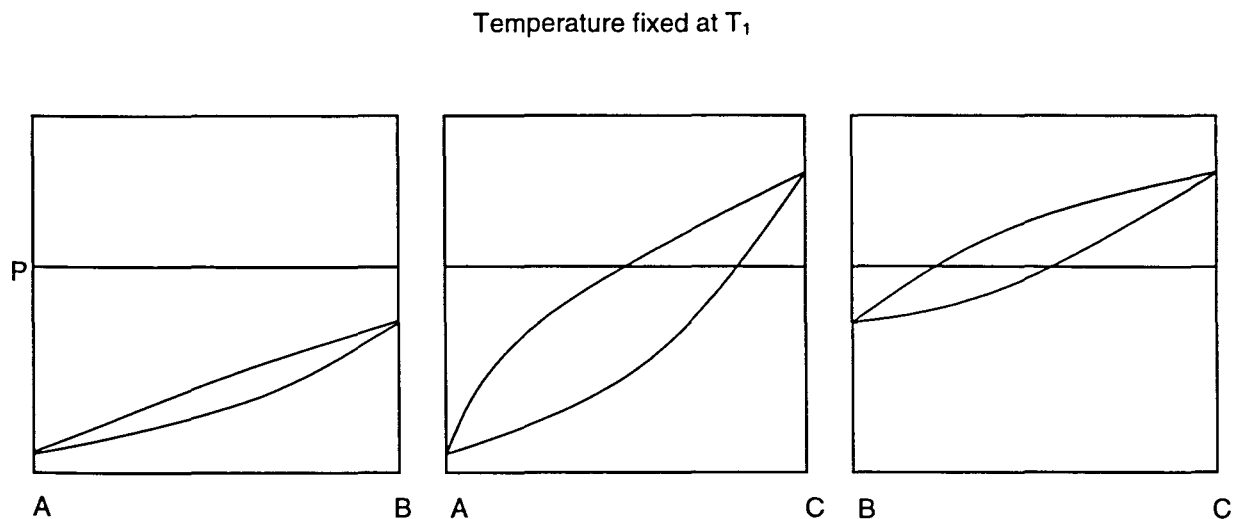


Figure 2.9 Isothermal P-xy diagrams for the A-B, A-C, and B-C binaries.

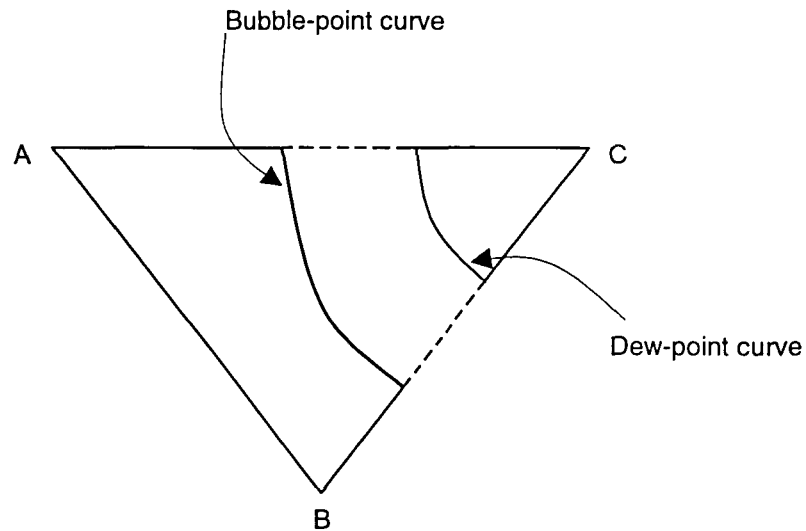


Figure 2.10 Planar diagram for the A-B-C ternary consistent with Figure 2.9.

Quaternary systems

A system consisting of four components is known as a quaternary. Constructing a ternary phase diagram is complicated. Introducing a fourth component to a ternary system increases the number of variables by one and creates an even more difficult, five-dimensional problem, with a total of three composition variables, pressure, and temperature for a two-phase system. Depending on which variable is chosen to be dependent, there are three basic ways that the dependent variable can be determined as a function of the four independent variables: the pressure can be expressed as a function of temperature and three composition variables as shown in equation (2.8); equation (2.9) shows temperature expressed as a function of pressure and three compositions; one of the composition

variables can be determined by fixing the temperature, pressure, and two other compositions as shown in equation (2.10).

$$P = f(T, x_A, x_B, x_C) \quad (2.8)$$

$$T = f(P, x_A, x_B, x_C) \quad (2.9)$$

$$x_A = f(T, P, x_B, x_C) \quad (2.10)$$

In this work the computation and construction of quaternary diagrams was based on the last of these methods. The detailed description is presented in CHAPTER 6 where the construction of quaternary diagrams is discussed. Quaternary systems are rarely shown in planar form. This is because the internal details cannot be represented in two dimensions. Three-dimensional space is required for displaying three independent composition variables. However, if it is necessary to display quaternary properties in two-dimensional form, there is one technique that can be used. Recall that quaternary, two-phase data are five-dimensional. Thus, three variables must be fixed to permit a two-dimensional plot. If temperature, pressure, and one composition variable (say X_D) are fixed, the remaining composition variables X_A , X_B and X_C can be considered to form a pseudo-ternary system and can be represented by a triangular section with a composition variable plotted along each side. Such a diagram is shown in Figure 2.11, and since the composition X_D has been fixed at a constant value, the remaining three variables are plotted from zero to the difference $1-X_D$.

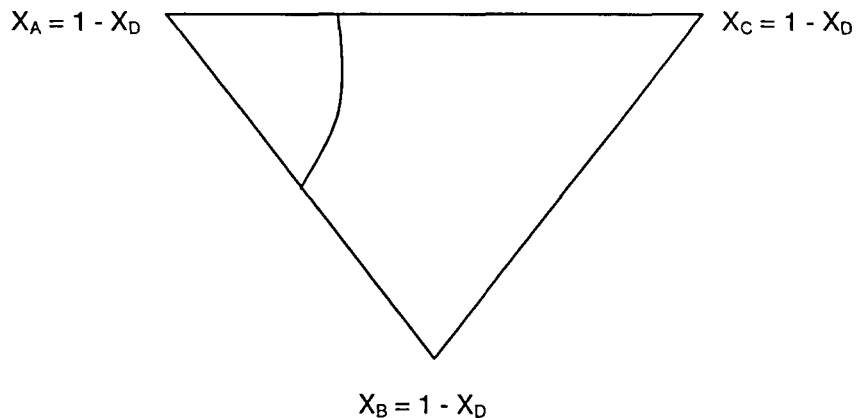


Figure 2.11 Planar representation of a quaternary system for fixed X_D .

Composition information can be read only from the curve in Figure 2.11 – which might represent all bubble-point states at a fixed temperature and pressure that have X_D equal to a constant. The disadvantage of constructing a constant-composition quaternary diagram is that it is not possible to draw tie lines that show coexisting liquid and vapor phases on the same plot. In general, the quaternary system diagram is represented by the equilateral tetrahedron shown in Figure 2.12. Such diagrams require both temperature and pressure to be fixed in order to permit a three-dimensional display of phase-equilibrium data.

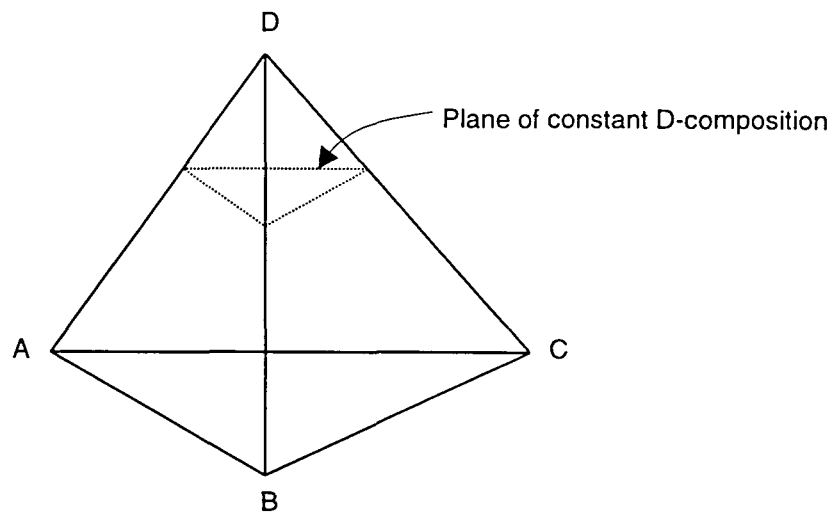


Figure 2.13 Constant-composition plane lying parallel to the triangular base ABC.

phase diagram of one ternary system from among the four components, drawn at the fixed temperature and pressure. The equilateral tetrahedron has the property that the sum of the perpendicular distances from any point inside the tetrahedron to the four triangular faces is equal to a constant¹. If the point is located on one of the triangular faces, say the BCD triangle, then the perpendicular distance from the point to the triangle BCD is zero. However, the summation of the perpendicular distances from lines BC, CD and BD to such a point is still equal to one.

Each point in the tetrahedron represents a possible composition of a quaternary system at the fixed temperature and pressure of the diagram. The smooth and continuous connection of all saturated liquid states forms the bubble-point surface and of all saturated vapor states forms the dew-point surface.

¹ This constant is the altitude of the tetrahedron.

Coexisting points on the bubble- and dew-point surfaces can be connected by tie lines. Any bulk composition that lies between the bubble- and dew-point surfaces will split to form coexisting liquid and vapor phases according to the tie line through that composition.

Due to its high dimensionality, a quaternary phase diagram is more complicated to construct than a diagram for a ternary. To get an idea of the basic construction, a step-by-step procedure, starting from studying the binary and ternary components, has to be followed. A simple quaternary system is chosen such that there is neither azeotropic behavior nor liquid immiscibility among the four components. They are arranged in such a way the component A has the least volatility and, therefore, the lowest vapor pressure among the others at a fixed temperature. Component D has the greatest volatility and, therefore, the highest vapor pressure at a fixed temperature. Components B and C are intermediate in ascending order.

Recall that for a simple quaternary system there is no azeotropic behavior among the components. The temperature is fixed at T_1 and the pressure is fixed at P_1 , which is above the vapor pressure of B but below the vapor pressure of C at that temperature. There are six possible binary systems among the four components, which leads to the six binary P-xy diagrams shown in Figure 2.14. By translating this information to the unit-length tetrahedron, the outline structure of the quaternary phase diagram can be observed as in Figure 2.15, with the bubble- and dew-point surfaces implied by the binary data.

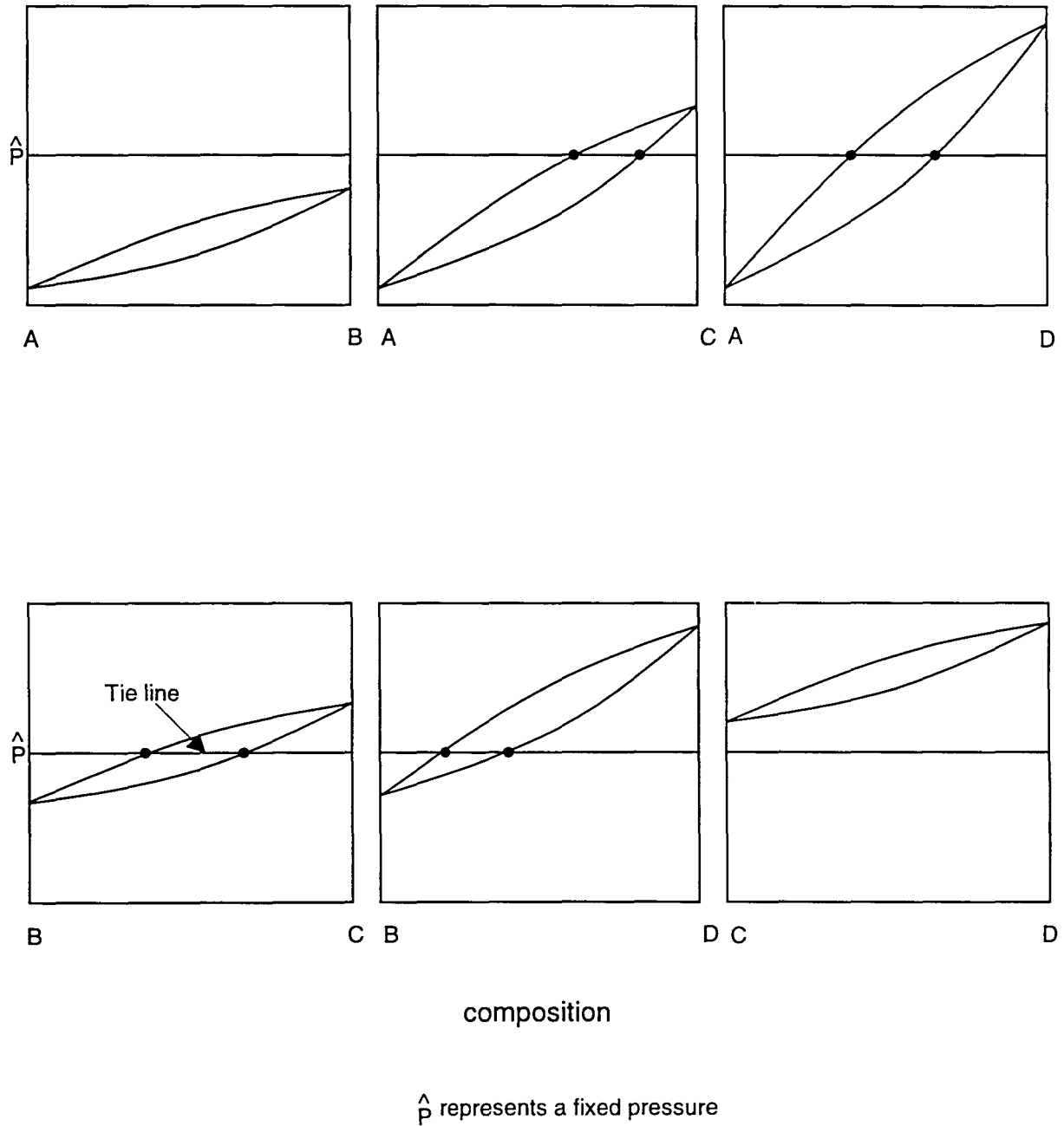


Figure 2.14 P-xy diagrams for the six binary sub-systems at temperature T_1 .

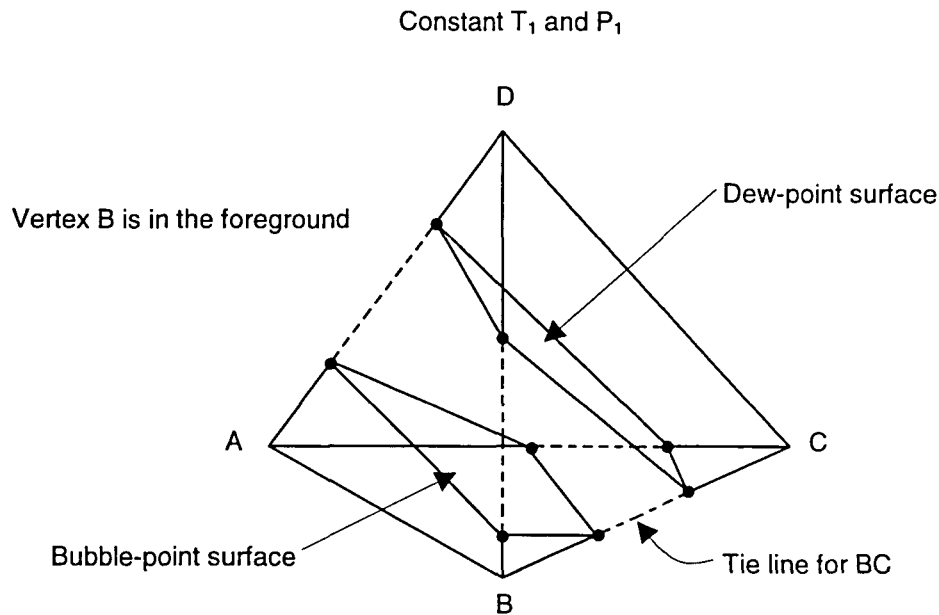


Figure 2.15 Outline structure of the quaternary diagram obtained from the binaries in Figure 2.14.

Quinary system

A Quinary system consists of five components. In addition to the temperature and pressure, there are four other free composition variables in the system. Therefore, with two phases present it is a complicated six-dimensional display problem. To determine the properties of the system in phase equilibrium, five independent variables must be defined. For example, bubble-point pressure can be shown as a function of temperature and four other composition variables. Conversely, dew-point temperature can be expressed as a function of pressure and four compositions. In addition, one of the composition variables can be expressed as a function of temperature, pressure, and three compositions. These three cases are shown by the following equations.

For two phases in equilibrium:

$$P = f(T, X_A, X_B, X_C, X_D) \quad (2.11)$$

$$T = f(P, X_A, X_B, X_C, X_D) \quad (2.12)$$

$$X_D = f(T, P, X_A, X_B, X_C) \quad (2.13)$$

In the quaternary system, the three independent composition variables used up the coordinates available in three-dimensional space. Now, in a quinary system, there is no method to display four independent composition variables in three-dimensional space. As a result, the complete quinary phase diagram can not be created. However, by fixing three of the system variables - temperature, pressure and one of the compositions (say X_E) - quinary phase behavior can be represented in a limited way by a tetrahedron having each of its four composition variables plotted from zero to the difference $1-X_E$. As in the quaternary case, either the bubble-point or dew-point surface can be shown, but not both.

With high-speed computation and animation programming, the continuous effect of the component-E mole fraction on this type of diagram could be shown through real-time motion. As was discussed for the quaternary system, the disadvantage of such a plot is that the bubble-point and dew-point surfaces cannot be shown simultaneously. This loses the real value of a phase-equilibrium diagram. Therefore, this project excluded quinary diagrams as well as constant-composition diagrams of any order and emphasized three-dimensional construction procedures for binary, ternary, and quaternary systems.

CHAPTER 3. THEORIES AND APPLICATIONS

Equations of state

Before the popularization of equations of state, scientists and engineers had to go to the laboratory to do experimental work to obtain phase-equilibrium information. Such work was slow and it always took a long time to collect data. In addition, they often had to deal with dangerous chemicals during the experiments.

With the evolution from the Van der Waals equation of state [4] to the later, more sophisticated, cubic equations such as the Soave-Redlich-Kwong and the Peng-Robinson [5,6], the prediction of fluid-phase behavior via digital computation has become easy and convenient. However, none of these equations can predict the phase behavior of a mixture precisely. Mixture rules and binary interaction parameters for a given equation must be chosen so as to obtain the best fit possible to the behavior of each multicomponent system [18].

In this project, the Peng-Robinson equation was used to predict the fluid-phase behavior for binary, ternary, and quaternary systems. The Peng-Robinson equation produces fairly accurate results for nonpolar and mildly polar hydrocarbon mixtures. Some of the binary interaction parameters for light hydrocarbons can be retrieved from the data bank of the ASPEN PLUS chemical process simulator. If ASPEN PLUS does not have an interaction parameter for a specific binary pair, it can be determined by finding the value which gives the best match to phase-

equilibrium data. The DECHEMA chemistry data series [7] provided those data in this research.

Most mixture equations of state are expressed in such a way that the pressure of the system is an explicit function of the temperature, volume, and composition.

$$P = f(T, \underline{V}, N_1, N_2, \dots, N_n) \quad (3.1)$$

where \underline{V} is the *total* volume of the system. For a mixture of n components, the Peng-Robinson equation has the form,

$$P = \frac{NRT}{\underline{V} - Nb_m} - \frac{N^2 a_m}{\underline{V}(\underline{V} + Nb_m) + Nb_m(\underline{V} - Nb_m)} \quad (3.2)$$

where,

$$a_m = \sum_{i=1}^n \sum_{j=1}^n N_i N_j a_{ij}$$

$$b_m = \sum_{i=1}^n N_i b_i$$

$$a_{ij} = (1 - \xi_{ij}) \sqrt{a_i a_j} \quad (i \neq j)$$

$$\xi_{ii} = 0 \quad (i = j)$$

$$a_{ii} = a_i$$

$$a_i = \left(\frac{0.45724 R^2 T_{ci}^2}{P_{ci}} \right) \left(1 + \kappa_i \left(1 - \sqrt{\frac{T}{T_{ci}}} \right) \right)^2$$

$$\kappa_i = 0.37464 + 1.54226 \omega_i - 0.26992 \omega_i^2$$

$$b_i = \frac{0.07780 R T_{ci}}{P_{ci}}$$

Note that T_{ci} , P_{ci} , ω_i , and N_i are the critical temperature, critical pressure, acentric factor, and the number of moles of component i in the mixture. The value of the binary interaction parameter ξ_{ij} gives an empirical measure of the interaction between components i and j . In other words, it accounts for the dissimilarity between components i and j . The closer the physical properties of the two components, the smaller the binary interaction parameter ξ_{ij} . Moreover, it is assumed that the binary parameter is independent of system temperature, pressure, and composition. Studies have shown that binary interaction parameters are often in the vicinity of 0.1, but the final result of the phase-behavior prediction from the Peng-Robinson equation is very sensitive to the exact value chosen.

The ASPEN PLUS chemical process simulator has many built-in equations of state for thermodynamic property evaluation. They are listed on the `Properties.Main` form, which is obtained from the ASPEN PLUS `Form` pull-down menu, and then from the `Properties` and `Main` sub-menu. A new window will open named `Properties.Main` on the title bar. To select the Peng-Robinson equation for the calculation, use the right mouse button to click on the space beside `Opsetname` to list all of the equations available; then select `PENG-ROB` for Peng-Robinson. In order to get the best phase-equilibrium result, a binary interaction parameter must be specified for each pair of components in the system. ASPEN PLUS stores a large number of interaction parameters in its data bank. Choosing the Peng-Robinson equation automatically retrieves the correct interaction

parameter from the data bank named EOS-LIT¹ and displays it on the Binary.Scalar form for the two components specified. The Binary.Scalar form is obtained from the Form pull-down menu, then from the Properties, Parameter, and Binary sub-menu. When a form manager appears, click to choose PRKIJ-1 Scalar to get the binary interaction parameter entry form for the Peng-Robinson equation. If it is necessary to replace the built-in interaction parameter for a particular binary mixture, remove the data bank EOS-LIT from the Data Bank field on the Binary.Scalar form and enter a new value in the space where the retrieved value was deleted. If the EOS-LIT data bank does not contain an interaction parameter for a given mixture, one can be entered manually from the keyboard.

Phase equilibrium

Phase equilibrium in fluid systems is both common and important in industrial processes such as absorption, distillation, and extraction. Equilibrium between coexisting phases can occur in solid-vapor, solid-liquid, liquid-liquid, and vapor-liquid systems. Among these, liquid-liquid, and vapor-liquid coexisting phases are more frequently observed in chemical industrial processes. Therefore, they are more often studied than solid-vapor and solid-liquid coexisting phases. This project

¹ The EOS-LIT binary data bank stores binary interaction parameters recorded by D. Behrens,, and R. Eckermann, eds: *Vapor-Liquid Equilibria for Mixtures of Low Boiling Substances*, DECHEMA Chemistry Data Series, Volume VI, 1977- and Watanasiri et al., *AICHE J*, 28, 638, 1982. [11].

emphasized exclusively the analysis and construction of phase diagrams for liquid-liquid and vapor-liquid systems.

Vapor-liquid equilibrium

If two phases of a system of n components having different properties (e.g., different temperatures, pressures, and compositions) are brought together in an isolated system, the driving forces between the phases will bring the system into an equilibrium state through internal heat, momentum, and mass transfer. If both phases persist, they will ultimately coexist at equilibrium in the system such that there is no additional net transport. In so doing, the total entropy of the isolated system will reach a maximum. The total entropy change $\delta\underline{S}$, equals the entropy change in the liquid phase ($\delta\underline{S}^l$) plus the entropy change in the vapor phase ($\delta\underline{S}^v$) ([8], Page 128).

For a small perturbation from equilibrium,

$$\begin{aligned}\delta\underline{S} &= \delta\underline{S}^l + \delta\underline{S}^v = 0 \\ &= \frac{1}{T^l} \delta\underline{U}^l + \frac{1}{T^v} \delta\underline{U}^v + \frac{P^l}{T^l} \delta\underline{V}^l + \frac{P^v}{T^v} \delta\underline{V}^v - \sum_{i=1}^n \left(\frac{\mu_i^l}{T^l} \right) \delta N_i^l - \sum_{i=1}^n \left(\frac{\mu_i^v}{T^v} \right) \delta N_i^v\end{aligned}\quad (3.3)$$

The total internal energy change ($\delta\underline{U}$), the total volume change ($\delta\underline{V}$), and the total material change (δN) of the isolated system are also equal to zero.

$$\delta \underline{U} = \delta \underline{U}^l + \delta \underline{U}^v = 0 \quad (3.4)$$

$$\delta \underline{V} = \delta \underline{V}^l + \delta \underline{V}^v = 0 \quad (3.5)$$

$$\delta \underline{N} = \delta \underline{N}^l + \delta \underline{N}^v = 0 \quad (3.6)$$

By substituting equations (3.4), (3.5), and (3.6) into equation (3.3), it can be simplified as,

$$\delta \underline{S} = \left(\frac{1}{T^l} - \frac{1}{T^v} \right) \delta \underline{U}^l + \left(\frac{P^l}{T^l} - \frac{P^v}{T^v} \right) \delta \underline{V}^l - \sum_{i=1}^n \left(\frac{\mu_i^l}{T^l} - \frac{\mu_i^v}{T^v} \right) \delta N_i^l = 0 \quad (3.7)$$

Since the variations $\delta \underline{U}^l$, $\delta \underline{V}^l$, and δN_i^l are independent, the following conditions must be satisfied in order to achieve the equilibrium criterion $\delta \underline{S} = 0$,

$$T^l = T^v \quad (3.8)$$

$$P^l = P^v \quad (3.9)$$

$$\mu_i^l = \mu_i^v \quad (i = 1, 2, \dots, n) \quad (3.10)$$

Temperature uniformity accounts for thermal equilibrium in the system. Two contacting phases of equal temperature guarantee that there is no net energy transfer between the phases. Pressure accounts for mechanical equilibrium. When the liquid and vapor phases coexist at the same pressure, the system is in a stationary state. Finally, uniform chemical potentials account for material equilibrium. When each component has the same chemical potential in the two

contiguous phases, there is no net mass transfer taking place. These three conditions must be met in order for a system of two (or multiple) phases to reach a state of stable equilibrium.

To determine whether a system is at equilibrium, a thermometer and a barometer could be used to measure the numerical values of temperature and pressure. However, unlike temperature and pressure, there is no such instrument that can be used to measure chemical potential. A numerical value assigned to the chemical potential has no real physical meaning unless it is referred to a reference state. To derive this relationship for a pure component, the chemical potential can be expressed in terms of temperature and pressure as follows,

$$Nd\mu = -\underline{S}dT + \underline{V}dP \quad (3.11)$$

where \underline{S} and \underline{V} represent the total entropy and volume of the component. To express the chemical potential at a specific temperature and pressure $\mu(T,P)$ in relation to the chemical potential in a reference state at a given reference temperature and pressure $\mu(T_o, P_o)$, integrate equation (3.11) from the reference conditions to the final conditions,

$$\int_{\mu(T_o, P_o)}^{\mu(T, P)} d\mu = \int_{T_o}^T -S(T, P_o) dT + \int_{P_o}^P V(T, P) dP \quad (3.12)$$

$$\Rightarrow \mu(T, P) = \mu(T_o, P_o) - \int_{T_o}^T S(T, P_o) dT + \int_{P_o}^P V(T, P) dP \quad (3.13)$$

Expressing phase equilibrium through equality of chemical potential involves quantities (arbitrary constants) that are not physically real. To avoid this, a function called the fugacity (f) is introduced as a substitute for chemical potential.

Fugacity is a quantity that has the same units as pressure. Under ideal-gas conditions, the fugacity of a pure component is equal to its pressure. In a similar manner, the fugacity of a component in an ideal-gas mixture is equal to its partial pressure. At higher pressures, fugacity is related to pressure through a quantity called the fugacity coefficient (ϕ). These relationships are shown below.

$$(dG)_T = VdP = RTd \ln f \quad (3.14)$$

$$\lim_{p \rightarrow 0} \frac{f}{P} \rightarrow 1 \quad (\text{pure}) \quad (3.15)$$

$$\lim_{p \rightarrow 0} \frac{\hat{f}_i}{y_i P} \rightarrow 1 \quad (\text{mixture}) \quad (3.16)$$

$$\frac{f}{P} = \phi \quad (3.17a)$$

$$\frac{\hat{f}_i}{y_i P} = \hat{\phi}_i \quad (3.17b)$$

In order to derive a useful expression to replace chemical potential equality, G.N. Lewis suggested that for an ideal-gas mixture at constant temperature and composition, the variation of chemical potential with pressure for a particular component i is equal to the molar volume of that component,

$$\left(\frac{\partial \mu_i}{\partial P}\right)_{T,y} = V_i \quad (3.18)$$

By substituting the expression for an ideal-gas mixture ($PV = NRT$, thus $PV_i = RT$ for each component) into equation (3.18), we obtain,

$$\left(\frac{\partial \mu_i}{\partial P}\right)_{T,y} = \frac{RT}{P} \quad (3.19)$$

$$\Rightarrow d\mu_i = RT \frac{dP}{P} \quad (\text{at constant temperature and composition}) \quad (3.20)$$

Integrate equation (3.20) from a reference state P° to a final pressure P .

$$\int_{\mu_i(T,P^\circ)}^{\mu_i(T,P)} d\mu_i = RT \int_{P^\circ}^P \frac{dP}{P} \quad (3.21)$$

$$\Rightarrow \mu_i(T,P) - \mu_i(T,P^\circ) = RT \ln \frac{P}{P^\circ} \quad (3.22)$$

Since it was derived for an ideal-gas mixture, equation (3.22) is true for that condition only. Lewis defined the fugacity function so that it could be generalized to include non-ideal behavior in the fluid phase,

$$\mu_i(T,P) - \mu_i(T,P^\circ) = RT \ln \frac{\hat{f}_i}{f_i^\circ} \quad (3.23)$$

Equation (3.23) gives the chemical potential difference for a component between a given state and a reference state within a single phase. It can be expressed for both the liquid and vapor phases as shown by the following (assuming the same reference condition applies to both):

$$\mu_i^l(T,P) - \mu_i^l(T,P^\circ) = RT \ln \frac{\hat{f}_i^l}{\hat{f}_i^{\text{ol}}} \quad (3.24)$$

$$\mu_i^v(T,P) - \mu_i^v(T,P^\circ) = RT \ln \frac{\hat{f}_i^v}{\hat{f}_i^{\text{ov}}} \quad (3.25)$$

By substituting equations (3.24) and (3.25) into the phase-equilibrium equation (3.10), we obtain

$$\mu_i^l(T,P^\circ) + RT \ln \frac{\hat{f}_i^l}{\hat{f}_i^{\text{ol}}} = \mu_i^v(T,P^\circ) + RT \ln \frac{\hat{f}_i^v}{\hat{f}_i^{\text{ov}}} \quad (3.26)$$

Again, assuming that the chemical potential and fugacity reference states are the same for both the liquid and vapor phases, we obtain the following equalities²,

$$\mu_i^l(T,P^\circ) = \mu_i^v(T,P^\circ) \quad (3.27)$$

$$\hat{f}_i^{\text{ol}} = \hat{f}_i^{\text{ov}} \quad (3.28)$$

² This assumption is the basis for predicting phase equilibrium solely from an equation-of-state.

Substituting equations (3.27) and (3.28) into equation (3.26) gives an alternate criterion for phase equilibrium.

$$\hat{f}_i^l = \hat{f}_i^v \quad (3.29)$$

Equation (3.29) indicates that for a system of liquid and vapor phases in equilibrium, not only the temperature and pressure must be the same in both phases but also the fugacity of each component must be the same. Fugacity equality provides a more convenient way to carry out the computations than does the chemical potential relationship.

The fugacity of component i in a mixture of a specific phase can be written as the mole fraction of that component times the fugacity coefficient times the pressure. Substituting in equation (3.29), we obtain

$$x_i \hat{\phi}_i^l P = y_i \hat{\phi}_i^v P \quad (3.30)$$

and

$$x_i \hat{\phi}_i^l = y_i \hat{\phi}_i^v \quad (3.31)$$

where x_i and y_i are the mole fractions of component i in the liquid and vapor phases, respectively. We introduce a new variable called the equilibrium vaporization ratio (K factor).

$$K_i = \frac{y_i}{x_i} = \frac{\hat{\phi}_i^l}{\hat{\phi}_i^v} \quad (3.32)$$

Since summation of the mole fractions of all components in the vapor must equal one, it follows that the summation of the $K_i x_i$ products must also sum to one.

$$\sum_{i=1}^n y_i = 1 \quad (3.33)$$

$$\Rightarrow \sum_{i=1}^n K_i x_i = 1 \quad (3.34)$$

Equation (3.34) is the criterion for bubble-point calculations. Since the liquid-phase mole fractions (x_i) are known, work is required to find a set of K-values that satisfies equation (3.34). Similarly, since summation of the mole fractions of all components in the liquid phase must also equal one, that leads to the dew-point criterion: summation of y_i/K_i equals one.

$$\sum_{i=1}^n x_i = 1 \quad (3.35)$$

$$\Rightarrow \sum_{i=1}^n \frac{y_i}{K_i} = 1 \quad (3.36)$$

As in the first example, work is required to find a set of K-values that will satisfy equation (3.36).

In order to calculate values of the K factor, both the fugacities in the vapor and liquid phases must be determined. We begin with the fundamental equation in Helmholtz energy form for a system of n components ([8], Pages 154-155),

$$\underline{A} \equiv \underline{H} - T\underline{S} - P\underline{V} \quad (3.37)$$

$$\underline{A} = f(T, \underline{V}, N_1, \dots, N_n) \quad (3.38)$$

$$d\underline{A} = -\underline{S}dT - P d\underline{V} + \sum_{i=1}^n \mu_i dN_i \quad (3.39)$$

where n is the total number of components in the system. By fixing the number of moles of each component, the final term in equation (3.39) vanishes.

$$d\underline{A} = -\underline{S}dT - P d\underline{V} \quad (\text{all } N_i \text{ constant}) \quad (3.40)$$

The temperature is set constant, and equation (3.40) becomes,

$$d\underline{A} = -P d\underline{V} \quad (\text{constant temperature, mole numbers}) \quad (3.41)$$

By integrating equation (3.41) from a finite volume \underline{V} to an infinite volume, we first obtain the unbounded expression,

$$\int_{\underline{A}(T, \underline{V}, N)}^{\underline{A}(T, \infty, N)} d\underline{A} = - \int_{\underline{V}}^{\infty} P d\underline{V} \quad (3.42)$$

$$\text{or} \quad \underline{A}(T, \infty, N) - \underline{A}(T, \underline{V}, N) = - \int_{\underline{V}}^{\infty} P d\underline{V} \quad (3.43)^3$$

³ \underline{A} continues to decrease as $\underline{V} \rightarrow \infty$ and is thus unbounded. Since it appears again in equation (3.45), it will be cancelled out.

We assume that the fluid-phase system behaves as an ideal gas as the volume of the system becomes infinitely large. We also assume that as the volume of the system approaches a large but finite value \underline{V}° , the fluid-phase system behaves closely enough to an ideal gas. Therefore, integrating equation (3.41) from an infinite volume to \underline{V}° gives

$$\int_{\underline{A}(T,\infty,N)}^{\underline{A}(T,\underline{V}^\circ,N)} d\underline{A} = - \int_{\infty}^{\underline{V}^\circ} P^{id} d\underline{V} \quad (3.44)$$

or

$$\underline{A}^\circ(T, \underline{V}^\circ, N) - \underline{A}(T, \infty, N) = - \int_{\infty}^{\underline{V}^\circ} P^{id} d\underline{V} \quad (3.45)$$

where P^{id} represents the ideal-gas pressure. By adding equations (3.43) and (3.45) and by adding and subtracting the term

$$\int_{\underline{V}}^{\infty} \frac{RT}{\underline{V}} d\underline{V}$$

we obtain the bounded expression

$$\underline{A}^\circ(T, \underline{V}^\circ, N) - \underline{A}(T, \underline{V}, N) = - \int_{\underline{V}}^{\infty} P d\underline{V} + \int_{\underline{V}}^{\infty} \frac{NRT}{\underline{V}} d\underline{V} - \int_{\infty}^{\underline{V}^\circ} \frac{NRT}{\underline{V}} d\underline{V} - \int_{\underline{V}}^{\infty} \frac{NRT}{\underline{V}} d\underline{V} \quad (3.46)$$

$$\Rightarrow \underline{A}^\circ(T, \underline{V}^\circ, N) - \underline{A}(T, \underline{V}, N) = - \int_{\underline{V}}^{\infty} \left(P - \frac{NRT}{\underline{V}} \right) d\underline{V} - NRT \ln \frac{\underline{V}^\circ}{\underline{V}} \quad (3.47)$$

Recall that the partial derivative of Helmholtz energy with respect to the number of moles of component i , with the temperature, volume, and the quantities of

the remaining components held constant, is equal to the chemical potential of i .

$$\left(\frac{\partial \underline{A}}{\partial N_i} \right)_{T, \underline{V}, N_j (j \neq i)} = \mu_i \quad (3.48)$$

Therefore, by differentiating the Helmholtz energy in equation (3.47) and substituting the result into equation (3.23), where \hat{f}_i° is equal to the partial pressure of component i under ideal-gas conditions ($y_i P$), the fugacity coefficient for a single phase can be represented as,

$$\int_{\underline{V}}^{\infty} \left(\left(\frac{\partial P}{\partial N_i} \right)_{T, \underline{V}, N_j} - \frac{RT}{\underline{V}} \right) d\underline{V} - RT \ln \frac{P\underline{V}}{NRT} = RT \ln \frac{\hat{f}_i}{y_i P} \quad (3.49)$$

or

$$\ln \hat{\phi}_i = \frac{1}{RT} \int_{\underline{V}}^{\infty} \left(\left(\frac{\partial P}{\partial N_i} \right)_{T, \underline{V}, N_j} - \frac{RT}{\underline{V}} \right) d\underline{V} - \ln Z \quad (3.50)$$

where Z is the compressibility factor $P\underline{V}/NRT$. The remaining work is to evaluate the term with the pressure derivative from the mixture form of the Peng-Robinson equation. The details of the differentiation will not be shown here, but can be found in reference ([8], Pages 204-205). The final expression for the fugacity in either phase is given by

$$\ln \hat{\phi}_i^\sigma = \frac{b_i}{b_m^\sigma} \left(\frac{PV^\sigma}{RT} - 1 \right) - \ln \frac{P(V^\sigma - b_m^\sigma)}{RT} + \frac{a_m^\sigma}{2RTb_m^\sigma \sqrt{2}} \left(\frac{2 \sum_{j=1}^n x_j a_{ij}}{a_m^\sigma} - \frac{b_i}{b_m^\sigma} \right) \ln \frac{V^\sigma + (1 - \sqrt{2})b_m^\sigma}{V^\sigma + (1 + \sqrt{2})b_m^\sigma} \quad (3.51)$$

where σ represents either liquid or vapor and b_m^σ , a_m^σ represent Peng-Robinson mixture constants evaluated at the composition of the σ phase. The fugacity coefficients are now substituted into equation (3.32) to evaluate a set of K-factors that satisfies equation (3.34) for a bubble-point calculation or equation (3.36) for a dew-point calculation.

A flow sheet is shown in Figure 3.1 to illustrate the procedure for a bubble-point pressure determination. Figure 3.2 shows an ASPEN PLUS-generated P-xy diagram for the cyclohexane-cyclohexanone binary mixture at $T=400\text{K}$. The pressure \hat{P} in Figure 3.2 is the bubble-point pressure determined for a liquid cyclohexane mole fraction of 0.7. Iterative calculations for bubble-point pressure and the corresponding vapor-phase composition were performed as shown in Figure 3.1. In order to draw a smooth, continuous bubble-point curve, the procedure for evaluating the pressure and equilibrium y-values was repeated at many values of x . The P-y data points were then used to draw a smooth dew-point curve.

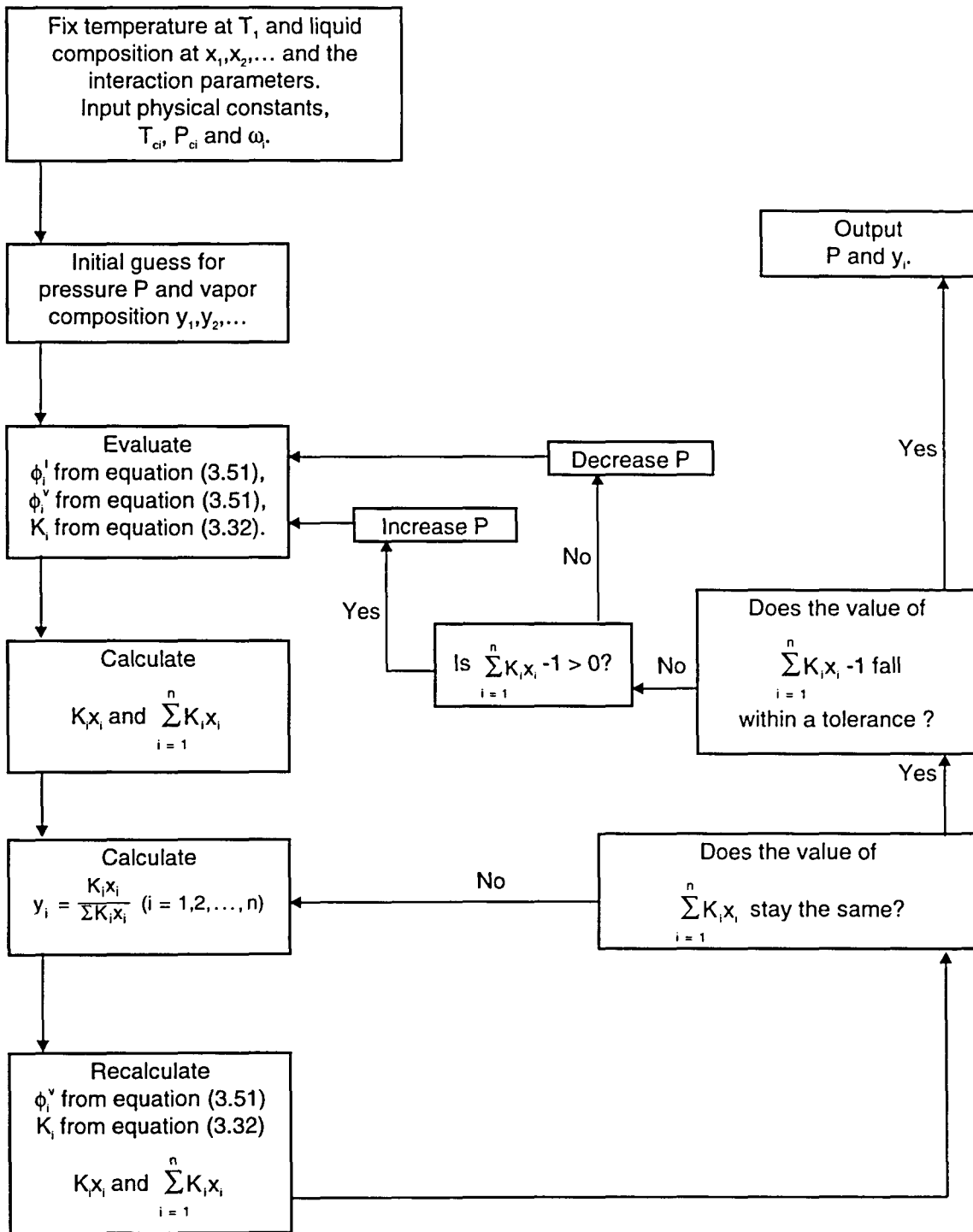


Figure 3.1 Flow sheet diagram for bubble-point pressure calculation [9].

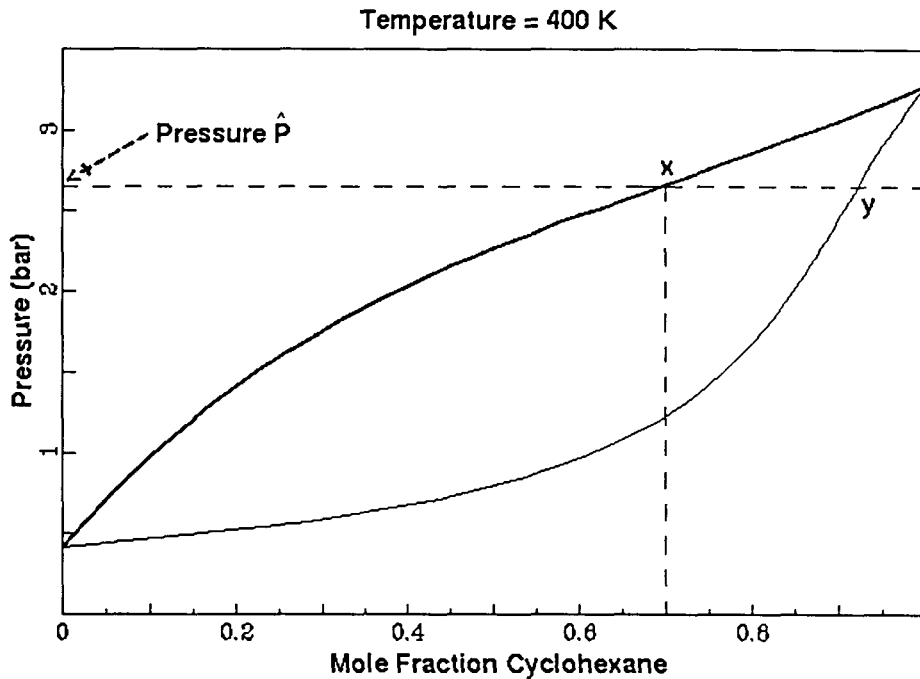


Figure 3.2 P-xy phase diagram for cyclohexane and cyclohexanone illustrating a bubble-point pressure calculation at $x = 0.7$.

Application

The ASPEN PLUS chemical process simulator uses an operation called FLASH2 to perform simple flash, bubble-point pressure and temperature, and dew-point pressure and temperature calculations. The process simulated is shown in Figure 3.3. An inlet stream 1 containing one or more components is connected to the FLASH2 block, and the thermal and phase conditions are set. The calculated liquid-state properties (product stream 3) and the equilibrium vapor-state properties (stream 2) are tabulated on the Stream-Sum.Main form. This can be obtained from the Form pull-down menu, then from the Result-Summary and Stream-Sum sub-menus. To specify the thermal and phase conditions in FLASH2, use the left

mouse button to click and select `FLASH2`, and then use the right mouse button to click the selected `FLASH2` for a pop-up menu. Choose `input` from the pop-up menu, and click `Main` from the next pop-up window manager to get the `Flash2.Main` entry form. There are four categories on the `Flash2.Main` form: temperature (`Temp`), pressure (`Pres`), heat duty (`Duty`), and vapor fraction (`Vfrac`). `FLASH2` accepts a combination of any two of these options except the combination of heat duty and vapor fraction. Specify a temperature and `Vfrac=0` for a bubble-point pressure calculation, or specify a pressure and `Vfrac=1` for a dew-point temperature calculation. The composition of the inlet mixture can be specified on the `Stream 1 (Stream.Main)` form.

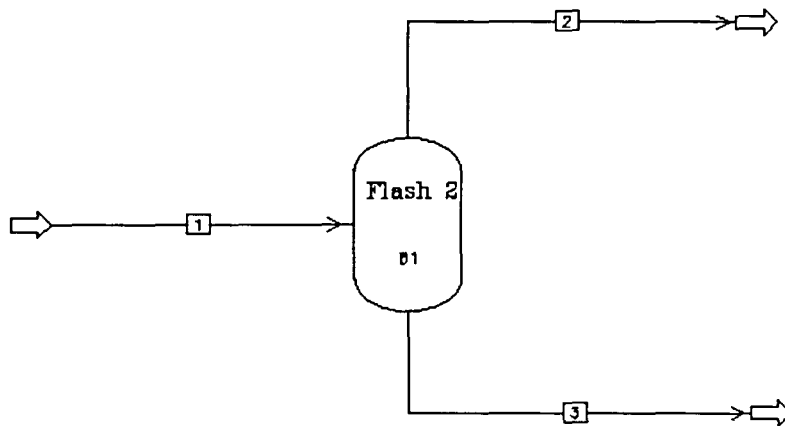


Figure 3.3 Setting up vapor-liquid equilibrium calculations using the `FLASH2` routine.

Take Figure 3.2 as an example of a bubble-point pressure calculation. Specify the temperature(400K) and Vfrac(0.0001) on the `Flash2.Main` form and the mole fraction of cyclohexane(0.7) on the Stream 1 (`Stream.Main`) form. The reason for specifying Vfrac to be 0.0001 is to pass a tiny amount of vapor to product stream 2 and thus have the equilibrium vapor-state properties specified without having an appreciable effect on the total amount of liquid in product stream 3. The results of the calculation show the equilibrium pressure to be 2.620 bar and the equilibrium vapor mole fraction of cyclohexane to be 0.9235.

ASPEN PLUS also has a utility to draw the complete binary P-xy diagram in one operation. From the `Analysis` pull-down menu, select the `Binary` and then `Pxy` sub-menus. The P-xy Diagram form will appear with all required information set at default values. Change the binary components and temperature accordingly. Notice that `Option Set` uses the Peng-Robinson equation by default. It is retrieved from the `Opsetname` variable specified on the `Properties.Main` form. To draw more than one P-xy curve on a single plot, specify two or more temperatures on the `P-xy Diagram` form. Then click OK to generate the diagram. The results are displayed in two forms, a window with the P-xy plot(Figure 3.2) and a window containing the tabulated numerical results. From the latter window, many other related plots can be generated from the `Plot` pull-down menu, such as P-x, y-x, gamma-x (liquid activity coefficients for either component), KVL-x (K-values for either component), and more.

To generate a T-xy phase diagram, again from the *Analysis* pull-down menu, select the *Binary* and then *Txy* sub-menus. The T-xy Diagram form will appear in the same format as the P-xy Diagram form, except that pressure is now the chosen variable. Change the binary components and the pressure accordingly, and then click *OK* to generate the T-xy diagram.

Liquid-liquid equilibrium

Liquid-liquid equilibrium occurs when two immiscible, multicomponent liquid phases of different mixture compositions and densities coexist at a fixed temperature, pressure, and (component) chemical potentials. Equilibrium between liquid phases follows the same thermodynamic criteria as that between liquid and vapor phases. Therefore, the mathematical expressions of equilibrium conditions are the same as those between the vapor and liquid phases indicated earlier.

$$T^{l1} = T^{l2} \quad (3.52)$$

$$P^{l1} = P^{l2} \quad (3.53)$$

$$\mu_i^{l1} = \mu_i^{l2} \quad (i = 1, 2, 3, \dots) \quad (3.54)$$

The liquid and vapor phases are replaced by two distinct liquid phases *l1* and *l2*. To evaluate the fugacity of a specific component in either liquid, equation (3.51) is again used with the compositions for that particular phase.

CHAPTER 4. MAKING OF THREE-DIMENSIONAL BINARY DIAGRAMS

This chapter discusses the procedures for generating three-dimensional, P-T-xy phase diagrams for binary systems. Although this was not the prime objective of this project, it gives some basic ideas for phase-diagram construction that lead to the next two chapters dealing with three-dimensional ternary and quaternary diagrams. There are three important steps involved in making a three-dimensional phase diagram: (1) generating phase-equilibrium data points from the ASPEN PLUS process simulator, (2) generating critical-condition data by using the Heidemann and Khalil method [10], and (3) displaying the spatial drawing using Open Inventor software running on a Silicon Graphics IRIS Workstation.

Generating phase-equilibrium data

The ASPEN PLUS chemical process simulator uses its Table Generation System (TGS) to tabulate the thermodynamic properties of mixtures. Therefore, it is not necessary to draw a flow-sheet diagram for property generation alone. When ASPEN PLUS is starting up, on the `Create New Run` form, click to choose `Property Table Generation (TGS)` under `Run Type`. Then click on `OK` to bring up a dark gray background in the ASPEN PLUS main window. Before doing any specification, check to make sure that the unit settings are correct. A numerical result can give misleading information if the units are used incorrectly in the course of the calculation. Therefore, clarifying the unit settings is important.

From the `Forms` pull-down menu, select `Setup` and the `Units-Sets` sub-menu. A `Units-Sets Object Manager` form appears. Highlight a unit set and click on `Input` to view the unit specification in that set. On the other hand, a new unit set can be created by clicking `Create` on the `Units-Sets Object Manager` form. Specify an ID name for the new unit set in the pop-up dialog box, and click on `OK` to bring up the `Units-Set Input Menu` form. There are three sections in this form. Click on `Units-Set1` and note that in the upper section of the `Setup.Units-Set1` form there is a space beside `Copy From/View`. Use the right mouse button to click on that space to get a list of unit sets. Highlight a unit set to copy its unit setting to this new unit set, and make the changes accordingly by clicking the right mouse button on a specific unit. Throughout this project, the units used for temperature and pressure are K and bar, respectively. After the unit specification, a dialog box appears. For setting this unit set globally, click on `Yes` to accept. After clarifying the unit setting, proceed to specify the names of the binary components on the `Components.Main` form.

In this work the Peng-Robinson equation of state was selected as the `Opsetname` variable on the `Properties.Main` form, and the corresponding binary interaction parameter was entered on the `PRKIJ-1 (Binary.Scalar)` form as described in Chapter 3. ASPEN PLUS uses the `Flashcurve` routine to tabulate the physical and thermodynamic properties for multi-phase mixtures resulting from flash calculations (vapor and liquid phases in this project) [11]. To use the `Flashcurve` routine, from the `Forms` pull-down menu select `Properties` and

then the Prop-Tables sub-menu. Click on 'Create' on the pop-up Prop-Tables Object Manager form. Select FLASHCURVE for the Prop-Tables type and click on OK. Enter an ID name for the new Flashcurve routine or accept the default name PT-1 so that ASPEN PLUS can recognize its existence. Finally, click on OK to bring up the Flashcurve Input Menu form. There are three sections in this input menu: (1) the Flashcurve.System form requires an input for the component flow rates in the lower section of the form. Note that the keyboard entry in the upper section of the form has been deactivated for the Table Generation System (TGS). (2) Use the Flashcurve.Vary form to specify at least one independent variable (e.g., composition) in the upper section of the form. A range of the independent variable must be specified. In addition, two of the variables, temperature (Temp), pressure (Pres), or vapor fraction (Vfrac), have to be specified in the lower section of the form; (3) the Flashcurve.Tabulate form tabulates the thermodynamic properties resulting from the flash calculations. However, it is necessary to specify at least one Property Sets name to define the tabulated properties. A list of the Property Sets names are defined on the Prop-Set.Main form. This form can be obtained from the Forms pull-down menu, then from the Properties and Prop-Sets sub-menu. The Prop-Sets Object Manager form appears and lists all the available Property sets ID names. Highlight an ID name and click on Input to check the thermodynamic properties defined. A new property set can be created using the 'Create' button. Specify an ID name for the new property set or accept the default name PT-1. On the Prop-Set.Main form, define the tabulated

thermodynamic properties, units, and phases. Finally, specify the name of this new property set on the `Flashcurve.Tabulate` form.

There are five sets of data points that are used to generate the three-dimensional diagram. The first two are: (1) a series of constant-temperature bubble-point (P-x) curves and (2) a series of constant-temperature dew-point (P-y) curves. On the `Flashcurve.System` form, enter '1' for the flow rates of both components. In the upper section on the `Flashcurve.Vary` form, enter 'TEMP' for the first `Varname`, and specify the temperature range and its increment. If the temperature increment is not constant, use the spaces along side of `List` to enter a list of the actual temperatures desired. In the next `Varname`, enter 'MOLE-FRAC' and enter the component name in the space beside 'Component.' Usually, it is component 1. Then set the range of mole fractions from '0' to '1' with '0.05' increments. This increment is small enough to produce smooth curves. In the lower section of the form, in the space beside `Vfrac`, enter '0' to perform bubble-point calculations or '1' for dew-point calculations. Finally, create a new property set 'PT-1' as described above, and specify its name on the `Flashcurve.Tabulate` form in the space next to `Property Sets`. On the newly created `Prop-Set.Main` form, set the tabulated parameter 'PRES' in the space under `Property`, and set the unit type to 'BAR'. The bubble-point or dew-point pressures evaluated for each independent value of temperature and composition will be tabulated on the `Flashcurve.Results` form.

The next two data sets are (3) a series of constant-pressure bubble-point (T-x) curves and (4) a series of constant-pressure dew-point (T-y) curves. The settings on the `Flashcurve.System` form stay the same as they were specified for calculating P-xy curves. On the `Flashcurve.Vary` form, replace `Vname` 'TEMP' by 'PRES' and change the range of the pressure accordingly. The rest of the setting will remain unchanged as described above. On the `Flashcurve.Tabulate` form, use the ID name of the property set which defines 'TEMP' as the tabulated property and 'K' as the unit. After the flash calculation the `Flashcurve.Results` form will tabulate the bubble-point or dew-point temperatures evaluated at each independent value of pressure and composition.

Finally, data set (5) gives the vapor pressure curves for the pure components. On the `Flashcurve.System` form, set the flow rate of component 1 to be '0' to calculate the vapor pressure curve of component 2 (or vice-versa). On the `Flashcurve.Vary` form, specify 'TEMP' as an independent variable in the upper section, and set an appropriate range and increment for the temperature. Enter '1' for `Vfrac` in the lower section. On the `Prop-Set.Main` form, set the tabulated property to be 'PRES' with unit type 'BAR' and specify the name of this property set on the `Flashcurve.Tabulate` form. The `Flashcurve.Results` form will tabulate the vapor pressure of either component as a function of temperature at the end of the flash calculation.

Generating data points in the critical region

The critical point of a pure component is at the highest temperature and pressure where separate vapor and liquid phases can coexist. These conditions are known as the critical temperature and pressure of the component. But for a binary mixture this is not the case. The critical points of a mixture are composition dependent. They can be represented by a critical locus that connects to the critical point of each pure component and passes through the critical points of all successive mixture compositions.

Heidemann and Khalil[10] have developed a computational algorithm to calculate the critical points of a multicomponent mixture where all fluid-phase properties are predicted by an equation of state, such as the Peng-Robinson. In his doctoral work, Daniel Coy [3] created a FORTRAN program to execute Heidemann and Khalil's algorithm for the Peng-Robinson case. Dr. Coy's 'critical' programs were written originally as sub-units within his 'Trace' program for thermodynamic properties. The details of the work were presented in his doctoral dissertation.

For this work, Dr. Coy's programs were extracted and modified to produce an independent program for calculating the critical locus of a binary mixture. The compiled and executable code has the name CR and is stored in the local drive of

`pv0415.vincent.iastate.edu`

in the directory

`/local/dcoy/Trace/Code/CR.`

The modified source programs are stored in

```
/local/dcoy/Trace/Code/CRCode/.
```

The CR program reads an input data file with extension `.pro`. Table 4.1 shows the format of the input file used for calculating the critical locus of the binary mixture ethylene / n-butane

Table 4.1 CR program input file for the ethylene/n-butane binary.

2	{ Number of components }
Component 1: Ethylene	
50.36d0	{ Pc (bar) }
282.4d0	{ Tc (K) }
0.086	{ Acentric factor }
Component 2: n-Butane	
37.97d0	{ Pc (bar) }
425.16D0	{ Tc (K) }
0.201	{ Acentric factor }
0.092	{ Binary interaction parameter }

The CR program needs values for the critical temperature, critical pressure, and acentric factor of each pure component, as well as the binary interaction parameter for the mixture. To execute the program, type `CR propfile` after the command prompt. `propfile` is the name of the property file shown in Table 4.1 with extension `.pro`. The results are tabulated on the computer screen with the mole fractions of component 1 in the left column (0.01 increment), critical pressures in the second column (with the unit bar), and critical temperatures on the right (with the unit K). To save the results in a specific file, use the command `CR propfile > filename`.

Generating images using Open Inventor software

Open Inventor is a trademark of Silicon Graphics, Inc. It is an object-oriented graphical application [12] used to generate interactive, three-dimensional images of mathematically defined surfaces. Open Inventor provides detailed rendering options for a three-dimensional object, such as the lighting model and the color and method of rendering. It also has a trackball interface for rotation, translation, and enlargement. These features make it possible to study phase-diagram structures in detail. In the early stage of diagram construction, a C++ program reads an Inventor-format, three-dimensional data file for rendering. The program utilizes OpenGL object libraries [13] to draw lines and wireframes. As a result, a different source program is required to draw each individual diagram. This is obviously not an effective way to construct a large number of diagrams, insofar as time and file organization are concerned. However, there are two major three-dimensional viewers that reside in the Silicon Graphics workstation: `ivview` and `SceneViewer`. These are end-user programs created by the Open Inventor Architecture Group that provide fast data readback and easy display of three-dimensional data. They were used extensively in constructing and rendering the phase diagrams studied throughout this project. Therefore, being familiar with the utilities and functions of these programs is very important.

`ivview` is a fast, interactive, three-dimensional viewer. It reads an Inventor-format, three-dimensional data file, called an `iv` file, and runs `ivquicken` to

accomplish the object-rendering process [14]. Two major utilities are involved when `ivview` is invoked: an Inventor `examiner viewer`, which allows interaction between mouse and three-dimensional object for rotation, translation, and enlargement, and a `menu bar` which provides simple manipulating functions.

`SceneViewer` is a more sophisticated three-dimensional viewer as well as a graphics editor. It reads only one `iv` file when it is executed. However, its `import` utility (which can be found from the `File` pull-down menu) allows the viewer to read more than one `iv` file for object rendering. Similar to `ivview`, `SceneViewer` utilizes the `Inventor examiner viewer` to interact with the mouse operation so as to change the viewpoint of a three-dimensional object. `SceneViewer` provides more sophisticated and better-developed menu options. These allow object editing such as selecting, cutting, copying and pasting, printing, light source and material editing, view control, trackball manipulation, and many more. By using these two well-designed three-dimensional viewers, additional programming effort is not required.

An `iv` file contains Inventor-format ASCII or binary codes which are used to define the nature of a three-dimensional object, such as the spatial data, the connectivity, and the lighting, shading, and color models. The format of an `iv` file is important because everything about the three-dimensional object is defined in the file. Binary-coded `iv` files will not be discussed because the code is interpretable only by the Inventor application. Table 4.2 shows a sample ASCII-coded `iv` file

which is used to create four simple line curves of different visual properties. Note that the first column shows the numbers corresponding to the lines of code. They are used as reference numbers while describing the code format but should not be used in the `iv` file¹.

Table 4.2 A sample `iv` file.

1	#Inventor V2.0 ascii
2	
3	Separator {
4	
5	Material {
6	ambientColor 0.0 0.0 0.0
7	diffuseColor 1.0 0.0 0.0
8	specularColor 0.0 0.0 0.0
9	emissiveColor 0.5 0.0 0.0
10	shininess 1.0
11	transparency 0.0 }
12	
13	Separator {
14	
15	# Draw two solid lines
16	DrawStyle {
17	style LINES
18	lineWidth 2
19	pointSize 1
20	linePattern 0xffff }
21	
22	Coordinate3 {
23	point [
24	0.0 0.0218 2.0851 ,
25	0.0 0.0794 1.6597 ,
26	0.0 0.1890 1.2343 ,
27	0.0 0.3668 0.8089 ,
28	0.0 0.6278 0.4686 ,
29	0.0 0.9214 0.05]}}
30	

¹ The description of the `iv` file format is extracted from the Inventor "on-line" Help Manual. For detailed instructions, type "man SoNodename" after the command prompt. SoNodename is replaced by the name of the node with the `So` prefix. For example, type "man SoSeparator."

Table 4.2 (Continued)

31	LineSet {
32	startIndex 0
33	numVertices [3, 3] }
34	
35	}
36	
37	Separator {
38	
39	# Draw a dashed line
40	DrawStyle {
41	style LINES
42	lineWidth 1
43	pointSize 1
44	linePattern 0xf0f0 }
45	
46	# Draw a dashed line
47	Coordinate3 {
48	point [
49	1.0 0.1571 2.0
50	1.0 0.3257 1.5746
51	1.0 0.5192 1.2343
52	1.0 0.7027 0.9791]}
53	
54	LineSet {
55	startIndex 0
56	numBertices 4 }
57	
58	}
59	

The first line shows the header used in every `iv` file. The header is used to identify the Inventor-format data file. It may be changed depending on the version of the Open Inventor software. The current version is 2.0. If the `iv` file is written in binary format, it should show `#Inventor V2.0 binary`.

`Separator`, `Material`, `DrawStyle`, `Coordinate3` and `LineSet`, shown respectively on lines 3, 5, 16, 22 and 31, are the names of the nodes². The node is

² Not to be confused with a node in a geometry file.

the basic building block that contains a set of data elements (called fields) used to define the properties of a three-dimensional object. For example, the `Material` node on line 5 consists of six fields: `ambientColor`, `diffuseColor`, `specularColor`, `emissiveColor`, `shininess`, and `transparency`. The format for writing a node should include the name of the node, followed by an open brace (`{`), a set of fields and parameters, and it should end with a closed brace (`}`).

The function of a `Separator` node is to isolate the properties of its “children” (nodes and fields) from the properties of the children specified in other `Separator` nodes. Therefore, each small part that makes up a three-dimensional object can have its own properties. An `iv` file allows for the specification of more than one `Separator` node. Since `Separator` nodes are relatively inexpensive as far as computing time is concerned, they can be used freely in defining the properties of a three-dimensional object. Note that the sample `iv` file shown in Table 4.2 uses two `Separator` nodes. Each of them defines a different line pattern for the line curves.

The `Material` node contains a set of color fields and red/green/blue (RGB) parameters to define the colors of a three-dimensional object. These parameters are set to zero by default, and they range from zero to one.

The `DrawStyle` node specifies the drawing style when a three-dimensional object is being rendered. `style` fields contain four possible parameters: `FILLED`, `LINES`, `POINTS`, and `INVISIBLE`. `FILLED` is assigned to the `style` field by default. The width of the line and the size of the points used to draw a three-dimensional object are defined in the `lineWidth` and `pointSize` fields. If the

parameter `LINES` is specified in the style field, the line pattern can be defined in the `linePattern` field. The value ranges from zero (an invisible line) to `0xffff` (a solid line). Dotted lines and dashed lines can be drawn also depending on the parameter specified.

The `Coordinate3` node defines the x, y, z coordinates of a three-dimensional object used for subsequent shading and rendering. The coordinates are specified in the brackets ([]) of the `point` field. Note that each point is separated by a comma, and its x, y and z coordinates are separated by spaces. There is no comma at the end of the final coordinate.

The `LineSet` node draws spatial polylines whose coordinates are defined by the `coordinate3` node. Each coordinate has its own index number in an ascending order. The first coordinate always starts with index zero. The `startIndex` field picks the starting coordinate and draws three-dimensional, spatial polylines through a set of coordinates in which the number of coordinates is specified in the `numVertices` field. For example, the `LineSet` field in line 31 with `startIndex 0` and `numVertices [3,3]` uses coordinates 0, 1, 2 for the first line and coordinates 3, 4, 5 for the second line.

The binary phase diagram is constructed in a rectangular coordinate box as shown in Figure 4.1. The mole fraction of component 1 (x_1), the pressure, and the temperature are plotted on the x, y and z axes, respectively. The box is constructed using an `iv` file called `block.iv`, and its coordinates are specified in Table 4.3.

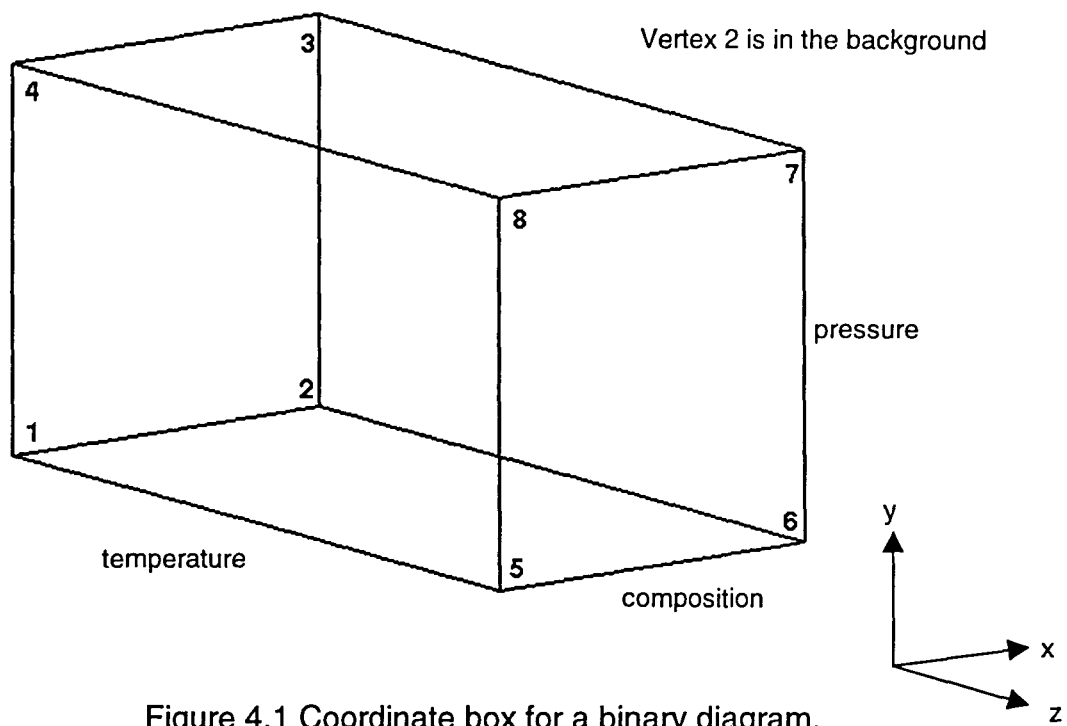


Figure 4.1 Coordinate box for a binary diagram.

Table 4.3 Box coordinates.

<u>Vertex</u>	<u>Coordinates</u> <u>(x,y,z)</u>
1	(0,0,0)
2	(1,0,0)
3	(1,1.05,0)
4	(0,1.05,0)
5	(0,0,2.085)
6	(1,0,2.085)
7	(1,1.05,2.085)
8	(0,1.05,2.085)

The binary phase-equilibrium data calculated by ASPEN PLUS are imported into an XESS spreadsheet for data extraction and rearrangement to form an `iv-` format data set. The data are then transferred to the `coordinate3` field in an `iv` file by the mouse-click action of copying and pasting data³. This procedure could also be accomplished using a program. However, as noted earlier, the objective of this project was not to generate large numbers of phase diagrams, so data-arranging by hand was faster and more convenient.

To generate a three-dimensional drawing, the physical coordinates of the phase-equilibrium data points must be transformed to the normalized coordinate system of the box. First, suitable ranges of temperature and pressure covering the phase behavior of the mixture must be determined. In other words, the maximum and minimum values of temperature and pressure must be set in the three-dimensional box. Then, the coordinate transformation from the physical data points to the normalized rectangular space are implemented by the following interpolation equations,

$$x = x_1 \quad (4.1)$$

$$y = 0.03 + (0.97 - 0.03) \cdot \left(\frac{P - P_{\min}}{P_{\max} - P_{\min}} \right)^n \quad (4.2)$$

$$z = 2.0 - \frac{2.0 - 0.05}{T_{\max} - T_{\min}} (T - T_{\min}) \quad (4.3)$$

³ Click and hold the left mouse button to highlight and copy a data set. Then click on the middle mouse button to paste the data into a specific place.

Since x ranges from zero to one in the same way as the mole fraction of component 1, there is no coordinate transformation required. For the y -coordinate transformation, P_{\max} and P_{\min} are the normalized maximum and minimum pressures set on the y -coordinate that cover the range of the phase diagram. P is the actual phase-equilibrium pressure calculated by ASPEN PLUS. The power term n determines how much the normalized y -coordinate is nonlinearized. It is useful when different pressure ranges are to be treated differently in the phase diagram. In this case, if the diagram is drawn with the power term n set to 1.0 (i.e., a linear transformation), the data in the lower pressure range will appear to be squeezed down along the normalized y -coordinate. With the power term n specified at a value less than one, the data in the lower pressure range will be enlarged and those in the upper pressure range slightly compressed. Thus the phase diagram is more easily visualized in the rectangular box. This is a technique for graphics visualization but not for accurate data analysis. The diagram is constructed in such a way that the top and bottom are offset by 0.03. In other words, when the pressure equals P_{\min} , y equals 0.03, and when pressure equals P_{\max} , y equals 0.97.

In the z -coordinate transformation, T_{\max} and T_{\min} are the maximum and minimum temperatures set on the normalized z -coordinate. T is the actual phase-equilibrium temperature calculated from ASPEN PLUS. The high-temperature end of the phase diagram is offset by 0.05 on the normalized z coordinate.

Several `iv` files are used to construct a three-dimensional binary phase diagram. `block.iv` specifies the rectangular bounding box. `tpline.iv` and

`tdline.iv` specify the constant-temperature bubble-point and dew-point contour lines, respectively. `pbline.iv` and `pdline.iv` specify the constant-pressure bubble-point and dew-point contour lines. `vapor.iv` specifies the vapor-pressure contour lines for the pure components, and `tie.iv` specifies the tie lines connecting the bubble- and dew-point curves.

Figure 4.2 shows the PTx diagram for cyclohexanone and cyclohexane [15]. The binary interaction parameter used for this mixture was 0.13 and was retrieved automatically from the ASPEN PLUS EOS-LIT data bank. Note that the pressure axis is nonlinear to prevent details at the low-temperature (and thus low-pressure) end of the diagram from being compressed [16].

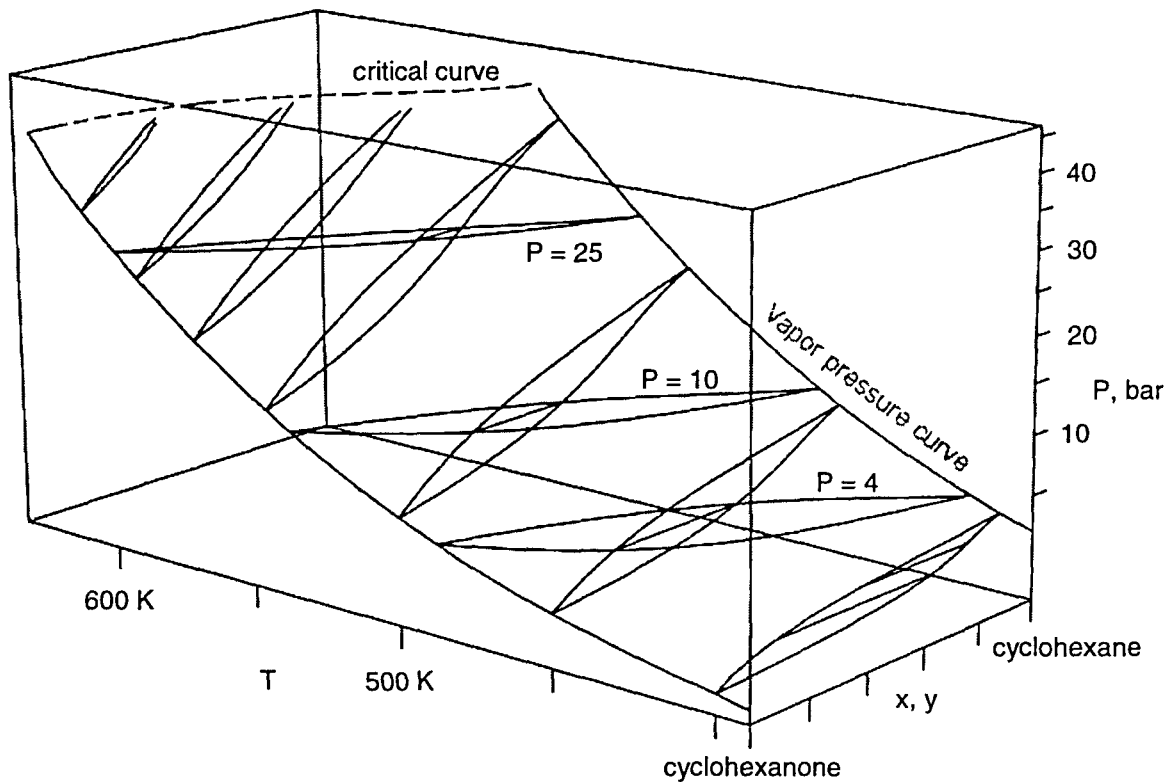


Figure 4.2 PTx diagram for cyclohexanone and cyclohexane.

Figure 4.3 shows the minimum-boiling azeotropic PTx diagram for cyclopentane and acetone [17]. The interaction parameter for this binary mixture is best fit at 0.119⁴. Since the pressure range is large, the details of the azeotropic loops (isotherms, isobars) are not shown clearly in Figure 4.3. The diagram is magnified in Figure 4.4 to show the azeotropic loops in greater detail.

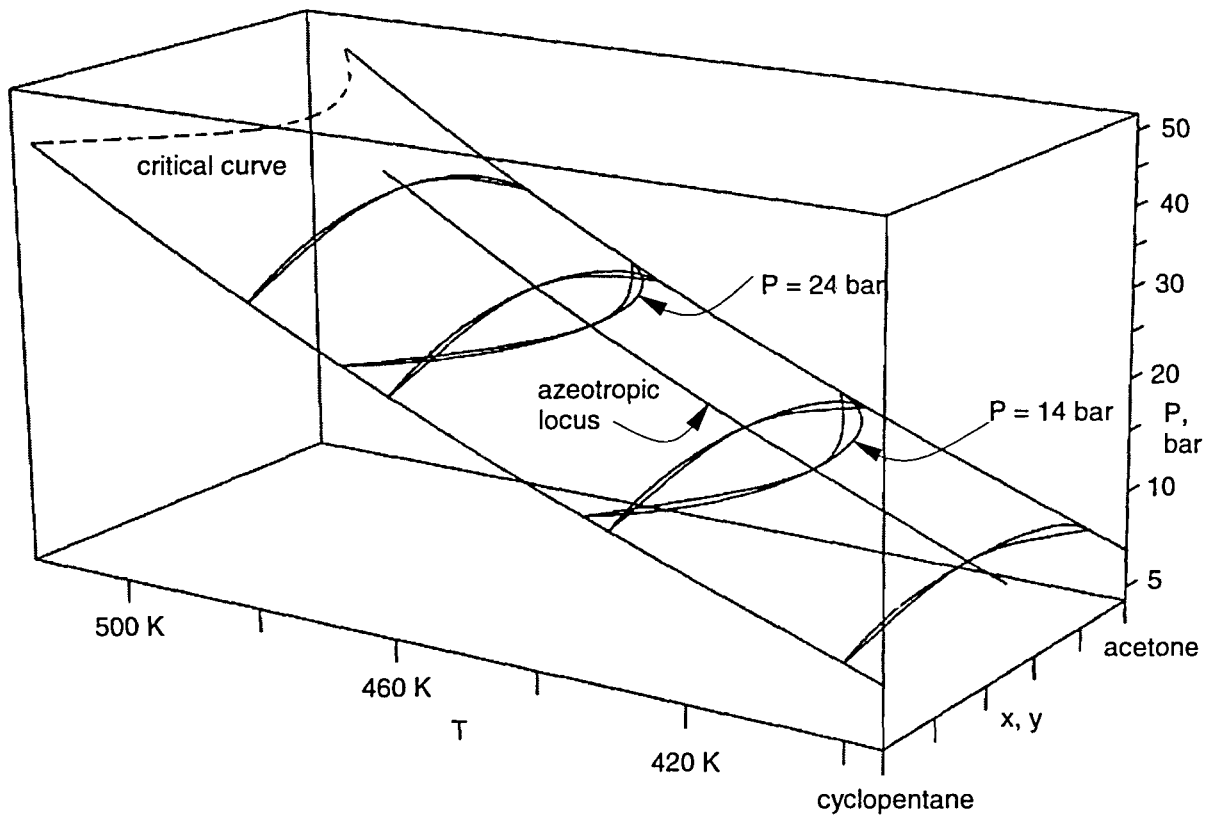


Figure 4.3 PTx diagram for cyclopentane and acetone.

⁴ The interaction parameter was adjusted according to the azeotropic composition and temperature given in Horsley, L. H., *Azeotropic data III, Advances in Chemistry Series 116*, American Chemical Society, Washington D. C. (1973), page 170.

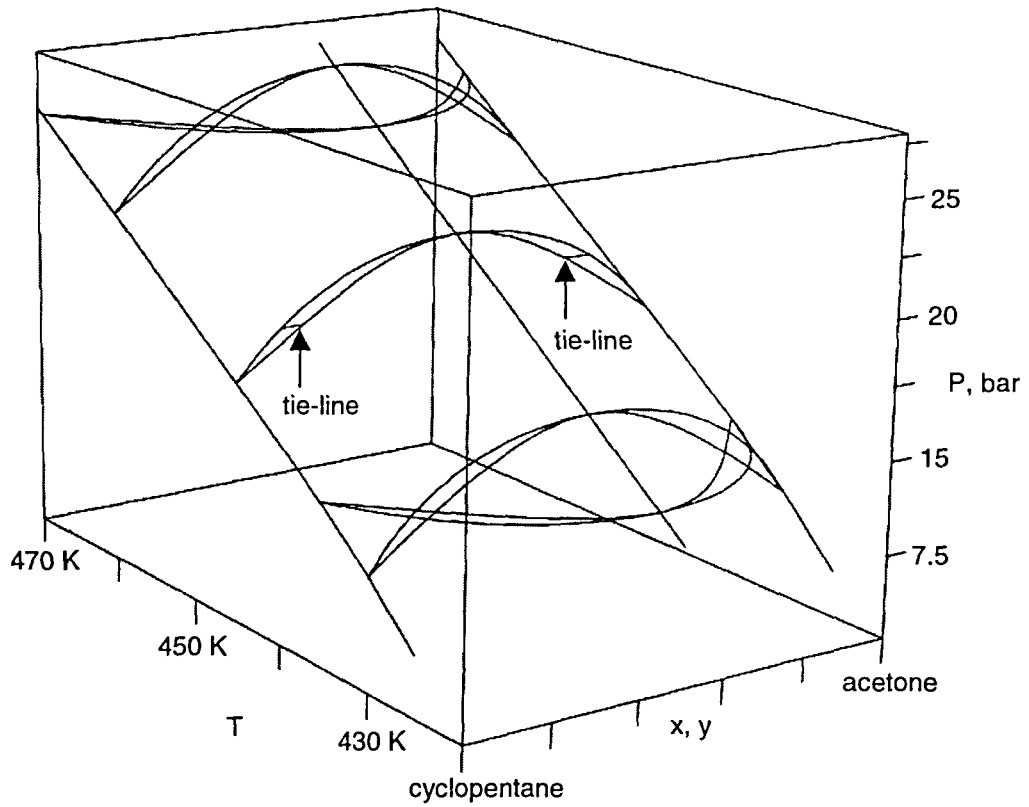


Figure 4.4 Magnified PTx diagram for cyclopentane and acetone.

Two tie lines have been added to the center loops. The homogeneous liquid phase lies above the loops whereas the vapor phase lies below.

CHAPTER 5. MAKING OF THREE-DIMENSIONAL TERNARY DIAGRAMS

The idea for making three-dimensional ternary phase diagrams arose from the Ph.D. dissertation of D.C. Coy [3] who showed graphic images of ternary-mixture properties in fundamental thermodynamic variables. Dr. Coy chose the ternary mixture carbon dioxide, ethylene, n-butane, in which carbon dioxide and ethylene form an azeotrope. As a consequence, it was decided to examine the phase behavior of ternary mixtures generally in this work by creating three-dimensional ternary diagrams.

Two FORTRAN programs were written to automate the construction of ternary diagrams: the ternary surface program (TS), which creates geometric-format data files for displaying the isothermal or isobaric phase-equilibrium surfaces of a ternary system using MOVIE.BYU software, and the GEOTOIV program, which converts the geometric data file format to `iv` file format for displaying graphics through OPEN INVENTOR software. These source files are named `TS.f` and `GEOTOIV.f`. They are stored in the directory `/home/kong/research/aspens/`. The TS program was written in the early stages of this work when all graphics were displayed using MOVIE.BYU, thus the geometric data format. At a later stage, alternate graphical software named OPEN INVENTOR was found that could draw dynamic views of three-dimensional objects. This also solved the line-drawing

problem in MOVIE.BYU¹.

OPEN INVENTOR software provides trackball interaction with the on-screen graphics, such as rotation, translation, and enlargement, and it allows detailed study of the structure of a three-dimensional object. These features make OPEN INVENTOR software a valuable tool for this work, and the GEOTOIV program became an important utility for converting geometric-format files to *iv*-format files.

There are four major functions in the TS program: (1) read a script file, create an ASPEN PLUS input file, and invoke the ASPEN PLUS simulator to execute the input file; (2) read the phase-equilibrium results computed by ASPEN PLUS and write the results to a temporary data file; (3) read the phase-equilibrium results from the temporary file, invoke a subprogram to triangulate the surface, and write the final results to a geometric-format data file; (4) rename the geometric-format data file and clean up all other files related to the ASPEN PLUS operations.

A script file with an extension *.scr* after its name must be prepared for executing the TS program. Table 5.1 shows a sample format of the script file prepared for a carbon dioxide, ethylene, n-butane ternary mixture. Note that the first column shows the line numbers in the script file but should not be

¹ MOVIE.BYU is incapable of drawing an individual line or a curve. This makes the drawing of tie lines to connect bubble-point surfaces and dew-point surfaces almost impossible. To solve the problem, a FORTRAN program called TIE was written to create a hexagonal tube with a very small radius to represent a line. The source file was named TIE.f and is stored in the directory */home/kong/research/aspn/*. Because of the different normal vectors on the surface of the hexagonal tube, its color could not be well represented by MOVIE.BYU without additional work to change the shininess factor of the tube to 1. OPEN INVENTOR has a line-drawing utility called *SoLineSet* as described in chapter 4 in Table 4.2. Moreover, OPEN INVENTOR is capable of linking to the OpenGL libraries which have their own line-drawing utility. In short, OPEN INVENTOR software makes line drawing much easier than MOVIE.BYU. Otherwise, making the figures in chapter 4 would have been almost impossible.

Table 5.1 The format of a script file for the TS program.

1	! SCRIPT FILE FOR CO2, C4H10-1 AND C2H4 TERNARY SYSTEM	
2		
3	CO2	{Component A}
4	C4H10-1	{Component B}
5	C2H4	{Component C}
6		
7	0.1333	{BIP for AB}
8	0.0552	{BIP for AC}
9	0.0922	{BIP for BC}
10		
11	D	{Bubble point or Dew point surface}
12	T	{T: isothermal prism, P: isobaric prism}
13	270.0	{fit temperature in K, or fit pressure in bar}
14		
15	41	{Number of constant mole-fraction lines, max=101}
16		
17	1.0	{parameter a: controls equal-spacing, 0:no control}
18	0.0	{parameter b: controls non-linear spacing}
19		
20	0	{constant composition line component}
21		{0: default component A}
22		{1: component A, 2: component B, 3: component C}

included in the script file itself.

The first line of the script file shows the title or comments about the content. One should avoid wordy sentences so that the title will not run over to the second line. The TS program reads only the title on the first line. Lines 3, 4 and 5 show the component identification names for components A, B and C, respectively. The components are arranged in a specific order as shown by the placement in the composition prism in Figure 5.1.

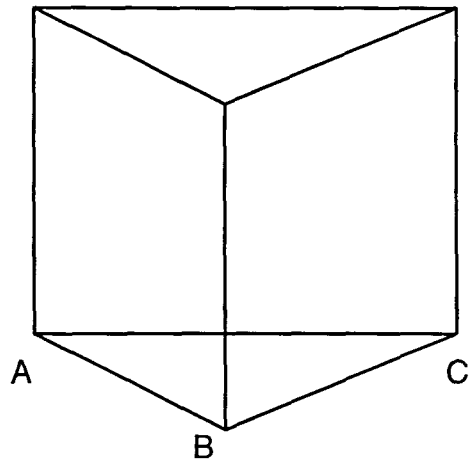


Figure 5.1 The order of components A, B and C in the (unturnd) prism.

Each component's identification name is its molecular formula as defined and recognized by ASPEN PLUS. It can be found on the `Component.Main` form in the ASPEN PLUS Forms pull-down menu, and then from the `Components` and `Main` sub-menus.

Lines 7, 8 and 9 show the binary interaction parameters for binary mixtures A-B, A-C, and B-C, respectively. Specifying 'B' on line 11 causes the TS program to perform a bubble-point surface calculation; 'D' results in a dew-point surface calculation. To draw an isothermal pressure-composition prism, specify 'T' on line 12 and its temperature value in Kelvin units on line 13. In a similar manner, to draw an isobaric temperature-composition prism, specify 'P' on line 12 and its pressure value in bar units on line 13.

The number on line 15 determines the total number of constant-composition contour lines that are drawn across the phase surface. To illustrate this idea, the

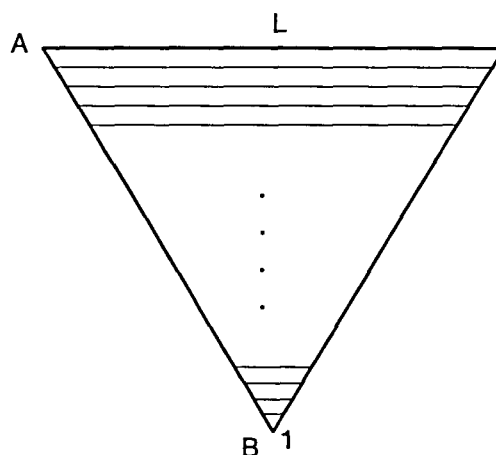


Figure 5.2 Surface contour lines projected onto a triangular base (equally spaced).

surface is projected onto a triangular base plane in Figure 5.2, and equally spaced contour lines are shown.

The number L is specified on line 15. The surface contour lines are drawn parallel to the constant mole-fraction lines of the component designated on line 21. To draw contour lines parallel to constant mole-fraction lines of component A, specify '0' or '1' on line 21. To draw contour lines parallel to constant mole-fraction lines of component B (as in Figure 5.2) or component C, specify '2' or '3' on line 21. Each surface contour line consists of a certain number of phase-equilibrium data points calculated from ASPEN PLUS. The set of lines is constructed in such a way that the first surface contour is a single point located at the pure-component vertex. As shown in Figure 5.2, the point marked 1 is at the B vertex. Each subsequent contour line will have one additional data point. For example, the n^{th} contour line

consists of n phase-equilibrium data points calculated from ASPEN PLUS. Such a construction makes it easy to triangulate the surface. The detailed procedure for surface triangulation is described in a later section. The total number of data points on the surface n_p is therefore determined by the number of surface contour lines specified on line 15, and it can be calculated from the following formula,

$$n_p = \frac{L(L+1)}{2} \quad (5.1)$$

where L is the total number of surface contour lines specified on line 15. For a relatively flat surface, a small number (e.g., 21) can be assigned to L , and that will be enough to generate a smooth surface, even though the triangular elements might be large. The advantage of using a small value of L is to save computing time and to reduce the size of the data files. However, with increasing complexity in surface curvature (such as with a saddle surface), it is necessary to make L larger to reduce the size of the elements and generate a smooth, nice-looking surface. The maximum number of surface contour lines that the program can accommodate is 101.

Lines 17 and 18 give the values for parameters a and b as defined in the linear expression $(a+bx)$. These values are used to adjust the non-equal spacing among the contour lines on a highly curved surface. The distance between each contour line (Δx_i) is normalized by the summation of all values as calculated in the following equation,

$$x_T = \sum_{i=1}^{L-1} |a + b \cdot i| \quad (5.2)$$

$$\Delta x_i = \frac{|a + b \cdot i|}{x_T} \quad (i = 1, 2, \dots, L-1) \quad (5.3)$$

The first contour line always starts at $x_1=1$, and the last contour line ends at $x_L=0$. In between, the positions of the surface contour lines are calculated by,

$$x_i = x_{i-1} - \Delta x_{i-1} \quad (i = 2, 3, \dots, L-1) \quad (5.4)$$

By specifying $a=1$ and $b=0$ on lines 17 and 18, the contour lines will be drawn with equal spacing as they are projected down onto the triangular base plane.

Figure 5.3 shows the equal spacing calculated from these values. Note that the y-axis in this figure has no physical meaning, whereas the x-axis represents the mole fraction of the component specified on line 20.

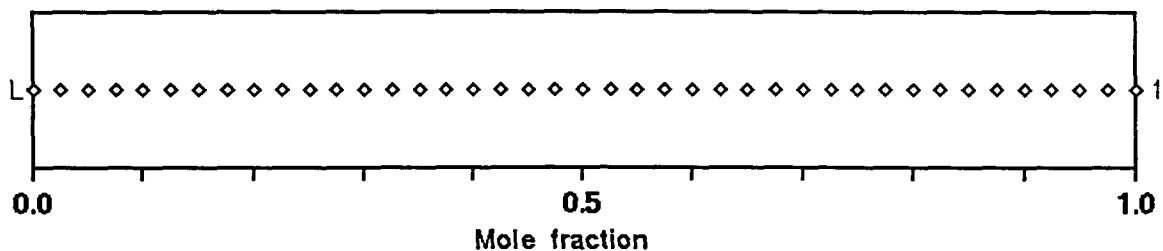


Figure 5.3 Surface contour lines with equal (default) spacing ($a=1$, $b=0$).

By default, the contour lines are equally spaced. This is suitable only for a simple surface with slight curvature. For highly curved surfaces needing contour lines that are not equally spaced, parameters a and b can be readjusted by trial and error until the triangulations between the lines are roughly the same size. For example, Figure 5.4 shows the contour line spacing calculated from $a=1$ and $b=0.2$. This setting is suitable for a surface with a slope that becomes steeper at the rich-component end of the range. For a surface with a peak in the middle, smaller line spacing is required around the peak, and Figure 5.5 shows roughly the way to set the line spacing. It is calculated from $a=-3$ and $b=0.1$. Finally, Figure 5.6 shows the line spacing for a surface with the steep slope on the lean-component end of the scale. This line spacing is calculated from $a=-4$ and $b=0.1$.

Readjusting parameters a and b on lines 17 and 18 contributes to a significant improvement in surface construction. In Figure 5.7, the dew-point surface for the ternary mixture carbon dioxide, n-butane, ethylene is constructed with the default settings shown in Table 5.1. The sizes of the triangular elements are significantly different over the surface and the definition will not be uniform. However, by setting $a=-4$ and $b=0.1$ to control the spacing of lines of constant n-butane composition (component B), the resulting dew-point surface in Figure 5.8 has triangular elements of roughly the same size.

Before executing the TS program, the ASPEN PLUS locker must be attached from the computer terminal by typing `add aspen` at the command prompt. Then follow the instructions printed on the computer screen to do the other necessary

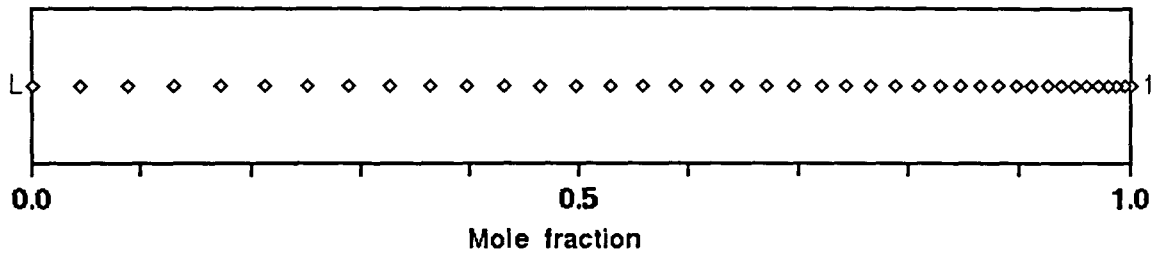


Figure 5.4 Surface contour-line spacing with $a=1$ and $b=0.2$.

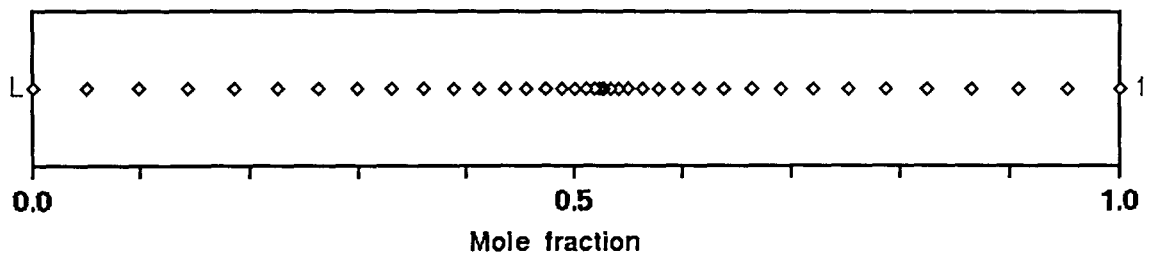


Figure 5.5 Surface contour-line spacing with $a=-3$ and $b=0.1$.

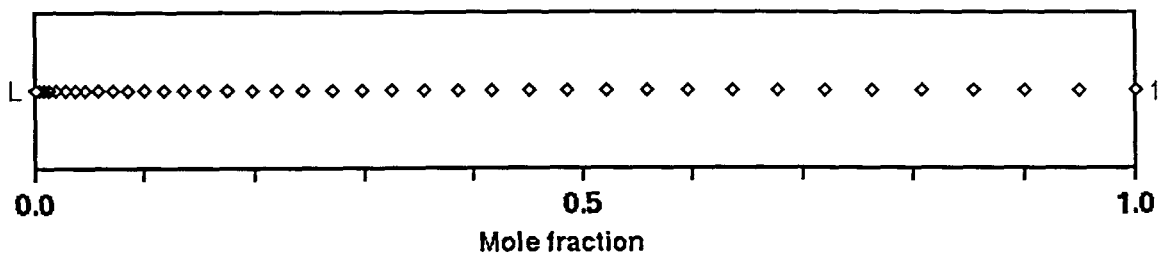


Figure 5.6 Surface contour-line spacing with $a=-4$ and $b=0.1$.

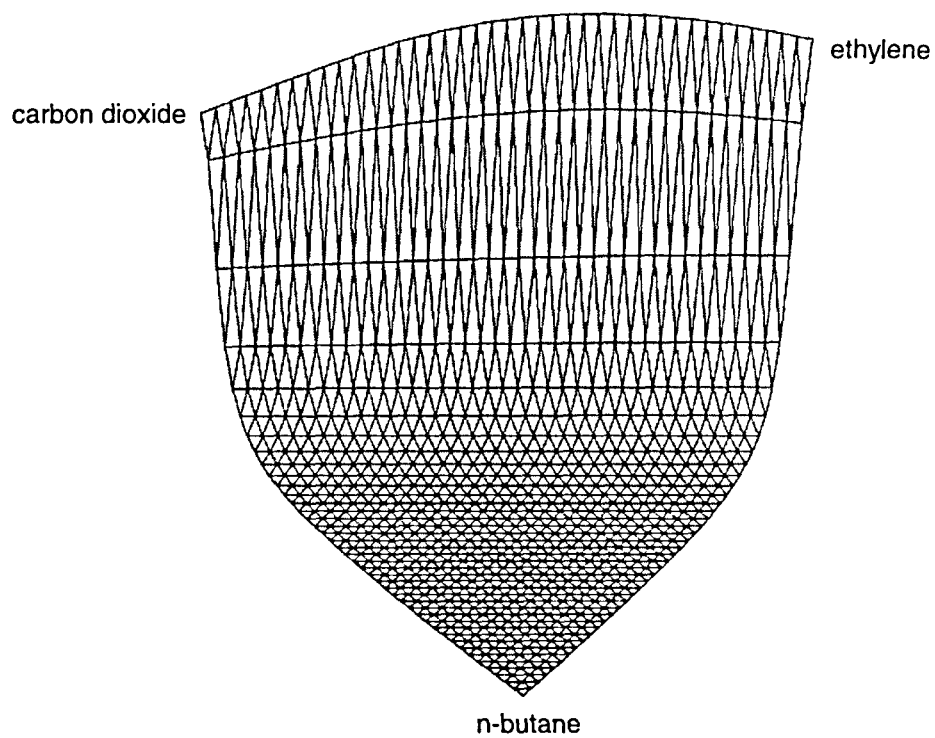


Figure 5.7 Dew-point surface with triangular elements of unequal size.

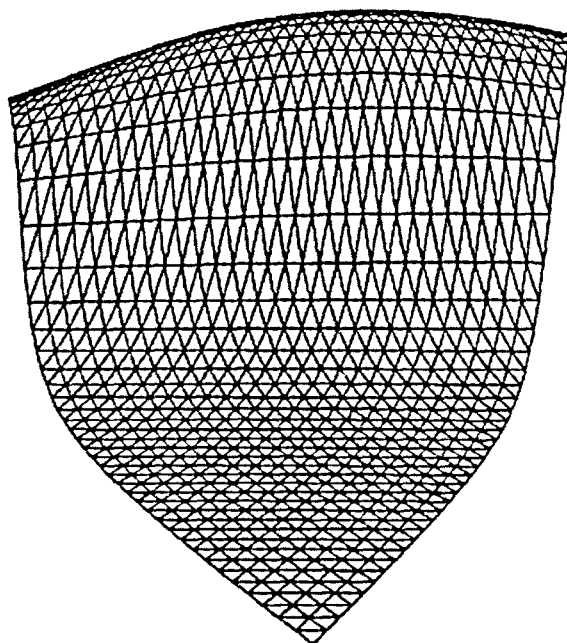


Figure 5.8 Dew-point surface with triangular elements of roughly the same size.

setup operations. This procedure is important since the TS program invokes the ASPEN PLUS simulator internally, and the external setup must be done prior to executing the program. TS was compiled on an alpha workstation and can be executed only on workstations of the same type. Alpha workstations also speed up the computation.

After the script file has been prepared, there are two options for executing the TS program – the default command `TS scriptfile` and the command `TS -w scriptfile` with option `-w`. In this illustration `scriptfile` is the name of the script file but without the extension `.scr`. If the command `TS scriptfile2` is issued, the TS program will first check the validity of the `scriptfile`. Then it invokes subprogram `MAKE_INP` to read the information written in the script file and create an ASPEN PLUS-format input file, which is named `ternary.inp`. This is a Table Generation System type input file (TGS) as described in chapter 4 under the section “Generating phase-equilibrium data points”. The flowsheet simulation is not required since the process is only to do a flash calculation and tabulate the phase-equilibrium properties.

In the final section of the `ternary.inp` file, the TS program creates L number of `flashcurve` property tables, named PT-1 to PT-L, where L is the number of constant-composition lines specified on line 15 in Table 5.1. Each `flashcurve` property table represents a constant-composition contour line

² I assume that readers are familiar with the computer directory structure and file locations. Describing the procedures for making three-dimensional phase diagrams will be too tedious if I need to give detailed instructions on manipulating a computer.

designated on the surface and contains a certain number of equally spaced points consisting of component compositions. For example, property table PT-10 represents the 10th contour line on the surface (counting from the pure component end) and contains 10 equally spaced points giving information about the overall composition along that line. As discussed in the section on Ternary systems in chapter 2, a 3-component, 2-phase system has 3 degrees of freedom. Drawing an isothermal pressure-composition phase diagram implies that two additional variables must be fixed in order to calculate the dew-point or bubble-point pressure. These two variables are the compositions of any two components. Therefore, after the `ternary.inp` file has been created, the TS program invokes ASPEN PLUS to execute the input file `ternary.inp` by issuing the command `aspen ternary.inp tttt`. This informs ASPEN PLUS to label all of its intermediate files with the name `tttt` before the extensions so that the clean-up procedures at the end of the execution can be carried out easily.

The command `TS -w scriptfile` can be used only if an input file `ternary.inp` is present. The `-w` option causes the TS program to skip the `MAKE_INP` subprogram and go straight to the execution of the input file `ternary.inp`. With this option, the information in the input file can easily be modified. The modification includes specifying any numerical values for constant-composition lines or using a different equation of state to predict the phase behavior, such as the Redlich-Kwong-Soave equation. This information cannot be specified in the script file.

After the input file is created, ASPEN PLUS reads the necessary information from the input file, and most importantly, it reads every composition point in each of the property tables (PT). Then it evaluates the corresponding bubble-point or dew-point pressure values and tabulates them in the ASPEN PLUS-format report file named `ternary.rep`. There are a total of L such tables with the ternary mixture compositions and the corresponding pressure values tabulated. The TS program also creates a data file named `highlow.dat`, which stores only two numbers. When pressure-composition values are being evaluated for an isothermal prism, `highlow.dat` stores the maximum and minimum pressure values. Conversely, when temperature-composition values are being evaluated for the isobaric prism, `highlow.dat` stores the maximum and minimum temperature values. These are used to locate the maximum and minimum points in the prism for size normalization.

The compositions and the corresponding pressure values in the `ternary.rep` file are later extracted and retabulated in a data file called `ternary.dat`. In the `ternary.dat` file, the first, second, and third columns tabulate mole fractions of components A, B, C, respectively, and the fourth column tabulates the corresponding pressure values (or temperature values for an isobaric prism). Next, the TS program invokes the `MAKE_TRI_COOR` subprogram to read the tabulated composition and pressure data points from `ternary.dat` and translate them to the prism coordinate system (shown in Figure 5.9) in accord with the following transformation equations,

$$x = \frac{x_B}{2} + x_C \quad (5.5)$$

$$z = x_B \cdot \cos\left(\frac{\pi}{6}\right) \quad (5.6)$$

$$y = 0.1 + \frac{0.9 - 0.1}{P_{\max} - P_{\min}} \cdot (P - P_{\min}) \quad (5.7a)$$

or

$$y = 0.1 + \frac{0.9 - 0.1}{T_{\max} - T_{\min}} \cdot (T - T_{\min}) \quad (5.7b)$$

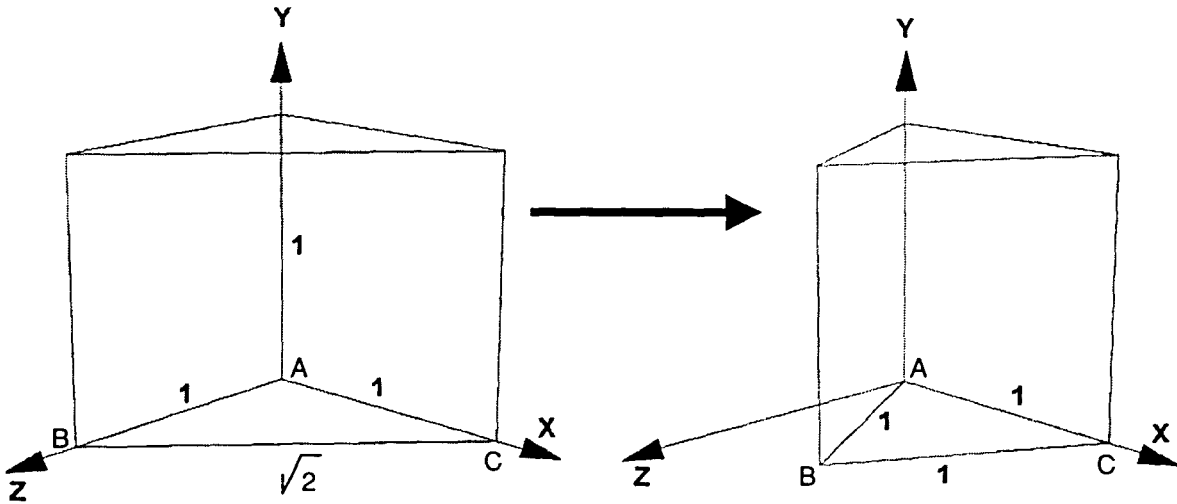


Figure 5.9 Schematic representation of the coordinate transformation, Cartesian (left) to equilateral triangular prism.

The mole fractions of components B and C are x_B and x_C . The mole fraction of component A (x_A) is not included in any of the transformation equations. In ternary systems, knowing the compositions of any two components gives the composition of the third (ie. $x_A = 1 - x_B - x_C$). Equations (5.7a) and (5.7b) are the

normalization equations used to calculate the height in the prism. The maximum and minimum pressure (or temperature) is set at a height of 0.1 and 0.9 in the prism. For an isothermal pressure-composition prism, equation (5.7a) will be used. If the TS program performs isobaric temperature-composition calculations, equation (5.7b) will be used. The values of P_{\max} , P_{\min} or T_{\max} , T_{\min} are recorded in the data file `highlow.dat`. P or T comes from the tabulated pressure or temperature values in the fourth column of the data file `ternary.dat`.

The TS program then creates a geometric-format file `ternary.geo` to store the x, y, z coordinates calculated from the transformation equations. The data stored in the geometric-format file can be displayed using MOVIE.BYU graphical software. There are three important sections in such a file. Table 5.2 shows a sample geometric-format data file which was used with MOVIE.BYU software to draw the square shown in Figure 5.10 consisting of two triangular elements. The numerical values in the left column of Table 5.2 indicate the line numbers in the sample data file for reference but should not be included in the actual geometric file.

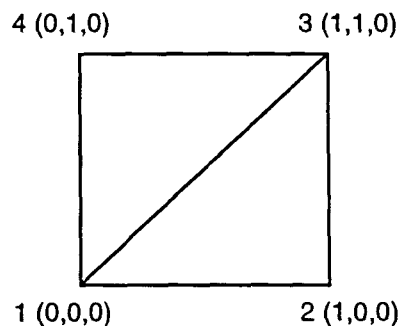


Figure 5.10 Square with two triangular elements drawn with MOVIE.BYU.

Table 5.2 Sample geometric-format data file.

1	1	4	2	6		
2	1	2				
3	0.000000E+00	0.000000E+00	0.000000E+00	1.000000E+00	0.000000E+00	0.000000E+00
4	1.000000E+00	1.000000E+00	0.000000E+00	0.000000E+00	1.000000E+00	0.000000E+00
5	1	2	-3	1	3	-4

The first section (lines 1 and 2) shows structural information about the square. On line 1 the first number indicates that the square has only one “group.” The second number indicates that there are four points (nodes) on the square. The third and fourth numbers show, respectively, that the square has two elements and a total of six nodes on the two elements. Obviously, a single triangle has three nodes and two have six. The information on line 2 tells MOVIE.BYU that the square is constructed from element 1 (the lower right triangle) to element 2. It is important to note that each number on line 1 and line 2 occupies a length of eight spaces and must be right-justified. In other words, the final numerical character should end in the eighth space.

The second section (lines 3 and 4) shows the x, y, z coordinates of the vertices of the square. Each line consists of two coordinate points written in scientific format. The third section (line 5) shows the node connectivity of the square. Unlike an *iv* file, the first coordinate in a geometric-format file starts at 1. Therefore, as indicated on line 5, the first triangular element is constructed by connecting the first, second, and third points. Using a minus sign before the 3 tells MOVIE.BYU to terminate the element by connecting the third point back to the

starting point. Similarly, the second triangular element is constructed by connecting the first, third, and fourth points. The node connection is ended by connecting the fourth point back to the first point.

Thermodynamic surface triangulation

After the surface structure information and the calculated x, y and z coordinates have been written to the `ternary.geo` file, the TS program invokes the `MAKE_CONNECT` subprogram to triangulate the surface according to the L value on line 15 in the script file. The triangulation algorithm was developed from a model consisting of five constant-composition lines connected by sixteen triangles as shown in Figure 5.11.

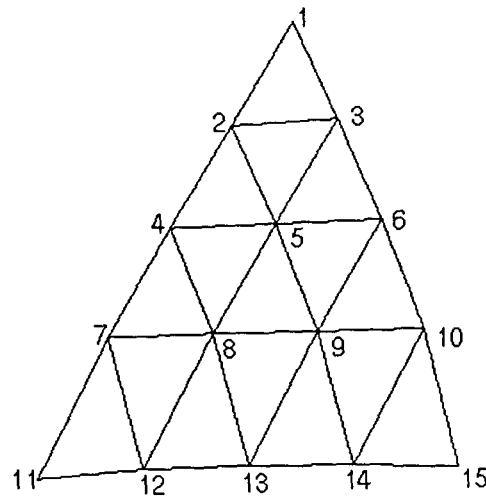


Figure 5.11 Model ternary phase surface with 5 constant-composition lines and 16 triangular elements.

The numerical values shown on each node are the indices of the coordinates. Note that the first index is placed on the first constant-composition line. The triangular elements are connected in a counterclockwise manner according to the connectivity shown in Table 5.3. There are two sets of connectivities, one for the upright triangles (123, 245, etc.) and the other for the inverted triangles (325, etc.).

The negative values tell the program to end the element by connecting the negative node to the starting node. The trend can be observed easily from the connectivity algorithm in Table 5.3. In connecting the upright triangles, the first column shows the coordinate indices beginning with 1 and running to the final index point on the $(L-1)^{\text{st}}$ constant-composition line. The indices in the second column are equal to the indices in the first column plus the current line number of the first column index. The indices in the third column are one greater than the indices in the second column multiplied by minus one. To find out on which constant-composition line (LINE) a given index (I) lies, the following inequalities may be applied.

Table 5.3 Connectivities for triangulating the surface shown in Figure 5.11.

Upright Triangles	Inverted Triangles
1 2 -3	3 2 -5
2 4 -5	5 4 -8
3 5 -6	6 5 -9
4 7 -8	8 7 -12
5 8 -9	9 8 -13
6 9 -10	10 9 -14
7 11 -12	
8 12 -13	
9 13 -14	
10 14 -15	

$$\frac{(LINE - 1) \cdot LINE}{2} < I \leq \frac{LINE \cdot (LINE + 1)}{2} \quad (5.8)$$

$$LINE^2 - LINE - 2I < 0 \quad \text{and} \quad LINE^2 + LINE - 2I \geq 0 \quad (5.9)$$

$$LINE < \frac{1 + \sqrt{1 + 8I}}{2} \quad (5.10a)$$

$$\text{and} \quad LINE \geq \frac{-1 + \sqrt{1 + 8I}}{2} \quad (5.10b)$$

I is the index number designated for the node of a small triangle, and $LINE$ is an integer-variable constant-composition line number to be determined. Figure 5.12 shows the mathematical algorithm for calculating constant-composition line numbers ($LINE$) as implemented by FORTRAN code in the TS program. The "WRITE" statement tabulates the triangulations as they appear under "Upright Triangles" in Table 5.3.

Only equation (5.10b) is used in this procedure. The TS program evaluates the right-hand term of inequality (5.10b) by substituting an index number (I). The resulting value is stored in the variable `CHECK`. Then the program iterates, starting

```

OPEN(UNIT=12, FILE='ternary.con', STATUS='UNKNOWN')

DO 100 I = 1, L*(L-1)/2
  CHECK = (SQRT(1+8.*REAL(I))-1.)/2.
  DO 200 J = 1, 101
    IF (CHECK .LE. J) THEN
      LINE = J
      GOTO 300
    ENDIF
  200 CONTINUE
  300 WRITE(12,'(3I8)') I, I+LINE, -(I+LINE+1)
  100 CONTINUE

```

Figure 5.12 FORTRAN code for triangulating upright triangles.

from one and increasing until it finds a number greater than or equal to CHECK. That number is assigned to the variable LINE. A series of connectivity indices for upright triangles, I , $I+LINE$, and $-(I+LINE+1)$, is then tabulated in a file named ternary.con.

The connectivity scheme for handling the inverted triangles is harder to follow. The numerical values in the first column are generated by the equation $I+LINE+1$, where I ranges from 1 to $L*(L-1)/2-L+1$. The range of I is gotten by observation and there is no specific analysis that describes it. The numerical values in the second and third columns are produced by $I+LINE$ and $-(2*(I+LINE+1)-I)$, respectively. The FORTRAN code for connecting the inverted triangles is shown in Figure 5.13.

The FORTRAN code shown in Figure 5.13 is similar to that used for triangulating the upright triangles shown in Figure 5.12 except for the range of I and the triangulation equations. The connectivity indices of the inverted triangles are

```

DO 400 I = 1, L*(L-1)/2-L+1
  CHECK = (SQRT(1+8.*REAL(I))-1.)/2.
  DO 500 J = 1, 101
    IF (CHECK .LE. J) THEN
      LINE = J
      GOTO 600
    ENDIF
500  CONTINUE
600  WRITE(12,'(3I8)') I+LINE+1, I+LINE, -(2*(I+LINE+1)-I)
400  CONTINUE

CLOSE (12)

```

Figure 5.13 FORTRAN code for triangulating inverted triangles.

appended to those of the upright triangles in the file `ternary.con`. The TS program finishes writing the geometric file `ternary.geo` by appending the connectivity indices from the file `ternary.con` to the x, y and z coordinates in the geometric file `ternary.geo`. At the end of the execution, TS cleans the directory by deleting some temporary files generated by ASPEN PLUS. It also renames the geometric file `ternary.geo` to `bsurf.geo` for a bubble-point calculation or to `dsurf.geo` for a dew-point calculation. Whether bubble- or dew-point calculations are performed is controlled in the script file on line 11 as shown in Table 5.1.

The geometric files `bsurf.geo` and `dsurf.geo` can be visualized through MOVIE.BYU graphical software. To get the best graphics display, use DECstation `pv0415.vincent.iastate.edu` because it has a 24-bit color screen, whereas other DECstations in the department have only 8-bit color screens. At the command prompt, type `add movie` to attach the MOVIE.BYU software locker. Then type `movX24` and three windows will appear on the computer screen. From the menu window, click on `read geo file` and type the name of the geometry file in the subsequent pop-up window. The three-dimensional object will appear on the computer screen in wireframe format. Shading, coloring, lighting, viewing position, and other graphical features can be manipulated in the menu window.

Since OPEN INVENTOR gave better graphics rendering for this work than MOVIE.BYU, all three-dimensional objects in this thesis are displayed through OPEN INVENTOR. A program called GEOTOIV was created to convert geometric files to `iv` files. As with the TS program, GEOTOIV was compiled on an alpha

workstation and is executable on alpha workstations only. At the command prompt, type `GEOTOIV geofile`, where `geofile` is the name of the geometric file without the `.geo` extension. The `GEOTOIV` program reads the geometric file and translates the information to an `iv` file having the same file name but with the extension replaced by `.iv`. Table 5.4 shows a sample `iv` file used to construct a bubble-point surface. Note that the first column shows the line number in the `iv` file but should not be included in the actual file itself.

The `iv` file for constructing ternary diagrams is similar to the `iv` file for binary diagrams as shown in Table 4.2. Table 5.4 uses the `ShapeHints` node on lines 5 and 6 to connect the indices in a counterclockwise manner and to turn on two-sided lighting for the rendered surfaces. Otherwise, the surfaces will be bright on one side and dark on the other. Since the `iv` file in Table 4.2 was used to draw lines, two-sided lighting was not required. Besides, the surface is constructed of many triangular facets whose connectivity is specified by `IndexedFaceSet` node as shown on line 23. Unlike the index numbering in `MOVIE.BYU`, `OPEN INVENTOR` starts the first coordinate with index zero. The color of the bubble-point surface is set to red and the color of the dew-point surface is set to green. This setting will be true for all drawings.

Since `OPEN INVENTOR` can only be executed on a Silicon Graphics workstation, `iv` files have to be transferred from an alpha workstation to an SGI workstation so that they can be displayed through `OPEN INVENTOR`. As described in the section “Generating images through `OPEN INVENTOR` software” in chapter 4,

Table 5.4 Sample iv file for constructing bubble point surface.

```

1 #Inventor V2.0 ascii
2
3 Separator {
4
5 ShapeHints {
6     vertexOrdering COUNTERCLOCKWISE    }
7
8 Material {
9     diffuseColor 1.0 0.0 0.0
10    emissiveColor 0.2 0.0 0.0
11    shininess 1
12    transparency 0.0          }
13
14 Coordinate3 {
15     point [
16         0.00000E+00 0.83758E+00 0.00000E+00,
17         0.25000E-01 0.84592E+00 0.00000E+00,
18         0.12500E-01 0.82120E+00 0.21651E-01,
19         .
20         .
21         .          ]}
22
23 IndexedFaceSet {
24     coordIndex [
25         0, 1, 2, -1,
26         1, 3, 4, -1,
27         2, 4, 5, -1,
28         .
29         .
30         .          ]}
31
32 }

```

there are two commands that can be used to display an iv file, `ivview` and `SceneViewer`. However, `ivview` is always preferable since it reads and displays many iv files at a time whereas `SceneViewer` imports iv files one by one. To do more complicated operations, such as copying, pasting, saving, printing, lighting, and others, `SceneViewer` will be the appropriate choice. The `bsurf.iv` file represents the bubble-point surface whereas the `dsurf.iv` file represents the dew-

point surface. `prism.iv` defines the prism geometry for the ternary bubble-point and dew-point surfaces. The coordinates of the prism can be calculated from the transformation equations (5.5) and (5.6) and are presented in Table 5.5. Other `iv` files can also be created to add isobaric planes, tie lines, and callouts to the drawing.

Table 5.5 The coordinates of the prism.

Lower Triangular Plane	x, y and z coordinates	Upper Triangular Plane	x, y and z coordinates
A	(0.0, 0.0, 0.0)	A	(0.0, 1.0, 0.0)
B	(0.5, 0.0, 0.866025)	B	(0.5, 1.0, 0.866025)
C	(1.0, 0.0, 0.0)	C	(1.0, 1.0, 0.0)

Figure 5.14 shows the simplest possible ternary pressure-composition diagram – for the mixture n-pentane, benzene, acetone at $T=298.15$ K. By “simple”, is meant that none of the three binary sub-systems within the ternary have azeotropes or critical points, and that the bubble-point curves are increasing (or decreasing) monotonically (implying no liquid immiscibility). The interaction parameters used for the binary mixtures n-pentane-benzene, n-pentane-acetone, and benzene-acetone were 0.0174, 0.020 and 0.020, respectively.

The upper and lower surfaces represent the bubble-point and dew-point functions, respectively. The triangular plane passing through the prism is for a particular pressure (0.5 bar). Tie lines (not shown at this pressure) form between the curves where the isobaric plane intersects the bubble- and dew-point surfaces. The three white tie-lines in Fig. 5.14 are placed at a pressure of 0.3 bar.

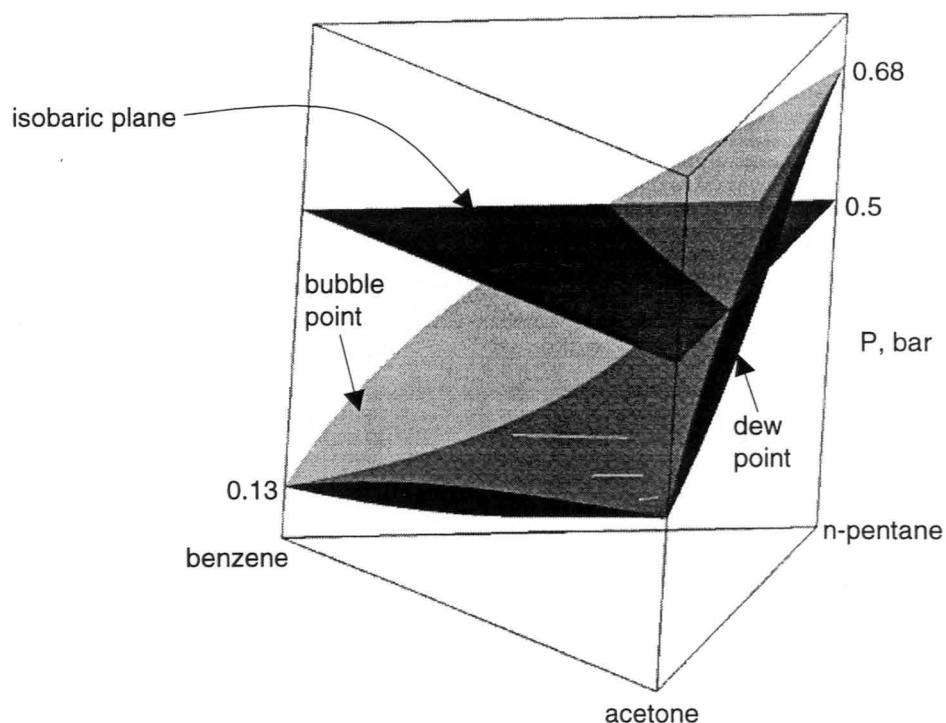


Figure 5.14 Ternary p-xy diagram for the system benzene, acetone, n-butane at $T=298.15$ K.

Figure 5.15 shows another non-azeotropic pressure-composition diagram, this time for the ternary mixture n-pentane, nitrobenzene, i-butane at $T=398.15$ K. The binary interaction parameters used for the n-pentane-nitrobenzene, n-pentane-i-butane, and nitrobenzene-i-butane binaries were 0.10, 0.020 and 0.020, respectively.

A wavy bubble-point surface can be seen in the prism, and it is confirmed by the extrema in the nitrobenzene, n-pentane binary diagram in Figure 5.16. This indicates the existence of a three-phase (vapor-liquid-liquid equilibrium) region. Two binary pressure-composition diagrams for this system were generated using ASPEN PLUS, and they are shown in Figures 5.16 and 5.17.

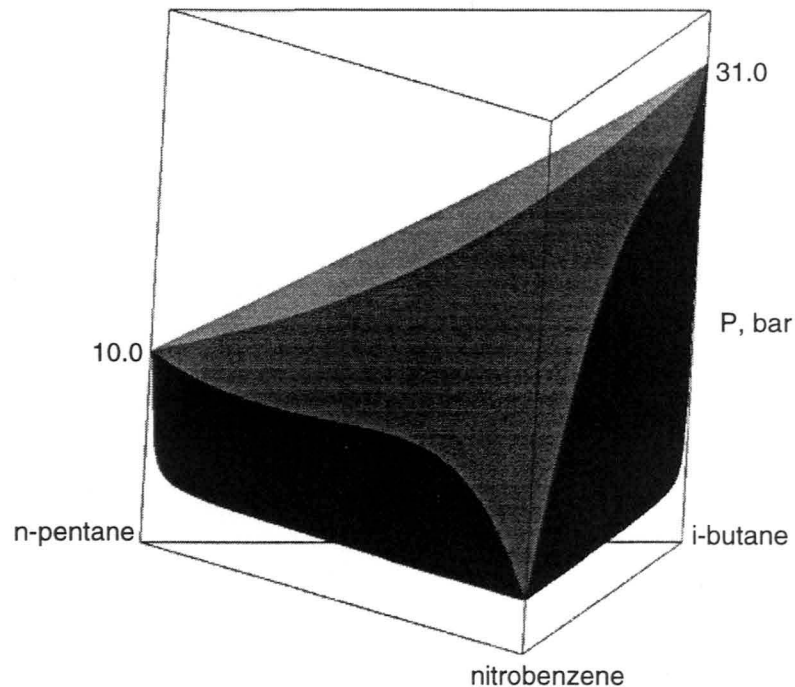


Figure 5.15 Isothermal pressure-composition prism for the n-pentane, nitrobenzene, iso-butane ternary at $T=398.15$ K (bubble-point surface is transparent).

The wavy bubble-point curve in Figure 5.16 indicates that three-phase equilibrium can exist at a pressure in the vicinity of 8.5 bar. Figure 5.17 shows the exact location of the three-phase points at compositions that give equal fugacities for the two components in the three phases. From the ASPEN data table that accompanies this diagram, the vapor-liquid-liquid equilibrium pressure was found to be 8.617 bar, and the compositions of the n-pentane-rich and lean liquid phases were 0.8005 and 0.2627, respectively.

With the addition of a third component (i-butane), the vapor-liquid-liquid equilibrium pressure and the coexisting compositions will be altered. The three-phase locus can be calculated by using the `FLASH3` block in ASPEN PLUS.

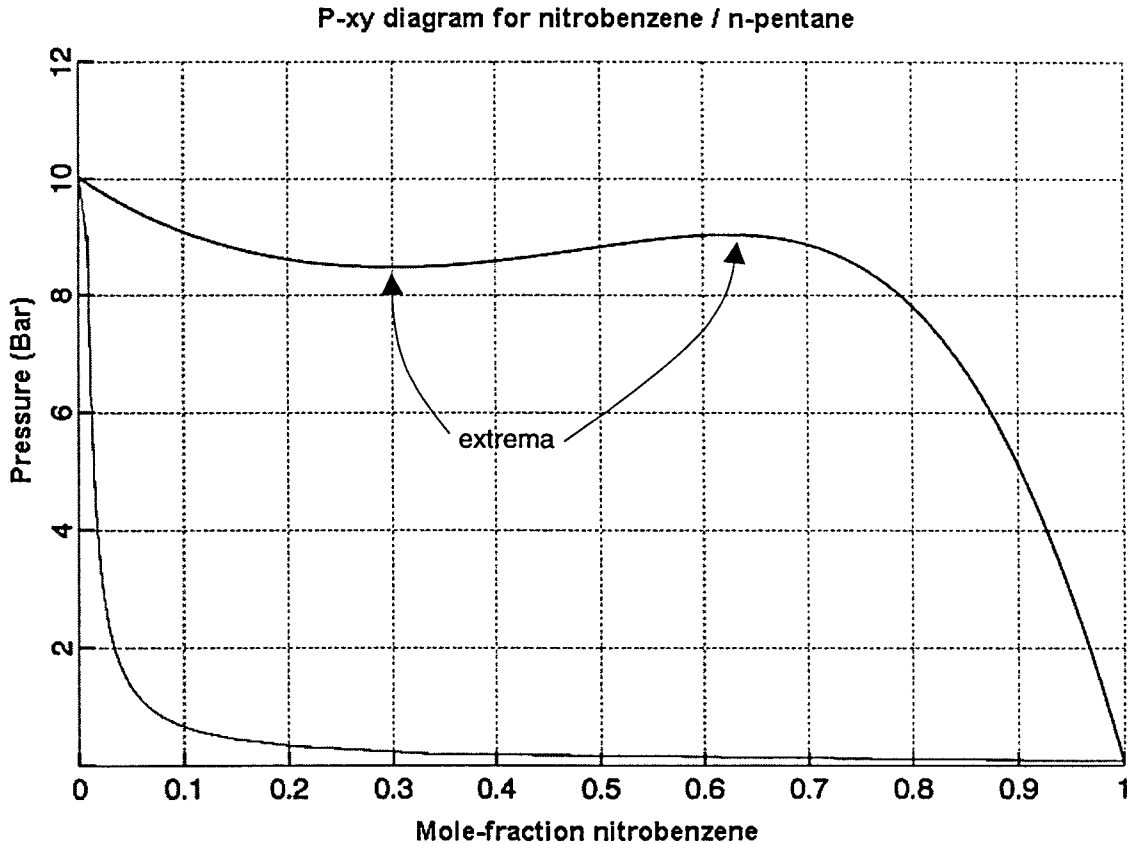


Figure 5.16 P-xy diagram for nitrobenzene and n-pentane at $T=398.15$ K.
The wavy bubble point curve indicates immiscible liquid phases.

FLASH3 determines the phase conditions of vapor-liquid-liquid equilibrium for a mixture. In the `Flash3.Main` input form, two of the following constraints must be specified: temperature, pressure, heat duty, and vapor fraction – except the combination of heat duty and vapor fraction.

In this project, points on the three-phase locus were determined (essentially) by isothermally compressing the ternary mixture³, initially at a pressure of 5 bar

³ This is done here by specifying a temperature of 398.15 K and a negative heat duty (heat out of the process).

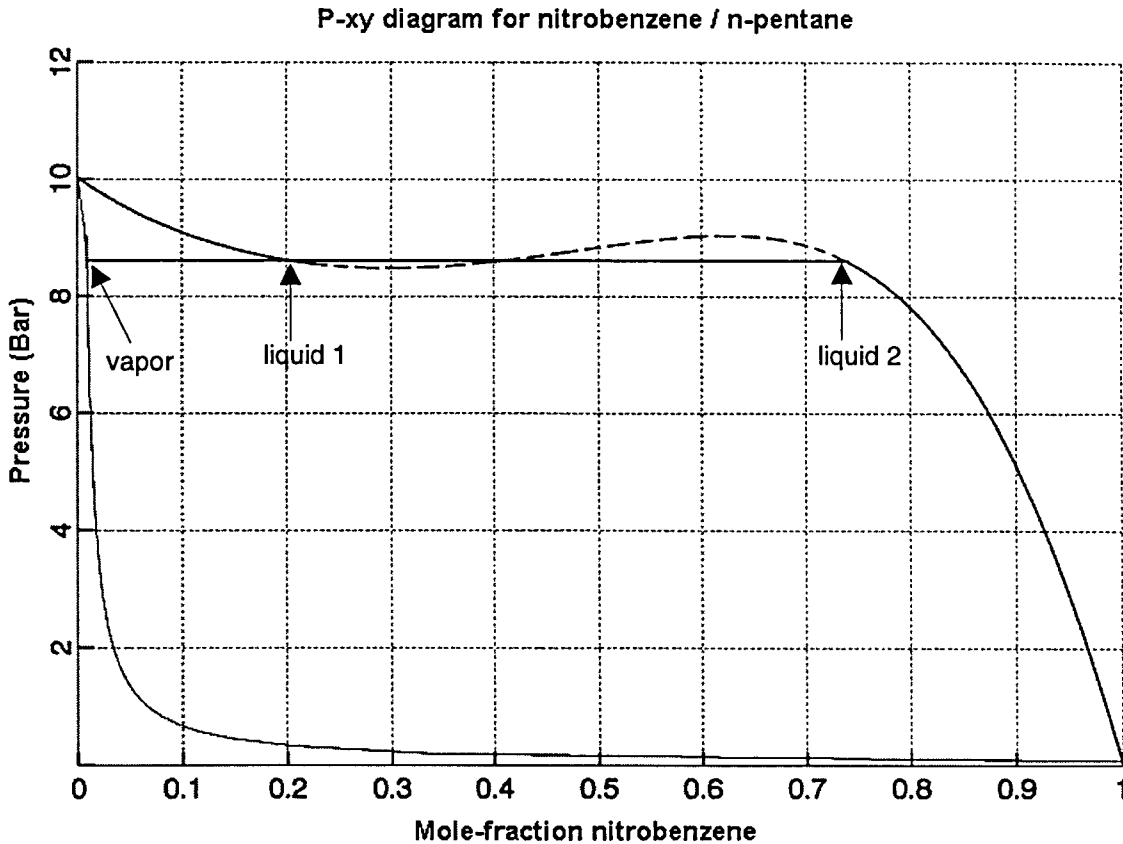


Figure 5.17 P-xy diagram for nitrobenzene, n-pentane at $T=398.15$ K.
Three phase line is at $P = 8.617$ bar.

(which is below the three-phase pressure) and at a composition that would result in a three-phase split. The mixture composition and inlet pressure of 5 bar are specified on the `Stream.Main` form, whereas the temperature and heat duty for the flash (compression) process are specified on the `flash3.Main` form. Table 5.6 shows the input ternary mixture compositions for the individual flash calculations and the corresponding heat duties (heat taken out of the system for isothermal compression). Table 5.7 shows the vapor-liquid-liquid compositions calculated from the `FLASH3` block.

Table 5.6 Input flash conditions for calculating the three-phase locus for the ternary mixture n-pentane, nitrobenzene, i-butane, T = 398.15 K.

Run #	n-Pentane		Nitrobenzene		i-butane		Heat Duty	
	(kmol/s)	(molefrac.)	(kmol/s)	(mole frac.)	(kmol/s)	(mole frac.)	(kw)	(kw/mol)
1	1	0.5000	1	0.5000	0	0.0000	-2300	-1150
2	1	0.4762	1	0.4762	0.1	0.0476	-3000	-1429
3	1	0.4545	1	0.4545	0.2	0.0909	-3100	-1409
4	1	0.4348	1	0.4348	0.3	0.1304	-3200	-1391
5	1	0.4167	1	0.4167	0.4	0.1667	-3500	-1458
6	1	0.4000	1	0.4000	0.5	0.2000	-4000	-1600
7	1	0.3846	1	0.3846	0.6	0.2308	-4300	-1654
8	1	0.3704	1	0.3704	0.7	0.2593	-4800	-1778
9	1	0.3571	1	0.3571	0.8	0.2857	-5300	-1893
10	1	0.3448	1	0.3448	0.9	0.3103	-6000	-2069
11	1	0.3436	1.01	0.3471	0.9	0.3092	-7371	-2533

Table 5.7 Three-phase compositions for n-pentane, nitrobenzene, i-butane, T = 398.15K.

Run #	n-pentane			nitrobenzene			Pressure (bar)
	Liquid 1	Liquid 2	Vapor	Liquid 1	Liquid 2	Vapor	
1	0.8005	0.2625	0.9907	0.1995	0.7375	0.009276	8.6173
2	0.7536	0.2641	0.8905	0.2077	0.7133	0.008755	9.3182
3	0.7099	0.2655	0.8095	0.2161	0.6898	0.008341	9.9639
4	0.6689	0.2670	0.7425	0.2249	0.6670	0.008006	10.5616
5	0.6286	0.2689	0.6831	0.2343	0.6429	0.007713	11.1469
6	0.5868	0.2716	0.6282	0.2455	0.6163	0.007449	11.7392
7	0.5486	0.2745	0.5825	0.2570	0.5905	0.007233	12.2739
8	0.5075	0.2786	0.5387	0.2719	0.5608	0.007031	12.8270
9	0.4669	0.2846	0.4993	0.2888	0.5276	0.006852	13.3622
10	0.4150	0.2953	0.4602	0.3203	0.4840	0.006680	13.9263
11	0.3791	0.3135	0.4368	0.3463	0.4385	0.006577	14.2870

Figure 5.18 shows the liquid-liquid equilibrium and vapor-liquid equilibrium tie lines for the three-phase region as viewed from the top of the prism. Figure 5.19 shows the isothermal, pressure-composition phase diagram with the wavy bubble-point surface cut out and replaced by the vapor-liquid-liquid equilibrium coexistence curves and tie lines. The VLE tie lines that connect to the pentane-rich vapor phase are visible through the transparent bubble-point surface.

Figure 5.20 shows the complete, isothermal, pressure-composition diagram for the n-pentane, nitrobenzene, i-butane ternary system. The vertical, U-shaped walls represent the liquid-liquid equilibrium region and are connected by four isobaric sections containing tie lines. Starting at the lowest section, the pressure values of the isobaric cuts are 17, 21, 26 and 31 bar.

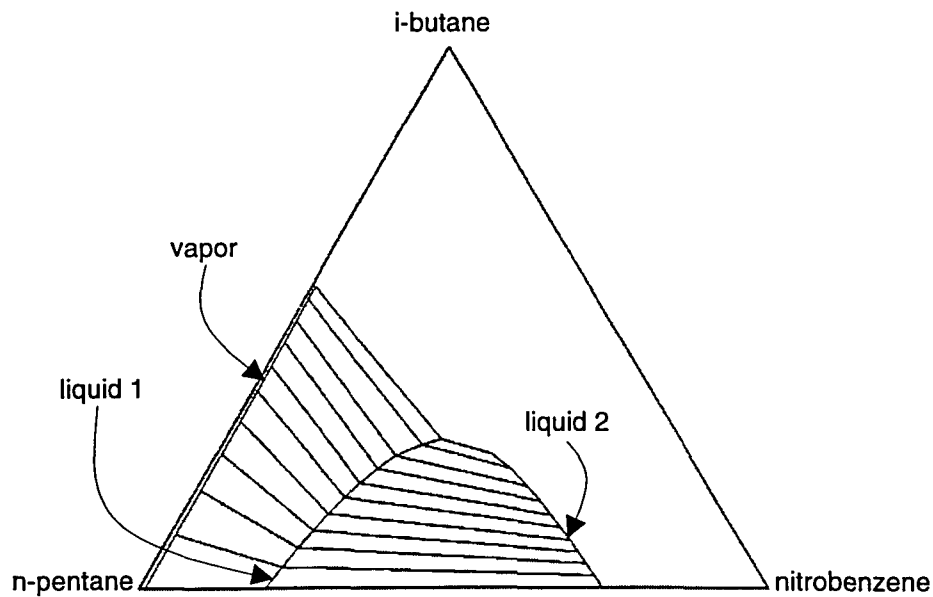


Figure 5.18 LLE and VLE tie lines for the ternary mixture, $T = 398.15 \text{ K}$.

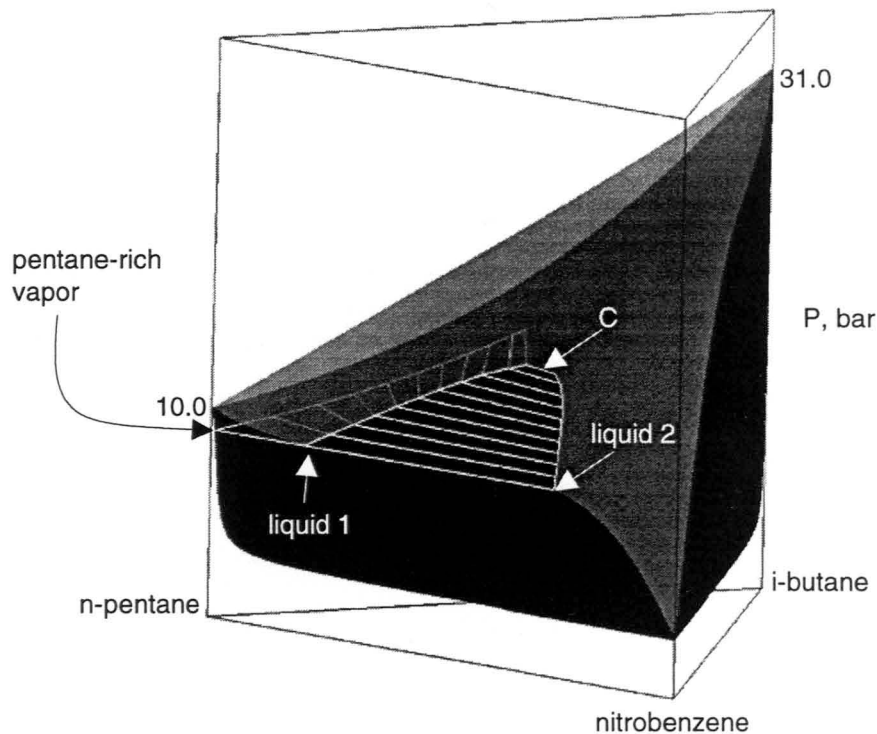


Figure 5.19 Isothermal ternary phase diagram for n-pentane, nitrobenzene, i-butane showing the VLLE coexistence curves and tie lines.

The liquid-liquid equilibrium data were calculated by the `DECANTER` and `SENSITIVITY` blocks implemented in the `ASPEN PLUS` simulator. Since `ASPEN PLUS` cannot carry the liquid-liquid equilibrium calculations all the way to the critical condition, the Heidemann and Khalil method [10] was used to predict the liquid-liquid equilibrium critical line.

`DECANTER` is a mathematical model implemented in `ASPEN PLUS` that can perform liquid-liquid equilibrium calculations for a mixture. Conditions such as the temperature and pressure of the mixture can be specified on the `Decanter.Main` form.

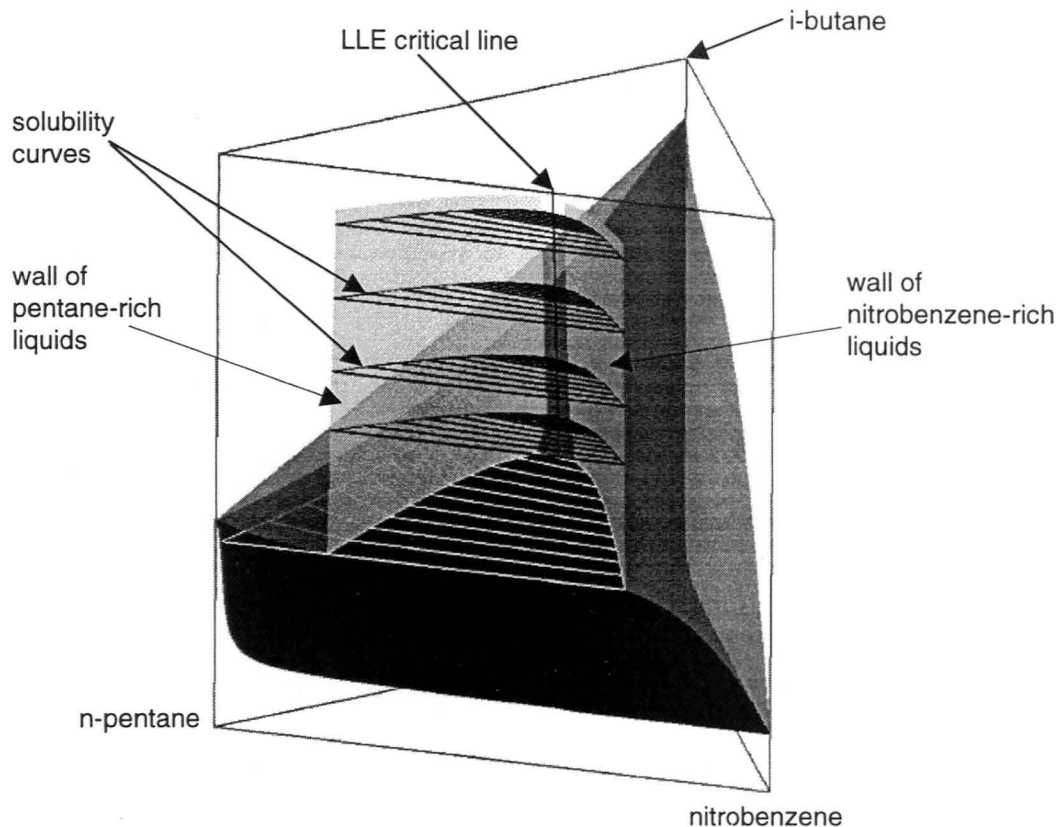


Figure 5.20 Complete, isothermal, pressure-composition diagram for the n-pentane, nitrobenzene, i-butane ternary mixture.

Sensitivity blocks examine the response of a simulated process to individual variables and tabulate the results as functions of those variables. From the `Forms` pull-down menu, select `Model Analysis Tools` and `Sensitivity` sub-menus. The `Sensitivity Object Manager` form will appear. Click on `Create` to create a new sensitivity block, or click on `Input` to change the information for an existing block. Sensitivity blocks consist of three sections: The `Sensitivity`. Define form is used to define the flowsheet variables that are to be tabulated on the

`Sensitivity.Tabulate` form. The variable names should be valid FORTRAN variable names. After each field is filled, press `Enter` on the keyboard and ASPEN PLUS will move the cursor to the next input field automatically. On the `Sensitivity.Vary` form, define the key (independent) variables for the flowsheet and specify ranges of their values for examining the response of the results. Finally, on the `Sensitivity.Tabulate` form, specify the variables for which results will be tabulated.

For determining the lowest section of liquid-liquid equilibrium tie lines, specify the temperature and pressure to be 398.15 K and 17 bar on the `Decanter.Main` form. On the `Sensitivity.Define` form, define variables for the mole fractions of n-pentane and nitrobenzene in both liquid phases and specify those variables on the `Sensitivity.Tabulate` form to obtain the results. There are two procedures for setting the values of independent variables on the `Sensitivity.Vary` form. For the region distant from the critical point (where liquid-liquid equilibrium calculations are easier), set the molar flow rates of n-pentane and nitrobenzene each to be 1 kmol/sec and vary the molar flow rate of i-butane from 0 to 1 kmol/sec. This varies the bulk composition from equimolar pentane/nitrobenzene to equimolar in the ternary.

The results tabulated on the `Sensitivity.Results` form show that there is liquid-liquid separation until the molar flow rate of i-butane equals 0.8 kmol/sec. This concentration region is close to the LLE critical point. To continue, since the

critical point is located slightly toward the nitrobenzene-rich side, increase the flow rate of nitrobenzene to approximately 1.2 kmol/sec. Then adjust the flow rate of i-butane from 0.7 to 0.8 kmol/sec, with an increment of 0.001 to locate the last possible LLE points before ASPEN fails. The results tabulated on the `Sensitivity.Results` form show that there is a discontinuity in numerical values when the flow rate of i-butane reaches 0.771 kmol/sec. Therefore, the LLE points calculated with this flow rate are the last data used before the critical point. The liquid-liquid equilibrium tie lines for the higher pressures are evaluated in the same way, and the LLE walls are constructed by simply connecting the various isobaric LLE data points.

The liquid-liquid critical locus can be determined by the Heidemann and Khalil method [10]. The `CR` program introduced in chapter 2 in the section called "Generating critical data points" was used to find the vapor-liquid critical locus for a mixture. In this work, A modified program called `CRL` was created to find the liquid-liquid critical locus. The `CRL` program is currently saved on DECstation `pv0415.vincent.iastate.edu` in the local drive `/local/dcoy/Trace/Code/`. The only difference between the `CR` and `CRL` programs is that the initial guesses for temperature and volume for `CRL` are smaller than those used in `CR`. By experiment it was found that the initial guess on temperature for the `CRL` program should be the mole-fraction-weighted average of the critical temperatures of the pure components. The initial guess on volume should be twice the value b_m which is defined for the Peng-Robinson equation of state in equation (3.2).

$$T = \sum_{i=1}^n x_i T_{ci} \quad (5.1)$$

$$V = 2b_m \quad (5.2)$$

Here n is the total number of components in the system. The initial guesses on the temperature and volume used in the CRL program are $2/3$ and $1/2$, respectively, of those used in the CR program.

To execute CRL, a property file for the ternary mixture must be prepared. Table 5.8 shows the format of the property file as written for the n-pentane, nitrobenzene, i-butane ternary mixture. Note that the numerical values in the first column are used for reference and should not be included in the actual property file.

This property file is similar to the one prepared for the binary mixture as discussed in Table 4.1. The only difference is that the ternary-mixture file has three

Table 5.8 CRL input file format for the n-pentane, nitrobenzene, i-butane ternary.

1	3	{ number of components }
2	Component 1: n-pentane	
3	33.65d0	{ Pc (bar) }
4	469.6d0	{ Tc (K) }
5	0.2486d0	{ Acentric factor }
6	Component 2: Nitrobenzene	
7	44.0d0	{ Pc (bar) }
8	719.0d0	{ Tc (K) }
9	0.4480d0	{ Acentric factor }
10	0.1	{ B.I.P 1-2 }
11	Component 3: i-Butane	
12	36.40d0	{ Pc (bar) }
13	408.10d0	{ Tc (K) }
14	0.177d0	{ Acentric factor }
15	0.02	{ B.I.P 1-3 }
16	0.02	{ B.I.P 2-3 }

binary interaction parameters corresponding to the three binary sub-mixtures. The binary interaction parameter for components 1 and 2 is placed after the properties of component 2 and appears on line 10. The binary interaction parameter for components 1 and 3 is placed after the properties of component 3, and the parameter for components 2 and 3 is located at the end of the file.

After the property file has been prepared, type `CRLI profile` at the command prompt. "profile" is the name of the property file with the extension `.pro`. The CRLI program first reads the information in the property file and then prompts for a first estimate of the mole fractions of components A and B at the critical point (the first base point) and also a composition increment δx for establishing a circular search path around this base point. CRLI then returns the temperature, pressure, and volume of the LLE critical point having this estimated composition. The calculated temperature ($T_{c,1}$) will, in general, be quite different from the temperature of the isothermal prism. This is then followed by a series of similar calculations at composition points along the circular path having a radius δx about the base point. That point along the path giving the temperature ($T_{c,2}$) closest to the prism temperature is chosen for a new base point, and a new search is begun using a composition radius of the same size as before.

This process is continued until one such search finds an exact match – a composition whose critical temperature is exactly that of the isothermal prism. The associated critical pressure is then noted and the complete coordinates of the point ($P_c, x_{A,c}, x_{B,c}$, and $T_c = T_{\text{prism}}$) are stored.

The final base point in the search is then perturbed to form a new first estimate for another series of “circular searches” for determining another set of exact critical coordinates. After about 10 such determinations the accumulated sets of critical coordinates are ordered and placed in a file for transfer to the graphics program. The connection of these (essentially random) points into a curve produces the LLE critical “line” for the isothermal prism. Figure 5.21 shows a typical series of base points and circular search paths to find LLE critical points corresponding to the prism temperature. An enlarged drawing is shown in Figure 5.22.

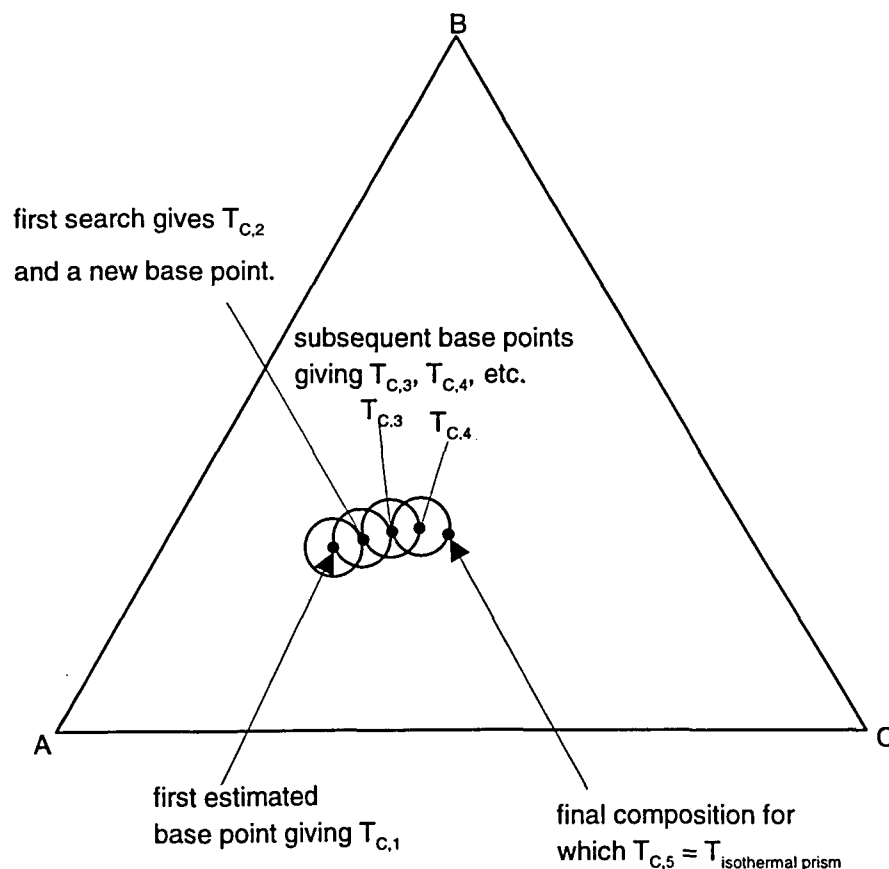


Figure 5.21 Schematic diagram showing a series of base points and circular search paths to find LLE critical points (exaggerated scale).

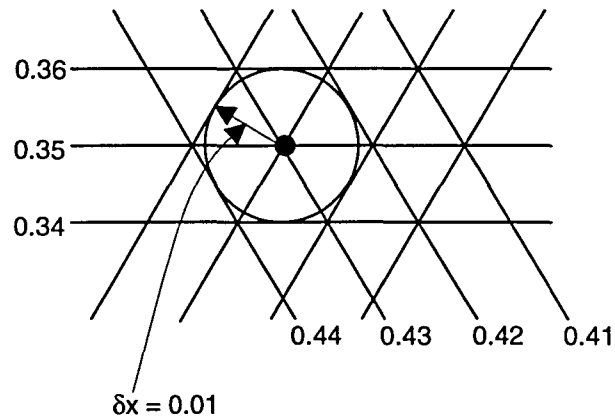


Figure 5.22 Magnified drawing of a particular base point and its circular search path.

The ternary phase diagrams shown thus far were rather simple, since none of the binary sub-mixtures had azeotropes. Figure 5.23 shows two views of the isothermal pressure-composition prism for the acetonitrile, benzene, ethanol ternary mixture at $T=333.15$ K. The interaction parameters used for the acetonitrile-benzene, acetonitrile-ethanol, and benzene-ethanol binaries were 0.074, 0.065, and 0.09, respectively.

This diagram has pressure-maximum azeotropes for each of the three binary sub-mixtures and a pressure-maximum azeotrope for the full ternary. The composition and pressure at which the ternary azeotrope occurs can be located by using an optimization method implemented in the ASPEN PLUS process simulator. From the `Forms` pull-down menu, select `Model Analysis Tools` and `Optimization sub-menus` – the `Optimization Object Manager` form will then appear. Click on `Create` to create a new optimization block or click on `Input`

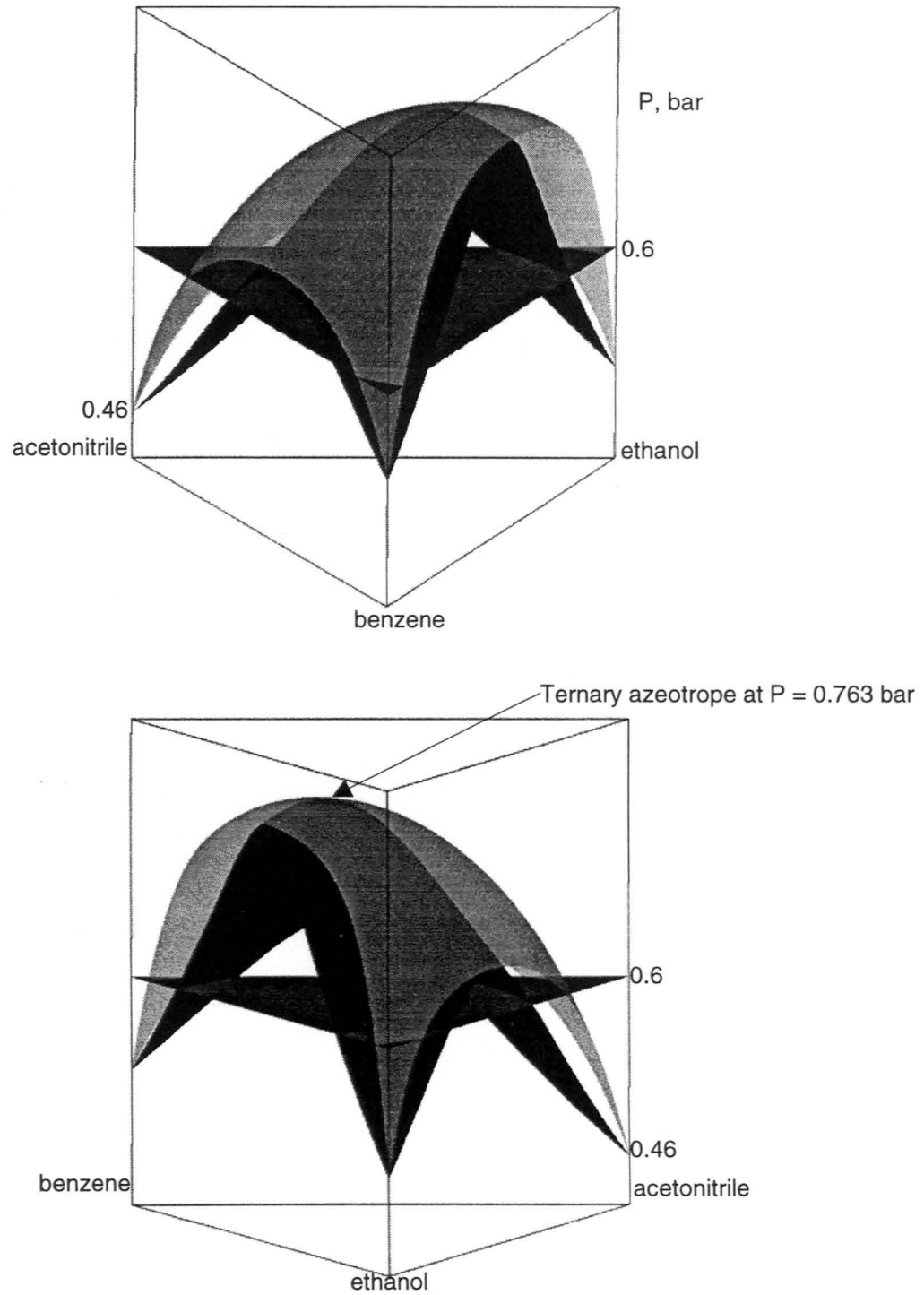


Figure 5.23 Two views of the isothermal p-xy diagram for the acetonitrile, benzene, ethanol ternary, $T = 333.15$ K.

to change the information in the current block. There are three sections to an optimization block: the `Optimization.Define` form is used to define the flowsheet variables that will be optimized on the `Optimization.Objective` form. The `Optimization.Vary` form is used to specify the independent variables and ranges that will be used to optimize the quantities specified on the `Optimization.Objective` form. For example, in this work set the temperature and vapor fraction to be 342.15 K and 0.001, respectively, on the `Flash2.Main` form⁴. Define the pressure variable for the liquid outlet stream from the `Flash2` block on the `Optimization.Define` form, and maximize the pressure on the `Optimization.Objective` form. Finally, define the molar flow rates for the three components and set them to vary from 0 to 1 kmol/sec. The results shown on the `Stream-Sum.Main` form indicate that the ternary, pressure-maximum azeotrope occurs at compositions of acetonitrile and benzene equal to 0.1534 and 0.4292, respectively, and at a pressure of 0.763 bar.

Figure 5.24 shows two views of another isothermal pressure-composition diagram, this time the ethylbenzene, acetic acid, pyridine ternary at $T=373.15$ K. The interaction parameters used for the ethylbenzene-acetic acid, ethylbenzene-pyridine, and acetic acid-pyridine binaries were 0.05, 0.015, and -0.23, respectively.

This phase diagram has a pressure-maximum azeotrope for the ethylbenzene-acetic acid binary and a pressure-minimum azeotrope for the acetic

⁴The purpose of setting the vapor fraction to 0.001 is to generate a tiny amount of vapor in the `Flash2` block so that the mole fractions of the three components in the vapor stream as well as in the liquid can be examined at the azeotropic point.

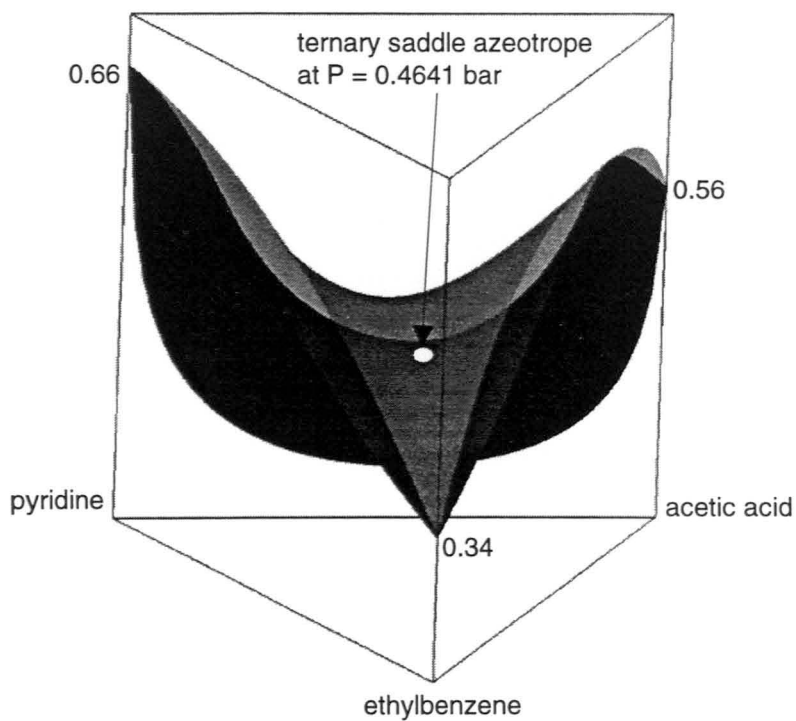
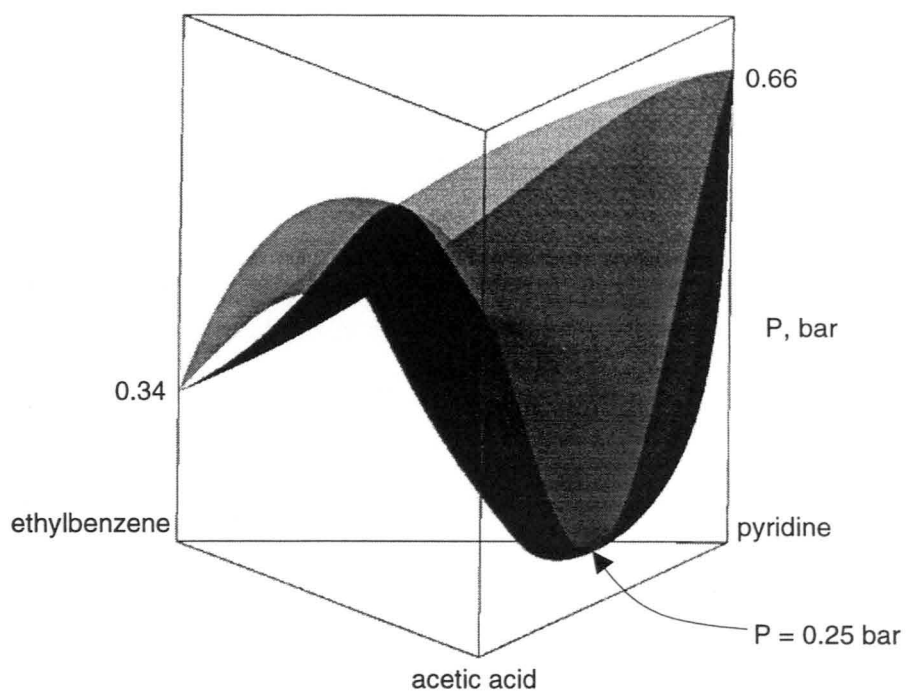


Figure 5.24 P-xy diagram for the ethylbenzene, acetic acid, pyridine ternary at $T=373.15$ K (two views).

acid-pyridine binary. It also has a ternary saddle azeotrope located in the middle of the prism. The composition of the saddle azeotrope is harder to locate than for the all-pressure-maximum case shown previously. A saddle azeotrope cannot be found by maximizing or minimizing the bubble-point or dew-point pressure. One must minimize the pressure *difference* between the bubble- and dew-point surfaces. First, a flowsheet has to be set up as shown in Figure 5.25. Set the flash temperature to 373.15 K for both flash blocks on the `Flash2.Main` form and set the vapor fraction for the upper and lower blocks to be 0.999 and 0.001, respectively. Then define the dew-point pressure for stream 2 and the bubble-point pressure for stream 5 on the `Optimization.Define` form and minimize the

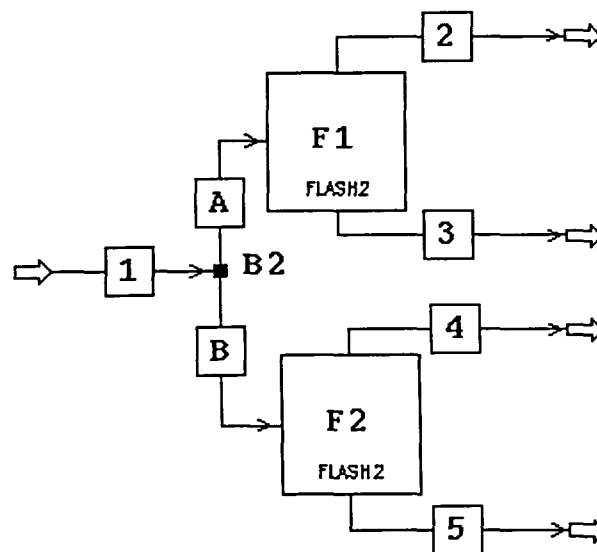


Figure 5.25 Flowsheet for locating the composition of a saddle azeotrope.

pressure difference on the `Optimization.Objective` form. Finally, on the `Optimization.Vary` form, vary the molar flow rate of ethylbenzene from 0.4 to 0.7 kmol/sec, acetic acid from 0.2 to 0.5 kmol/sec, and pyridine from 0.1 to 0.4 kmol/sec. The results shown on the `Stream-Sum.Main` form indicate that the saddle azeotrope occurs at compositions of ethylbenzene and acetic acid equal to approximately 0.5520 and 0.2146 and at a pressure of 0.4641 bar. Using the `Optimization.Vary` form, the flowrate of each component was varied over a range greater than zero because the difference between bubble- and dew-point pressures at each pure-component vertex is also zero.

CHAPTER 6. MAKING OF THREE-DIMENSIONAL QUATERNARY DIAGRAMMS

After working to make three-dimensional ternary phase diagrams, the next challenging project was constructing three-dimensional quaternary diagrams. Predicting the phase behavior for a quaternary fluid system involves solving a five-dimensional problem. The possible independent variables are temperature, pressure, and three compositions, thus making it an even more complicated system. The basic idea is to fix temperature and pressure and represent the four composition variables in a unit-length tetrahedron as shown in Figure 6.1. The Cartesian coordinates of the vertices A, B, C, D are shown in Table 6.1.

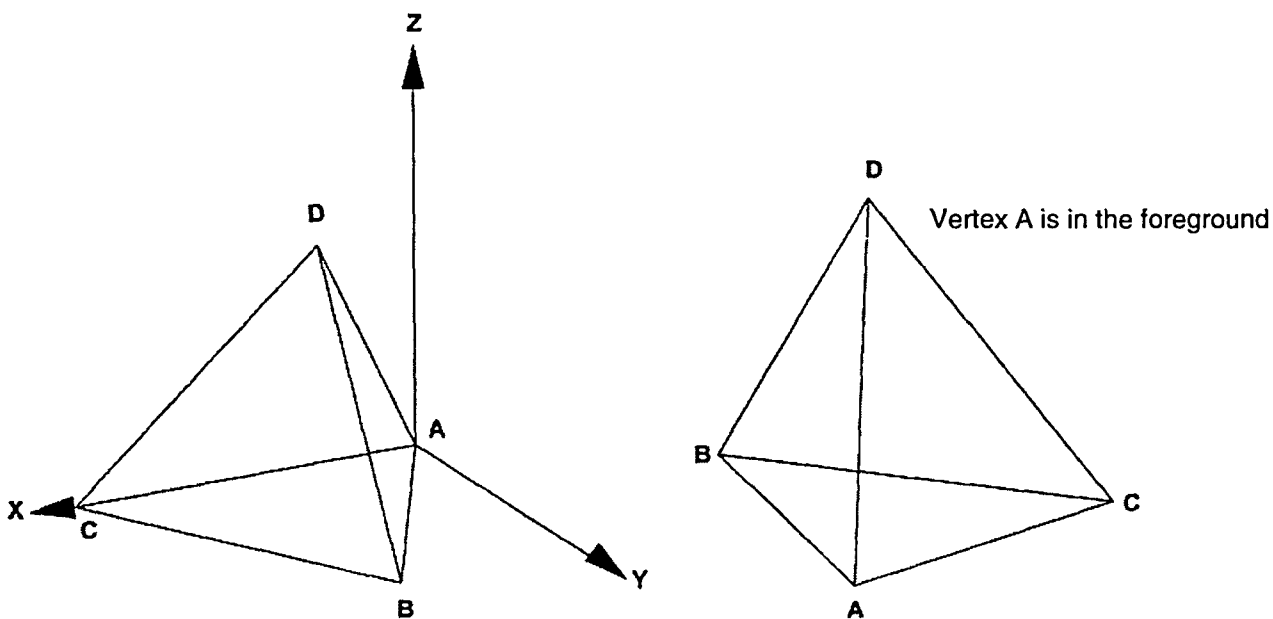


Figure 6.1 Two views of a unit-length tetrahedron for representing quaternary systems.

Table 6.1 Coordinates of the vertices of the tetrahedron.

Vertex	Coordinate (x, y, z)
A	(0.0, 0.0, 0.0)
B	(0.5, 0.866, 0.0)
C	(1.0, 0.0, 0.0)
D	(0.5, 0.433, 0.75)

In the example shown here, the components are arranged such that component A is always the least volatile, component B is more volatile than component A but less than component C, and component D is always the most volatile. Each triangular face shows the phase-equilibrium curves translated from an isothermal, isobaric section through one of the four ternary sub-mixtures.¹ Each edge of the tetrahedron shows the phase-equilibrium points from one of the six component binaries. Points inside the tetrahedron represent the composition of the complete quaternary mixture. The spatial coordinates in the tetrahedron can be calculated from the following transformation equations (according to Figure 6.2) based on the known mixture composition, X_B , X_C , X_D .

$$x = \frac{X_B}{2} + X_C + \frac{X_D}{2} \quad (6.1)$$

$$y = \left(X_B + \frac{X_D}{2}\right) \cdot \cos\left(\frac{\pi}{6}\right) \quad (6.2)$$

$$z = X_D \cdot \cos^2\left(\frac{\pi}{6}\right) \quad (6.3)$$

¹ The ternary sub-mixtures of the ABCD quaternary are ABC, ABD, ACD, and BCD.

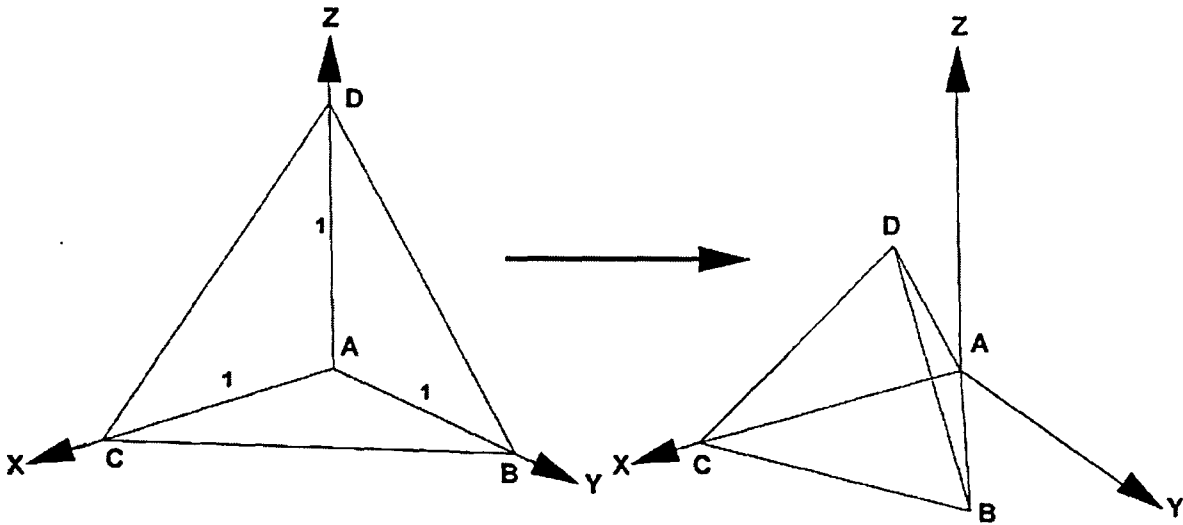


Figure 6.2 Schematic representation of a quaternary coordinate Transformation: Cartesian to equilateral tetrahedron.

There are several ways that phase-equilibrium composition points can be determined for a quaternary. In this work, the composition points are solved by first fixing the temperature and two of the component compositions. Then ASPEN PLUS varies the third composition until it finds the desired (fixed) pressure. Since the structure of the quaternary phase diagram is complicated and does not follow a unique pattern, making these diagrams automatically is not possible at this point. Much manual work is still required. In the remainder of this chapter we will focus on the procedures for calculating the phase-equilibrium points and constructing the tetrahedral diagrams for two specific systems.

The first quaternary system consists of benzene(A), acetone(B), n-pentane(C), and n-butane(D). These four components form one of the simplest possible quaternary mixtures. In other words, none of the six binary sub-mixtures

forms an azeotrope, and there is no liquid immiscibility. It was decided to select a simple quaternary at the beginning because the three-dimensional quaternary system is quite complicated. The Peng-Robinson binary interaction parameters used for the binary mixtures within the quaternary are listed in Table 6.2.

Table 6.2 Binary interaction parameters used for the quaternary system.

Binary pair	Interaction parameter
benzene(A)-acetone(B)	0.020 ⁺
benzene(A)-n-pentane(C)	0.0174 [*]
benzene(A)-n-butane(D)	0.020 ⁺
acetone(B)-n-pentane(C)	0.020 ⁺
acetone(B)-n-butane(D)	0.020 ⁺
n-pentane(C)-n-butane(D)	0.0174 [*]

* obtained from ASPEN PLUS

+ obtained by estimation

There are four steps to constructing a three-dimensional quaternary diagram:

- (1) Determine the isothermal, isobaric, coexisting binary compositions for the edges of the tetrahedron.
- (2) Determine the isothermal, isobaric, ternary bubble- and dew-point curves for the triangular faces.
- (3) Calculate meshes of quaternary bubble- and dew-point compositions.
- (4) Use these data to form geometry files for displaying the graphics through OPEN INVENTOR. Quaternary bubble-point and dew-point surfaces are constructed separately, but the procedures are the same in ASPEN PLUS except on the `Flash2.Main` form, where we specify the vapor fraction to be zero for bubble-point calculations and 1 for dew-point calculations.

To determine the isothermal, isobaric, coexisting binary pairs, a mathematical routine in ASPEN PLUS called *Design-Spec* was used. *Design-Spec* is a feedback control block that allows iteration of the manipulated variable until ASPEN PLUS finds a solution within a tolerance of the value specified for the target variable. *Design-Spec* uses the secant method for its convergence algorithm, and the convergence information can be found on the *Conv-Options.Secant* form obtained from the *Forms* pull-down menu, then from the *Convergence* and *Conv-Options* sub-menus. On the *Conv-Options.Secant* form, the maximum number of iterations, target tolerance, and step size for the calculation can be specified. There are two sections in *Design-Spec*: the *Design-Spec.Define* form is used to define the target variables in the flowsheet. On this form, enter a variable name in the *Vaname* field, then press *Enter* and ASPEN PLUS will bring the cursor to the next input field automatically. The *Design-Spec.SpecVary* form is used to specify the value of the target variable, the convergence tolerance, the manipulated variable, and its range. All of these specifications will overwrite the information in the original flowsheet, and the final results will be displayed on the *Stream-Sum.Main* form.

Since the procedures for calculating all binary points are the same, only one example will be presented here. The schematic procedure is shown in Figure 6.3. To calculate the bubble-point composition for benzene and n-butane at $T=298.15$ K and $P=0.5$ bar, specify the mole fraction of benzene and n-butane each to be 0.5 and the other components in the quaternary to be zero in the inlet stream on the

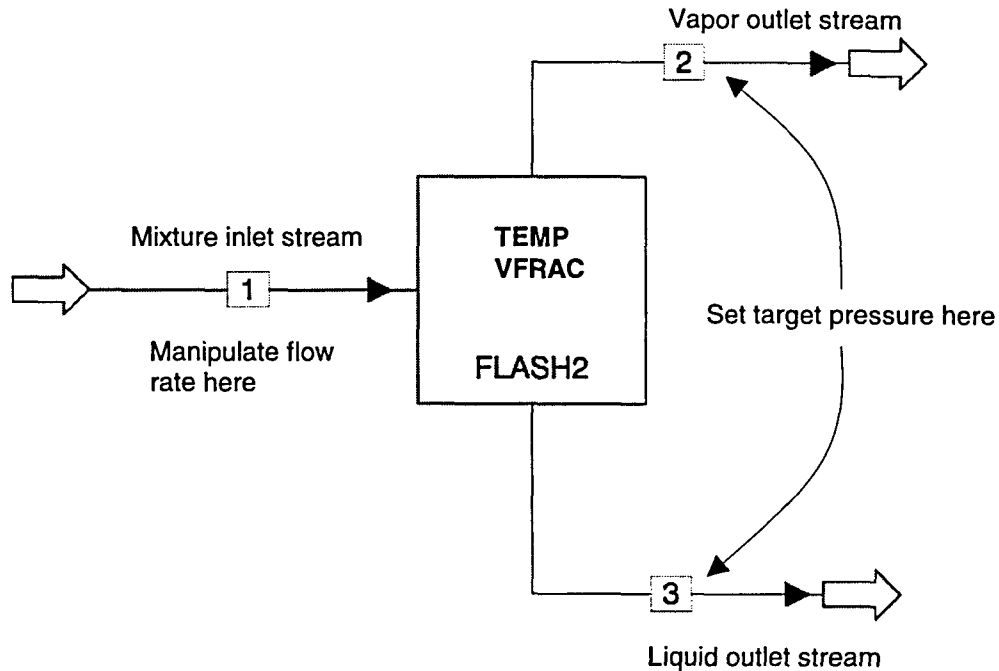


Figure 6.3 Schematic diagram for flash calculation using Design-Spec.

Stream.Main form. Then specify temperature and vapor fraction to be 298.15 K and zero, respectively, on the Flash2.Main form. Create two Design-Specs - in one define the pressure in the liquid outlet stream from the flash2 block as the target variable on the Design-Spec.Define form. Next, on the Design-Spec.SpecVary form, manipulate the molar flow rate of benzene from 0 to 1 kmol/sec and set the target pressure to be 0.5 bar. In the other Design-Spec, define the total flow rate in the inlet stream as the target variable on the Design-Spec.Define form. On the Design-Spec.SpecVary form, manipulate the molar flow rate of n-butane from 0 to 1 kmol/sec and set the target inlet molar flow rate to be 1 kmol/sec. After execution, the final results can be found on the Stream-

Sum.Main form; the bubble-point composition of benzene is found to be 0.9037. To calculate the corresponding dew-point composition of benzene (for the same VLE state), replace 0 by 1 in the vapor fraction input field on the Flash2.Main form. The dew-point composition is then found to be 0.2468. These results can be verified from the benzene/n-butane binary diagram as produced from the Analysis pull-down menu, then from the Binary and P-xy sub-menus. Similar procedures can be applied to calculate the remaining coexisting binary points. The results are shown in Table 6.3.

Table 6.3 Coexisting compositions for binary sub-mixtures.
T=298.15 K, P=0.5 bar.

Mixture	Coexisting pairs
benzene(A)-acetone(B)	Not found (all liquid)
benzene(A)-n-pentane(C)	x(benzene) = 0.4259, y(benzene) = 0.1454
benzene(A)-n-butane(D)	x(benzene) = 0.9037, y(benzene) = 0.2468
acetone(B)-n-pentane(C)	x(acetone) = 0.6683, y(acetone) = 0.4306
acetone(B)-n-butane(D)	x(acetone) = 0.9424, y(acetone) = 0.5613
n-pentane(C)-n-butane(D)	Not found (all vapor)

By transferring these binary coexisting pairs to the edges of the tetrahedron (using the transformation equations shown in (6.1), (6.2) and (6.3)), an outline structure of the complete quaternary phase diagram can be constructed, first by connecting the binary bubble-points and then the binary dew-points. This is done in Figure 6.4 and shown in two orientations. Viewed from the top in Figure 6.4(b), the outline structure of the bubble-point surface alone appears in Figure 6.5.

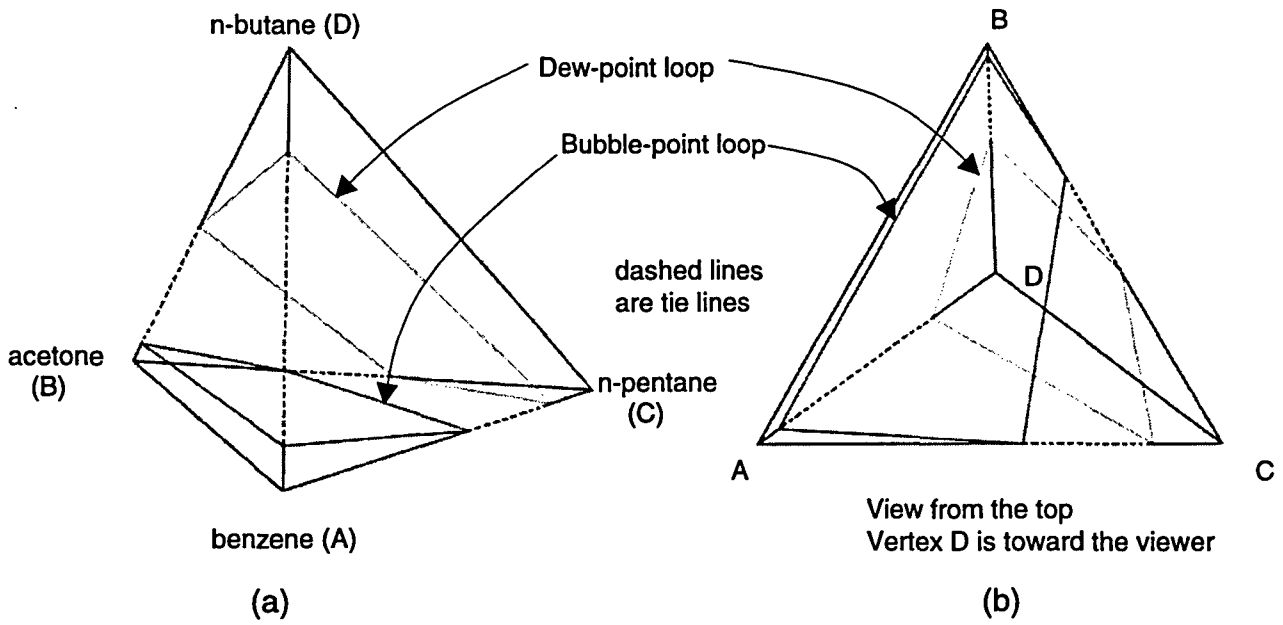


Figure 6.4 Outline structure of the bubble- and dew-point surfaces in the phase diagram for a simple quaternary mixture (two orientations).

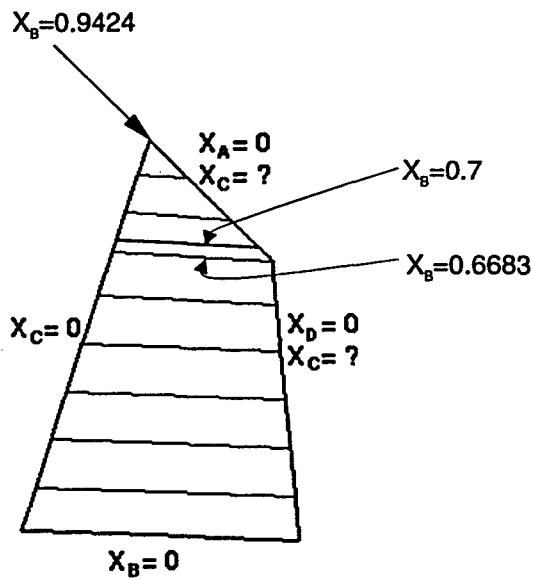


Figure 6.5 Outline structure of the bubble-point surface in Figure 6.4(b) as viewed from the top of the tetrahedron.

The idea of solving for phase-equilibrium composition points is to start from the point where $X_B=0$ and $X_C=0$, then move across the constant-B-composition line from left to right by increasing the value of X_C . When the point where $X_D=0$ is reached, increase the value of X_B and restart X_C from 0, doing the same iterations each time and continuing until $X_B=0.9424$. The composition of component D will be calculated along the constant-B-composition lines. The number of composition points that will be calculated depends upon the curvature of the surface. Since each iteration must stop at the end of a particular constant-B-composition line, the intersections between the constant-B lines and the lines where $X_D=0$ (or $X_A=0$ for the upper triangle) have to be calculated beforehand so that the iterations know where to stop.

To calculate the mole fraction of n-pentane (X_C) at the intersection of the constant-B (acetone) lines and the line $X_D=0$ (in the ABC face of the tetrahedron), both `sensitivity` blocks and `Design-Spec` must be utilized together. First, set the mole fraction of n-butane (D) to zero and the other components equal in mole fraction in the inlet stream on the `Stream.Main` form. Then set the temperature and vapor fraction to be 298.15 K and zero, respectively, on the `Flash2.Main` form. Again, create two `Design-Specs`. In one of the `Design-Specs`, define the pressure in the liquid outlet stream from the `flash2` block as the target variable on the `Design-Spec.Define` form. Next, on the `Design-Spec.SpecVary` form, manipulate the flow rate of n-pentane (C) from 0 to 1 kmol/sec and set the target pressure to be 0.5 bar. In the other `Design-Spec`, define the total flow rate in the

inlet stream as the target variable (`Design-Spec.Define` form), and manipulate the flow rate of benzene (A) from 0 to 1 kmol/sec and set the target inlet flow rate to be 1 kmol/sec (`Design-Spec.SpecVary` form). This ensures that the final flow rate of each component will be based on a total flow of 1 kmol/sec. In other words, the final results will be tabulated essentially in mole fractions.

Finally, on the `Sensitivity.Define` form, define the molar flow rate for each component and the pressure in the liquid outlet stream so that these results will be tabulated on the `Sensitivity.Tabulate` form for verification. Vary the molar flow rate of acetone (B) from 0 to 0.6683 kmol/sec with 0.1 kmol/sec increments². This increment is based principally on the curvature of the surface. For a more highly curved surface, a smaller increment is required, which will make the calculation process take longer.

To calculate the mole fractions of n-pentane (X_c) on the intersections along the line where $X_a=0$ (in the BCD face), the procedures are about the same as above. Only a few details need to be changed. On the `Stream.Main` form for the inlet stream, set the mole fraction of benzene to be zero. Then, in one of the `Design-Specs` – the `Design-Spec.SpecVary` form that manipulated the flow rate of benzene previously – replace it by n-butane. Finally, on the `Sensitivity.Vary` form, vary the molar flow rate of acetone from 0.0.6683 to 0.9424 kmol/sec³ with 0.1 kmol/sec increments (from 0.7 to 0.9 kmol/sec).

² $X_b=0.6683$ passes through the intersection of the lines for $X_b=0$ and $X_a=0$ (See Figure 6.5).

³ Shown in Table 6.3, the composition of the acetone (B), n-butane (D) binary ($X_c=0$ and $X_a=0$).

Table 6.4 Ternary compositions calculated on the lines where $X_D=0$ and $X_A=0$.

	Benzene (X_A)	Acetone (X_B)	n-Pentane (X_C)	n-Butane (X_D)
$X_D = 0$ (ABC face)	0.42593	0.0	0.57407	0.0
	0.36847	0.1	0.53153	0.0
	0.30796	0.2	0.49204	0.0
	0.24509	0.3	0.45491	0.0
	0.18035	0.4	0.41965	0.0
	0.11411	0.5	0.38589	0.0
	0.04662	0.6	0.35338	0.0
$X_D = 0, X_A = 0$	0.0	0.66826	0.33244	0.0
$X_A = 0$ (BCD face)	0.0	0.7	0.29453	0.00549
	0.0	0.8	0.17568	0.02432
	0.0	0.9	0.05342	0.04658
	0.0	0.94242	0.0	0.05758

The mixture compositions calculated for the intersections of constant-B (acetone) lines and the lines where $X_D=0$ and $X_A=0$ are listed in Table 6.4 for $T=298.15$ K and $P=0.5$ bar.

In the next step, each iteration loop will be set up in ASPEN PLUS to fix the value of the mole fraction of component B (acetone), increment X_C (n-pentane) along the constant-B-composition line, and solve for the corresponding bubble-point compositions of component D (n-butane). Therefore, the number of loops set up depends on the number of constant-B lines drawn across the bubble-point surface. At this stage, each loop must be set up manually since no simple way has been formulated yet to program a double loop that will vary X_B and X_C and calculate all of the composition points on the bubble-point surface automatically.

The set-up procedures for calculating the compositions of component D are similar to those for calculating the ternary compositions as discussed previously.

The four components are set equal in mole fraction in the inlet stream on the `Stream.Main` form. Then the temperature and vapor fraction are set to be 298.15 K and zero, respectively, on the `Flash2.Main` form. Next, create two `Design-Specs`; in one, manipulate the flow rate of n-butane from 0 to 1 kmol/sec so that the `flash2` block is operating under a fixed pressure of 0.5 bar. In the other `Design-Spec`, manipulate the flow rate of benzene from 0 to 1 kmol/sec so that the total flow rate in the input stream is fixed at 1 kmol/sec. Again, define the molar flow rate for each of the components and the pressure in the outlet stream on the `Sensitivity.Define` form so that the final results will be tabulated on the `Sensitivity.Tabulate` form.

Manipulate two variables (the molar flow rates of acetone (B) and n-pentane (C)) on the `Sensitivity.Vary` form to determine the composition of n-butane (D). First, fix the flow rate of acetone (B) at zero for the lowest constant-B-composition line in Figure 6.5. Then vary the flow rate of n-pentane (C) from 0 to 0.57407 kmols/sec, which gives the composition of the intersection between the zero B-composition line and the line where $X_D=0$. Finally, set the total number of points to be calculated on the constant-B line in the `Npoint` field. To calculate the composition of component D on the next higher B-composition line, change the molar flow rate of acetone on the `Sensitivity.Vary` form to the value corresponding to that line. Then vary the flow rate of n-pentane from 0 to 0.53153, the molar flow at the intersection with the line where $X_D=0$. A list of these values is given in Table 6.4.

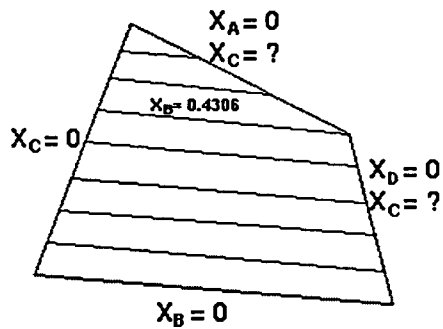


Figure 6.6 Outline structure of the dew-point surface in Figure 6.4(b).

To construct the dew-point surface, first examine its outline structure as shown above, viewed from the top in Figure 6.4(b).

The outline structure of the dew-point surface is similar to that of the bubble-point surface shown in Figure 6.5. Therefore, the procedures to calculate the composition of component D (n-butane) along the constant-B-composition lines are the same as discussed above. The only difference is that the vapor fraction is changed to 1 in the `flash2.Main` form.

The calculated quaternary data points are then transferred to an `xess` spreadsheet for data reorganization. This includes transforming the data points to the tetrahedron coordinate system using transformation equations (6.1), (6.2), and (6.3) and arranging the data points so that they can be copied and pasted directly into the `iv` files through mouse action.

Triangulation of the quaternary surface

The triangulation algorithm for making quaternary phase surfaces is different than the one discussed in chapter 5 for making ternary diagrams. Since there are so many possible patterns in the structure of VLE surfaces in quaternary phase diagrams, it is difficult to automate the triangulation process. Therefore, manual work is still required to triangulate the bubble- and dew-point surfaces for four-component systems.

First, examine the outline structure of the bubble-point surface shown in Figure 6.5. It is divided into two parts for triangulation, the lower quadrilateral bounded by the lines where $X_c=0$, $X_b=0$, $X_d=0$ and $X_b=0.6683$, and the upper triangle bounded by the lines $X_c=0$, $X_b=0.6683$ and $X_a=0$. In the lower quadrilateral, the data points are arranged in a “square” matrix. In other words, the numbers of data points across the constant-B-composition lines are the same. Therefore, a simple INVENTOR routine called `QuadMesh` node is used for triangulation instead of the more complex `IndexedFaceSet` node. `QuadMesh` node constructs the quadrilateral according to the coordinates located on the surface and then triangulates that surface. There are three parameters to support `QuadMesh` node: `startIndex` indicates the first index to be chosen - by default it is 0; `verticesPerRow` indicates the number of data points across the constant-B composition lines, and `verticesPerColumn` indicates the number of constant-B lines.

For the upper triangle, `IndexedFaceSet` node will be used for triangulation. Therefore, the number of data points calculated along the constant-B-composition lines in this section must be planned carefully so that it can be triangulated easily. The details of using `IndexedFaceSet` node can be referred to in Table 5.4 and in the accompanying discussion. Since the outline structure of the dew-point surface is similar to that of the bubble-point surface, the procedures for triangulation are exactly the same. The complete VLE phase diagram for the benzene, acetone, n-pentane, n-butane quaternary is shown in Figure 6.7.

Next we explore a more complicated quaternary diagram in contrast to the simple quaternary example discussed above. A system has been chosen which

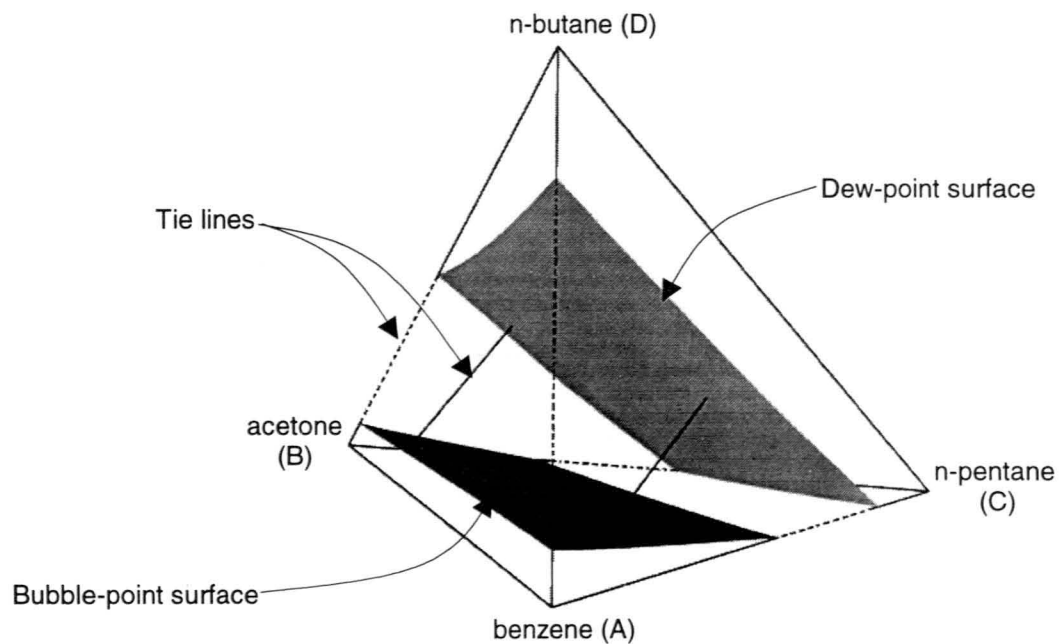


Figure 6.7 Quaternary phase diagram for benzene, acetone, n-pentane, n-butane at $T=298.15$ K and $P=0.5$ bar.

consists of the four components acetonitrile(A), benzene(B), ethanol(C) and acetone(D) at $T=333.15$ K. The ternary sub-mixture acetonitrile, benzene and ethanol forms a maximum pressure ternary azeotrope, and each of the binaries within the ternary forms a maximum pressure binary azeotrope. The fourth component, acetone, forms simple binary phase diagrams with acetonitrile, benzene, and ethanol. The interaction parameters used for the six binary sub-mixtures within the quaternary are listed in Table 6.5.

Table 6.5 Interaction parameters used for the binary pairs.

Binary sub-mixture	Binary interaction parameter (obtained by estimation)
acetonitrile(A)-benzene(B)	0.074
acetonitrile(A)-ethanol(C)	0.065
acetonitrile(A)-acetone(D)	0.017
benzene(B)-ethanol(C)	0.090
benzene(B)-acetone(D)	0.030
ethanol(C)-acetone(D)	0.024

The system pressure is fixed at $P=0.6$ bar for each of the following examples. Similar to the procedure for constructing the earlier quaternary diagram, there are also four steps for constructing the acetonitrile, benzene, ethanol, acetone diagram:

- (1) Examine the outline structure of the bubble-point and dew-point surfaces by evaluating all of the binary equilibrium compositions at the fixed temperature and pressure.
- (2) Evaluate the ternary composition points so that the quaternary calculation loops know where to stop.
- (3) Evaluate the quaternary composition points from the *Design-Spec* and *Sensitivity* blocks in the ASPEN PLUS

process simulator. (4) Export these data points to an `xess` spreadsheet for data reorganization.

It is more difficult to evaluate the binary equilibrium compositions for a quaternary system consisting of azeotropic binaries than for a quaternary consisting of simple binary phase behavior. Since the ternary mixture acetonitrile(A), benzene(B), ethanol(C) contains three binary-mixture azeotropes at pressures above the common pressure (0.6 bar), there will be *two* coexisting pairs along each of the AB, AC and BC edges and one coexisting pair along each of the AD, BD and CD edges in the tetrahedron shown in Figure 6.8. Therefore, there are a total of nine binary bubble points and nine binary dew points on the edges of the tetrahedron.

The procedures for evaluating the binary pairs in this case are similar to the procedures used to evaluate the binary pairs in the previous quaternary system. Again, specify the system temperature ($T=333.15$ K) and the vapor fraction on the `Flash2.Main` form. For bubble-point calculations, set the vapor fraction to be zero - for dew points the vapor fraction is 1. Then, for the two components that will not be evaluated, set their mole fractions to be zero in the inlet stream on the `Stream.Main` form. To evaluate the acetonitrile-benzene binary pairs, set the mole fractions of acetonitrile and benzene each to be 0.5, and set the mole fractions of ethanol and acetone to be zero on the `Stream.Main` form. Next, create two `Design-Specs`; use one `Design-Spec` to manipulate the molar flow rate of one of the components and to fix the value of the pressure at 0.6 bar. Use the other

Design-Spec to manipulate the molar flow rate of the other component so as to fix the total inlet flow at 1 kmol/sec. The ranges chosen for the manipulated molar flow-rate variables are different. To evaluate the binary bubble points on lines AD, BD and CD, the range can be set from 0 to 1 kmol/sec, since there is only one solution on each of these lines. However, when it comes to the binary bubble points on lines AB, AC and BC, restrictions must be applied, since there are two solutions on each of these lines. For example, if the binary bubble point is located on line AB at the A-rich end, the molar flow rates of components A and B have to be set roughly from 0.5 to 1 kmol/sec and from 0 to 0.5 kmol/sec, respectively, depending on the location of the binary states. This rule will stay the same for calculating the other binary coexisting points. The results of the calculations are listed in Table 6.6. By locating these binary coexisting points on the edges of the tetrahedron using the transformation equations (6.1), (6.2) and (6.3), the outline structure of the bubble-point and dew-point surfaces can be approximated by connecting like phases as shown in Figure 6.8.

Table 6.6 Coexisting points for binary sub-mixtures at $T=333.15$ K, $P=0.6$ bar.

acetonitrile(A)-benzene(B)	$x(\text{acetonitrile}) = 0.7853$, $y(\text{acetonitrile}) = 0.6359$
acetonitrile(A)-benzene(B)	$x(\text{acetonitrile}) = 0.1243$, $y(\text{acetonitrile}) = 0.2153$
acetonitrile(A)-ethanol(C)	$x(\text{acetonitrile}) = 0.7365$, $y(\text{acetonitrile}) = 0.6002$
acetonitrile(A)-ethanol(C)	$x(\text{acetonitrile}) = 0.1432$, $y(\text{acetonitrile}) = 0.2621$
benzene(B)-ethanol(C)	$x(\text{benzene}) = 0.9353$, $y(\text{benzene}) = 0.8279$
benzene(B)-ethanol(C)	$x(\text{benzene}) = 0.049$, $y(\text{benzene}) = 0.2031$
acetonitrile(A)-acetone(D)	$x(\text{acetonitrile}) = 0.8408$, $y(\text{acetonitrile}) = 0.6517$
benzene(B)-acetone(D)	$x(\text{benzene}) = 0.9322$, $y(\text{acetone}) = 0.8235$
ethanol(C)-acetone(D)	$x(\text{ethanol}) = 0.9313$, $y(\text{ethanol}) = 0.7791$

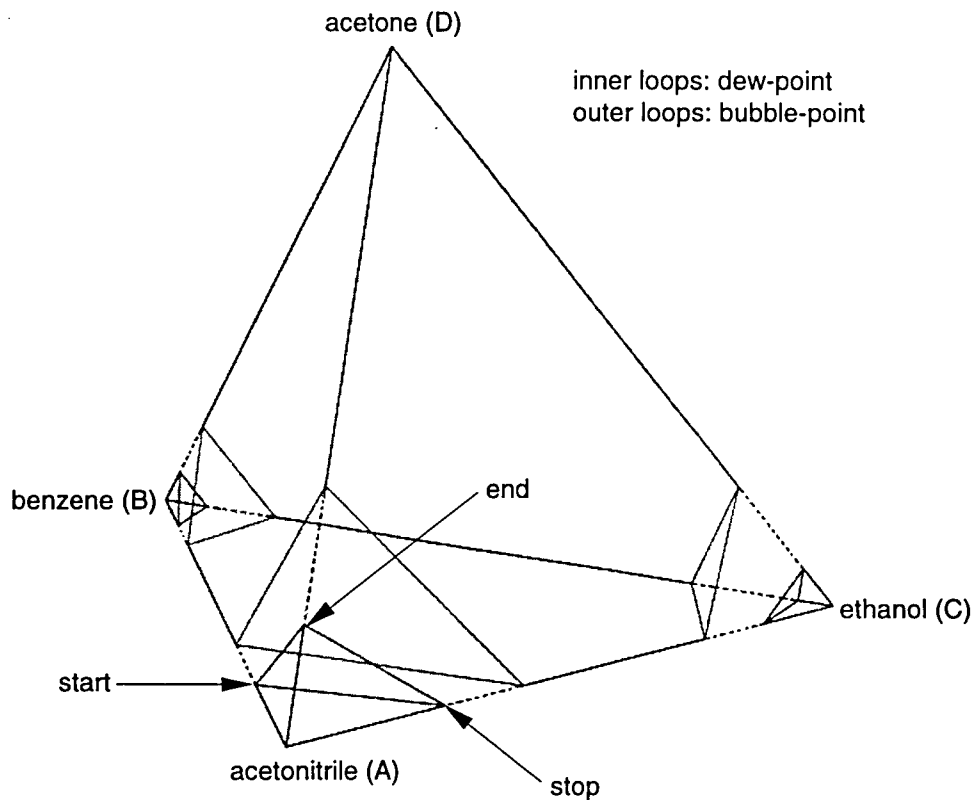


Figure 6.8 Outline structure of the quaternary bubble-point and dew-point surfaces using straight-line approximations in the ternary faces.

We see that there are pairs of triangular bubble-point and dew-point surfaces near each of the acetonitrile, benzene, and ethanol vertices. This is common for a quaternary phase diagram consisting of azeotropic binary sub-mixtures.

Next, depending on where the calculation loops end, it is necessary to evaluate the real ternary composition points on the triangular faces of the tetrahedron. For example, consider the bubble-point surface located near the benzene vertex (shown in Figure 6.8 and enlarged in Figure 6.9). The loop for calculating quaternary bubble-point compositions near the benzene vertex was

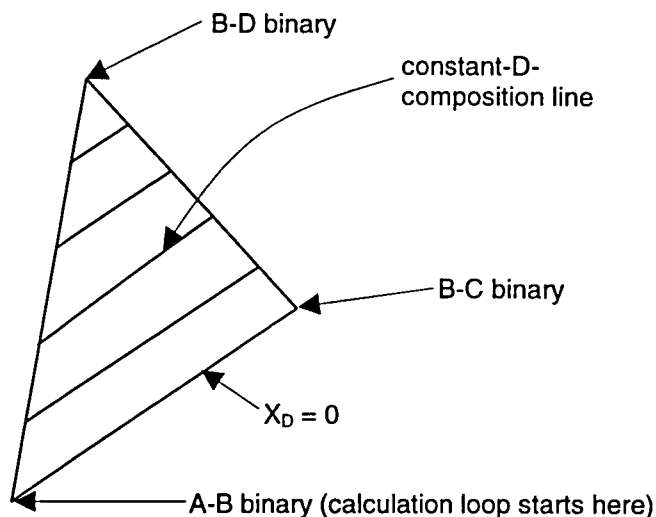


Figure 6.9 Enlargement of bubble-point surface near the benzene vertex in Figure 6.8.

performed from left (acetonitrile-benzene-acetone triangular face) to right (benzene-ethanol-acetone triangular face), starting along the constant-D (acetone) composition line $X_D=0$ and ending at the benzene-acetone binary bubble point.

The ternary bubble-point compositions on the benzene-ethanol-acetone face connecting the benzene-acetone and benzene-ethanol binaries were evaluated so that the calculation loop knows where to stop along each of the constant-acetone composition lines. Table 6.7 shows a list of the parameter settings that were used on the `Stream.Main` form, `Sensitivity` blocks, and `Design-Specs` for evaluating the ternary bubble-point compositions along the sides of each triangular bubble-point section. Table 6.8 shows the calculated results from the ASPEN PLUS simulator.

Table 6.7 ASPEN PLUS parameter settings for evaluating ternary bubble-point compositions for a specific triangular section.

	Bubble-point surface near the acetonitrile vertex	Bubble-point surface near the benzene vertex	Bubble-point surface near the ethanol vertex
Face of the tetrahedron on which ternary compositions are evaluated	Acetonitrile-ethanol-acetone	Benzene-ethanol-acetone	Benzene-ethanol-acetone
Inlet stream Stream.Main form	Set $X_B = 0$ The rest: equal molar	Set $X_A = 0$ The rest: equal molar	Set $X_A = 0$ The rest: equal molar
Sensitivity.Vary form	Range(XD): 0→0.1592 $\Delta XD = 0.04$	Range(XD): 0→0.0679 $\Delta XD = 0.018$	Range(XD): 0→0.0687 $\Delta XD = 0.018$
Design-spec. SpecVary form #1	Set $X_A: 0 \rightarrow 1$ Fix $P = 0.6$ bar	Set $X_B: 0.5 \rightarrow 1$ Fix $P = 0.6$ bar	Set $X_B: 0 \rightarrow 0.3$ Fix $P = 0.6$ bar
Design-spec. SpecVary form #2	Set $X_C: 0 \rightarrow 1$ Fix inlet flow rate = 1	Set $X_C: 0 \rightarrow 0.5$ Fix inlet flow rate = 1	Set $X_C: 0.7 \rightarrow 1$ Fix inlet flow rate = 1

A= Acetonitrile, B= Benzene, C= Ethanol, D= Acetone

Table 6.8 Ternary bubble-point compositions for the parameters specified in Table 6.7.

Face of the tetrahedron	X_A	X_B	X_C	X_D
Acetonitrile-ethanol-acetone (surface near vertex A)	0.73672	0.0	0.26328	0.0
	0.77518	0.0	0.19282	0.032
	0.80129	0.0	0.13471	0.064
	0.81936	0.0	0.08464	0.096
	0.83216	0.0	0.03984	0.128
	0.84084	0.0	0.0	0.15916
Benzene-ethanol-acetone (surface near vertex B)	0.0	0.93526	0.06474	0.0
	0.0	0.93507	0.04693	0.018
	0.0	0.93444	0.02959	0.036
	0.0	0.93330	0.01270	0.054
	0.0	0.93223	0.0	0.06787
Benzene-ethanol-acetone (surface near vertex C)	0.0	0.04919	0.95081	0.0
	0.0	0.03581	0.94619	0.018
	0.0	0.02280	0.94120	0.036
	0.0	0.01015	0.93585	0.054
	0.0	0.0	0.93127	0.06873

After the ternary bubble-point compositions have been determined for each of the triangular sections (which give the termination points for the final quaternary calculations), several iteration loops must be set up to evaluate the quaternary compositions on the three bubble-point sections in the tetrahedron. The procedures are similar to the ones used to evaluate the quaternary composition points in the earlier phase diagram. The idea is to fix one mole fraction, vary the second by discrete increments, and then iterate the third composition until the fixed bubble-point pressure for the system is found. For example, to evaluate the quaternary composition points for the triangular section located near the acetonitrile vertex, start from the binary bubble point where X_D (acetone) and X_C (ethanol) are zero (marked "start" in Figure 6.8) and go across the constant-D (acetone) composition line, terminating the calculation loop at the acetonitrile-ethanol-acetone face (marked "stop") with a certain number of points at fixed X_C spacing. Next, increase the mole fraction of D (acetone) by a small amount and repeat by going along the new constant-composition line in the same manner. The calculation loops will eventually terminate at the vertex of the bubble-point surface (marked "end"). To evaluate the remaining two bubble-point surfaces at the benzene-rich and ethanol-rich vertices, similar procedures are applied. The scheme to evaluate the quaternary dew-point compositions are very similar to those for the bubble-point compositions, except that the vapor fraction is specified to be 1 on the `Flash2.Main` form.

The triangulation procedures involve mostly manual work. The number of nodes on the surface is determined by the curvature of the bubble-point and dew-

point functions. This triangulation algorithm will not work for constructing all kinds of quaternary phase diagrams. In this work, however, the zero index always started at the first bubble-point or dew-point state evaluated.

The VLE phase diagram for the acetonitrile, benzene, ethanol, acetone quaternary is shown in Figure 6.10.

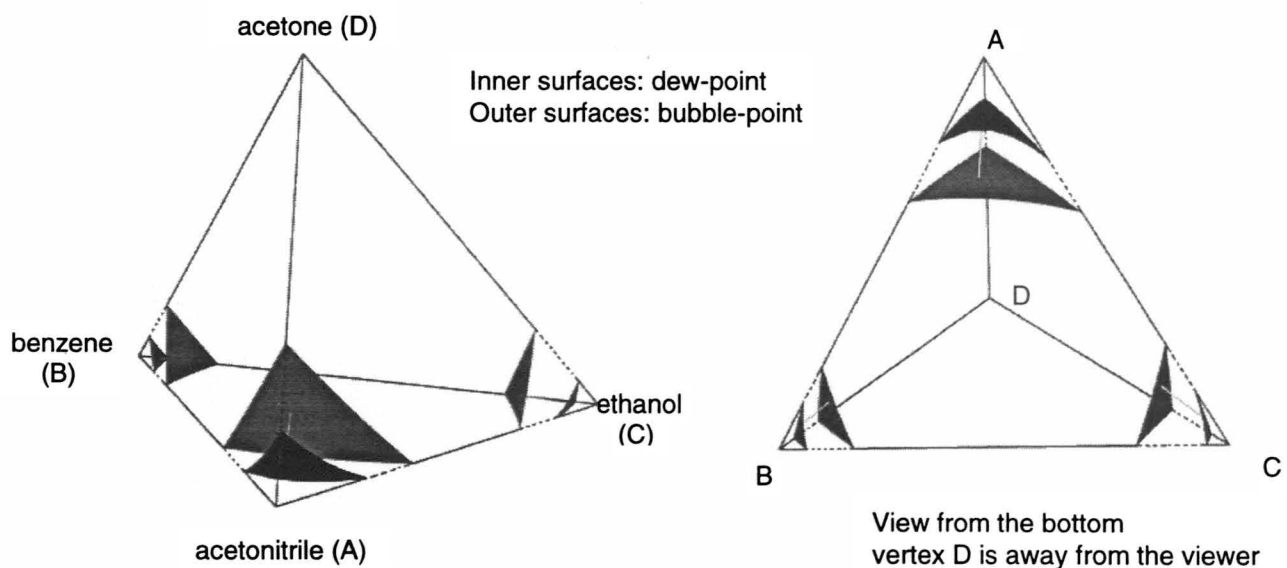


Figure 6.10 Phase diagram for the acetonitrile, benzene, ethanol, acetone quaternary, $T=333.15\text{ K}$, $P=0.6\text{ bar}$.

Next, the pressure of the quaternary system is raised to 0.6377 bar, and the structure of the phase diagram is re-examined. The pressure is chosen to be 0.6377 bar because that is the azeotropic pressure of the acetonitrile-ethanol binary at 333.15K. As a consequence, the triangular bubble-point and dew-point surfaces near the acetonitrile and ethanol vertices will contact along the binary line in the tetrahedron. Figure 6.11 shows the complete quaternary phase diagram

constructed at $T=333.15\text{ K}$ and $P=0.6377\text{ bar}$. The procedure for constructing this drawing was exactly the same as that used to construct the phase diagram shown in Figure 6.10. If the pressure continues to rise, the joined bubble-point and dew-point surfaces will detach from the acetonitrile-ethanol binary line, separate, and form two distinct quadrilateral surfaces.

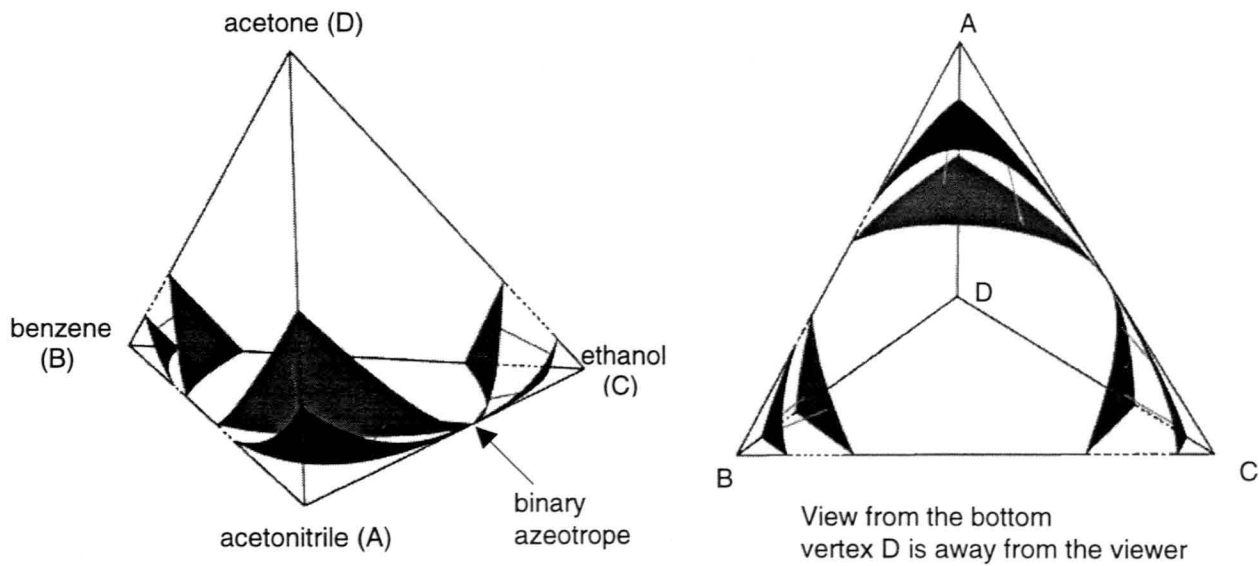


Figure 6.11 Phase diagram for acetone, benzene, ethanol and acetonitrile, $T=333.15\text{ K}$, $P=0.6377\text{ bar}$.

CHAPTER 7. CONCLUSIONS AND RECOMMENDATIONS

Two FORTRAN programs called TS and GEOTOIV have been developed to automate the construction of three-dimensional ternary phase diagrams. To execute the TS program, a script file must be prepared containing all of the important settings for the drawing. These settings include the kind of surface to be drawn (bubble point or dew point), the temperature for pressure-composition diagrams, the pressure for temperature-composition diagrams, the number of constant-composition lines, and others. The TS program invokes the ASPEN PLUS chemical process simulator and uses the Peng-Robinson equation of state to generate geometric-format, phase-equilibrium data files which are interpretable by MOVIE.BYU graphical software. However, MOVIE.BYU generates only static graphics. Therefore, the GEOTOIV program provides a way of converting geometric-format files to iv-format files which are interpretable by OPEN INVENTOR. This alternate software generates dynamic graphics and provides great flexibility for interaction with the screen display. The user can rotate, translate, and enlarge the graphics easily with mouse action to study the detailed structure of a particular drawing.

Since the procedures for making three-dimensional quaternary phase diagrams are very complicated, it is not yet possible to automate these procedures completely through computer programming. Therefore, a large amount of manual work is still required. From generating and compiling the phase-equilibrium data to

translating those data into an OPEN INVENTOR graphical format, an entire day may be required to construct a quaternary diagram, depending on its complexity. An even more sophisticated program might be created, both to automate making the diagram and also to simulate quaternary phase behavior through real-time motion (e.g., the continuous variation of the diagram for a series of different temperatures while the pressure is held fixed). I recommend organizing the structure of quaternary phase diagrams into categories and creating associated programs to automate the procedures for making each type of drawing, for example, quaternary systems that contain no azeotropes, one azeotrope, and up to six azeotropes among their six binary sub-mixtures.

The Peng-Robinson equation of state was used throughout this project to predict the phase behavior of vapor-liquid and liquid-liquid mixtures in the equilibrium state. It has been found that the Peng-Robinson equation produces fairly accurate results for non-polar and mildly polar hydrocarbon mixtures. Other equations of state, (such as the Redlich-Kwong-Soave equation, which is comparable to the Peng-Robinson) are also capable of predicting phase behavior for non-polar or mildly polar mixtures (e.g., light hydrocarbons and light gases – carbon dioxide, hydrogen, etc.) in the high-temperature and moderate pressure regions. I recommend that these alternate equations also be used for visualization purposes and their results compared with those presented in the thesis.

APPENDIX

The following lists all of the software used to create this thesis:

- 1) Microsoft Word 97 – For text and equations.
- 2) Microsoft Draw 97 – For graphics editing on thesis pages, such as callouts, lines, and arrows (implemented in Microsoft Word 97).
- 3) Adobe Photoshop 4.0 – For individual graphics editing, such as callouts, lines, graphics format, and resolution control.
- 3) Showcase – Used on the Silicon Graphics workstation to convert images of three-dimensional diagrams to encapsulated postscript files. They are then converted to GIF format by using Adobe Photoshop 4.0 to control the graphics resolution. All images in this thesis are in GIF format.
- 4) Snapshot – Used on the Silicon Graphics workstation to convert images of diagrams that have transparent surfaces to RGB files. Encapsulated postscript files cannot show the transparency property. The command 'tops' is then used to convert RGB files to postscript files. They are then converted again to GIF files by Adobe Photoshop 4.0 to control the graphics resolution.

BIBLIOGRAPHY

- 1 Schmitz, M. C., "Visualizing thermodynamic concepts through high-performance computer graphics," M.S. thesis, Iowa State University, 1991.
- 2 Willers, G. P., "The construction of thermodynamic phase diagrams through computer graphics," M.S. thesis, Iowa State University, 1978.
- 3 Coy, Daniel C., "Visualizing thermodynamic stability and phase equilibrium through computer graphics," Ph.D. dissertation, Iowa State University, 1993.
- 4 van der Waals, J.D., 1873, "On the Continuity of the Liquid and Gaseous State," Ph.D. dissertation, Sigthoff, Leiden, Holland.
- 5 Soave, G., 1972, "Equilibrium Constants From a Modified Redlich-Kwong Equation of State," *Chem. Eng. Sci.*, 27, No. 6, 1197-1203.
- 6 Peng, D.Y., and D. B. Robinson, 1976, "A New Two-Constant Equation of State," *Ind. & Eng. Chem. Fundamentals*, Vol. 15, No. 1, 59-64.
- 7 Gmehling, J., and U. Onken, 1980, *Vapor-Liquid Equilibrium Data Collection*, Chemistry Data Series, Vol. I, Part 1-6, DECHEMA, Frankfurt/Main, Federal Republic of Germany.
- 8 Modell, M., and R. C. Reid, 1983, *Thermodynamics and Its Applications*, Second Edition, Prentice Hall, Englewood Cliffs, New Jersey.
- 9 Smith, J.M., H.C. Van Ness, 1987, *Introduction to Chemical Engineering Thermodynamics*, Fourth Edition, McGraw-Hill, Inc., New York, New York, Page 490.
- 10 Heidemann, R.A., and A. M. Khalil, September 1980, "The Calculation of Critical Points," *AIChE Journal*, Vol 26, No. 5, 769-779.
- 11 ASPEN PLUS™, On-line Help Manual, 1996, AspenTech, Inc., Cambridge, Massachusetts.
- 12 Wernicke, Josie, 1994, *The Inventor Mentor. Programming Object-Oriented 3D Graphics with Open Inventor™*, Release 2, Addison Wesley, Reading, Massachusetts.

- 13 Neider, J., Davis, T., and M. Woo, 1993, *OpenGL™ Programming Guide. The Official Guide to Learning OpenGL*, Release 1, Addison Wesley, Reading, Massachusetts.
- 14 Open Inventor™, On-line Help Manual, 1994, Silicon Graphics, Inc., Mountain View, California.
- 15 Gmehling, J., U. Onken, and W. Arlt, 1980, *Vapor-Liquid Equilibrium Data Collection*, Chemistry Data Series, Vol. I, Parts 3 and 4, DECHEMA, Frankfurt/Main, Federal Republic of Germany, Pages 337-338.
- 16 Jolls, Kenneth R., and K. S. Tian, June 1997, "Fluid-phase Equilibria From a Chemical Process Simulator," Proceedings, American Society for Engineering Education, annual meeting, Milwaukee, WI., Page 2.
- 17 Horsley, L. H., Azeotropic DATA III, Advances in Chemistry Series 116, American Chemical Society, Washington, D.C. (1973).
- 18 Petersen, C. S., November 1989, "A Systematic and Consistent Approach To Determine Binary Interaction Coefficients for the Peng-Robinson Equation of State," *SPE Reservoir Engineering*, Page 488.
- 19 Walas, M. Stanley, 1985, *Phase Equilibria in Chemical Engineering*, Butterworth publishers, Stoneham, Massachusetts, Page 225.
- 20 Jolls, K.R., J. Burnet, and J. T. Haseman, "Computer-generated phase Diagrams for binary mixtures," *Chem. Engr. Educ.*, xvll (3):112 (1983).
- 21 Redlich, O. and Kwong, J.N.S., "On the Thermodynamics of Solutions. V. An Equation of State. Fugacities of Gaseous Solutions," *Chem. Rev.*, 1949, 44, 233-44.